DIFFERENT APPROACHES OF MODELLING AND ATTITUDE CONTROL OF MICROSATELLITE WITH INERTIAL COUPLING IN PRESENCE OF DISTURBANCE

A Thesis

Submitted in partial fulfilment of the requirement for the Degree of

Master in Control System Engineering

(Electrical Engineering Department)

By

Ayandeep Mandal

Registration No.: 163518 of 2022-2023

Examination Roll No.: M4CTL24001B

Under the Guidance of

Dr. Smita Sadhu (Ghosh)

Department of Electrical Engineering

Jadavpur University, Kolkata-700032, India.

November, 2024

FACULTY OF ENGINEERING AND TECHNOLOGY
JADAVPUR UNIVERSITY

CERTIFICATE

This is to certify that the dissertation entitled **"**Different Approaches of Modelling and Attitude Control of Microsatellite with Inertial Coupling in Presence of Disturbance**"** has been carried out by AYANDEEP MANDAL (University Registration No.: 163525 of 2022-2023) under my guidance and supervision and be accepted as partial fulfilment of the requirement for the Degree of Master in Control System Engineering.

Dr. Smita Sadhu (Ghosh)
Professor
Dept. of Electrical Engineering
Jadavpur University

Dr. Biswanath Roy
Head of the Department
Dept. of Electrical Engineering
Jadavpur University

Prof. Rajib Bandyopadhyay
Dean
Faculty of Engineering and Technology
Jadavpur University

FACULTY OF ENGINEERING AND TECHNOLOGY
JADAVPUR UNIVERSITY

CERTIFICATE OF APPROVAL*

The forgoing thesis is hereby approved as a creditable study of an engineering subject and presented in a manner satisfactory to warrant acceptance as prerequisite to the degree for which it has been submitted. It is understood that by this approval the undersigned do not necessarily endorse or approve any statement made, opinion expressed or conclusion drawn there in but approve the thesis only for which it is submitted.

Committee on final examination for the evaluation of the thesis.

Signature of the
Examiner

Signature of the
Supervisor

*Only in the case the thesis is approved.

FACULTY OF ENGINEERING AND TECHNOLOGY
JADAVPUR UNIVERSITY

DECLARATION OF ORIGINALITY AND COMPLIANCE OF ACADEMIC THESIS

I hereby declare that this thesis, titled **"**Different Approaches of Modelling and Attitude Control of Microsatellite with Inertial Coupling in Presence of Disturbance**"**, includes both a literature review and original research conducted by the undersigned as part of his Master's Degree in Control System Engineering. All information has been gathered and presented in compliance with academic standards and ethical guidelines. It is further affirmed that, in accordance with these standards, all sources and results not originating from this work have been duly cited and referenced.

Candidate Name: **AYANDEEP MANDAL**

Examination Roll. No.: M4CTL24001B

Thesis Title:

Signature of the candidate

Acknowledgement

I would like to express my heartfelt gratitude to my thesis supervisor, Dr. Smita Sadhu (Ghosh), from the Department of Electrical Engineering at Jadavpur University, for granting me the opportunity to work under her guidance and encouraging me to delve into the field of Control System Engineering. Her patient mentoring, insightful feedback, and unwavering support have been instrumental in shaping my research.

I specially thank Prof. Tapan Kumar Ghoshal, Emeritus Professor, ElectricalEngineering Department, Jadavpur University, Kolkata for his innovative discussions and for sharing his valuable suggestions, ideas and thoughts, which inspired me to doa project in this domain as well as helped me throughout my thesis work.

I would also like to thank respected faculties of Electrical Engineering Department Control System specialization Prof. Sayantan Chakraborty, Prof. Ranjit Kumar Barai and Prof. Madhubanti Maitra for all the guidance and knowledge that they imparted during the tenure of the course.

Finally, I extend my sincere thanks to my parents, Mr. Nabakumar Mandal and Mrs. Shipra Mondal and my sister Ishita Mandal and Debasmita Mandal, for their continuous support, encouragement and unending faith in my abilities.

Date:

Place:

AYANDEEP MANDAL

Department of Electrical Engineering

Examination Roll No.: M4CTL24001B

Jadavpur University.

Table of Contents

Chapter 4: Simulation Summary

Chapter 5: Conclusion

CHAPTER 1: INTRODUCTION

"Earth is the cradle of humanity, but mankind cannot stay in the cradle forever"

- *Carl Sagan, Cosmos (American astronomer and planetary scientist)*

Humankind's profound curiosity to know the unknown, to see the unseen has driven us in unimaginable quests and space exploration might be the most exciting of them all. The inherent urge to explore beyond this 'cradle' of earth had taken humanity to outer space in 1957 for the first time. Since then, we have achieved the unthinkable in the last 67 years, be it our probe traveling beyond the solar system into the interstellar space (Voyager 1&2), or developing reusable rockets (by SpaceX), or launching James Webb space telescope to second Lagrange point for infrared astronomy. Needless to say, today's space technology is giving us unprecedented insights into the universe's origin, formation of celestial bodies and possibility of existence of life in exoplanets. But, not only quenching the thirst of knowledge, space technology has increasingly permeated daily life, driving advancements across multiple sectors and significantly impacting how we live, work, and interact with the world.

One of the most notable impacts of space technology is in the realm of global communication. Satellite networks facilitate instant connectivity across vast distances, supporting everything from international telecommunication to internet services in remote areas. For instance, advancements in satellite internet technology have led to the deployment of mega-constellations of low Earth orbit (LEO) satellites, such as SpaceX's Starlink and OneWeb, aiming to provide high-speed internet access to underserved regions around the globe.

Another significant contribution of space technology is in the field of Earth observation. Modern satellites equipped with advanced sensors and imaging systems are pivotal in monitoring climate change, natural disasters, and environmental changes. Recent developments, such as NASA's Landsat 9 and the European Space Agency's Copernicus Sentinel missions, provide unprecedented data that helps in tracking deforestation, assessing the impacts of natural disasters, and managing natural resources more effectively.

Furthermore, space technology has enabled breakthroughs in navigation systems. The Global Positioning System (GPS), which relies on a network of satellites orbiting Earth, has revolutionized how we navigate

both in urban environments and remote regions. Recent enhancements in satellite navigation, including the development of the Galileo system by the European Union and the modernization of GPS, offer improved accuracy and reliability, benefiting applications ranging from autonomous vehicles to precision agriculture. Nearly Every Mobile application that makes our life easy today, directly or indirectly uses this (or similar) service, which is enough to understand its massive impact in modern human life.

In this context, the control of satellite attitude—the precise orientation of satellites in space—has become increasingly critical. Maintaining the correct orientation is essential for ensuring that satellite systems function optimally and achieve their intended missions. Attitude control is essential for ensuring that a satellite's instruments are correctly oriented to achieve mission objectives. Whether it's aligning a communication antenna with a ground station, positioning a scientific sensor for optimal data collection, or maintaining a specific orientation for imaging, precise control of attitude is crucial. In the absence of gravity and atmospheric forces, achieving and maintaining the desired orientation involves complex dynamics and requires sophisticated control systems.

Historically, attitude control has evolved from basic systems relying on gyroscopes and magnetic torquers to advanced techniques utilizing reaction wheels, control moment gyroscopes, and modern thrusters. The development of these systems has been driven by the need for higher accuracy, greater reliability, and enhanced mission capabilities. Contemporary challenges in attitude control include managing the effects of external disturbances, such as solar radiation pressure and gravitational forces from secondary celestial bodies, as well as addressing the limitations of onboard resources like power and computational capacity.

This thesis aims to contribute to the field of satellite attitude control by exploring various control approaches and solutions. Through a combination of theoretical analysis, utilization of different mathematical models and simulation based on different controllers, this research seeks to address emerging real-case challenges inherent in managing satellite orientation in the ever-evolving space environment.

1.1 What is Attitude control?

The attitude control system (ACS) controls the spacecraft body axes such that the errors in roll, pitch and yaw angles are within defined limits to control the orientation of the spacecraft as the main objective. The schematic of the attitude control system is as shown in figure 1.

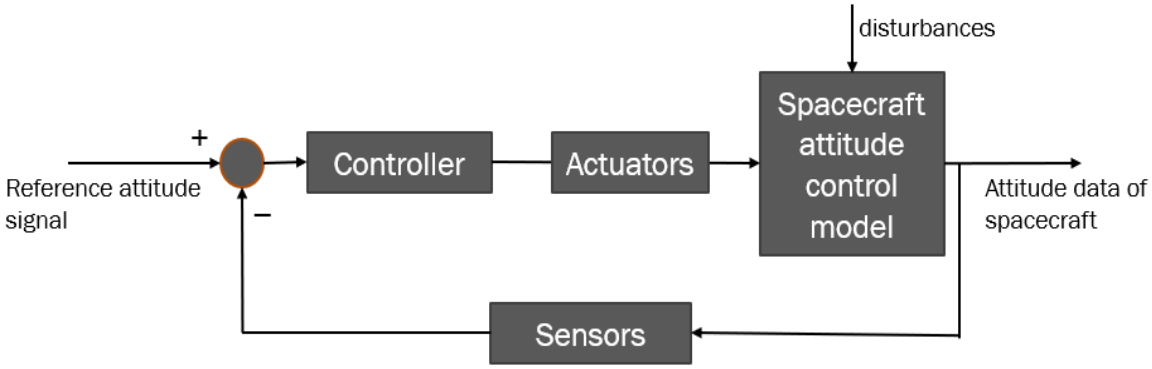

Figure 1: Block Diagram of Attitude Control System

1.2 Roll, Pitch and Yaw Angle

To expedite on the orientation of a body roll, pitch and yaw angle are to be explained. Roll, pitch, and yaw are fundamental concepts in three-dimensional space that describe the orientation of an object, typically an aircraft or a vehicle. Here's a brief overview of each:

1. **Roll**: This refers to the rotation around the longitudinal axis (the axis that runs from the front to the back of the object). When an spacecraft rolls, one wing goes up while the other goes down. This movement is crucial for banking turns.

2. **Pitch**: Pitch involves rotation around the lateral axis (the axis that runs from wingtip to wingtip or along the y axis in conventional right hand Cartesian frame system). When an spacecraft pitches, its nose moves up or down. This motion affects altitude and is essential for climbing or descending.

3. **Yaw**: Yaw is the rotation around the vertical axis (the axis that runs from the top to the bottom of the object or the z axis in the conventional right hand cartesian system). When an aircraft yaws, its nose moves left or right. This movement helps in changing direction horizontally.

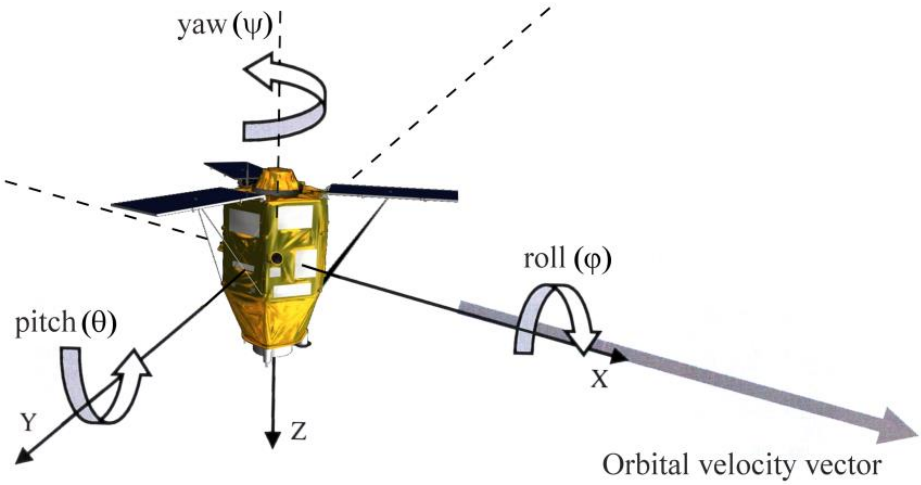

Fig 2: Roll, Pitch and Yaw axis representation of a spacecraft [1]

Together, these angles describe the complete orientation of an object in 3D space and are essential for navigation, stability, and control in various vehicles, especially in aviation.

1.3 Sensors and Actuators:

Two of the most important parts of the attitude control system are sensors and actuators as they measure the instantaneous orientation of the spacecraft and perform required maneuvers for desired change in the orientation of the object respectively. Different kinds of sensors and actuators used in spacecrafts are discussed below.

1.3.1 Sensors

1. Inertial Measurement Units (IMUs):

- Description: IMUs consist of accelerometers and gyroscopes that measure linear acceleration and angular velocity, respectively.
- Function: They provide real-time data on the spacecraft's motion and orientation.

2. Sun Sensors:

- Description: These sensors detect the position of the Sun relative to the spacecraft.
- Function: They help determine the spacecraft's attitude by providing reference points for solar positioning.

3. Star Trackers:

- Description: Optical sensors that capture images of stars and compare them to a star catalog.
- Function: They provide precise attitude information by identifying the spacecraft's orientation in relation to known stars.

4. Magnetic Field Sensors:

- Description: These sensors measure the local magnetic field.
- Function: They help determine the spacecraft's orientation with respect to Earth's magnetic field, useful for attitude stabilization.

5. GPS Receivers:

- Description: These systems receive signals from GPS satellites.
- Function: They can provide position and velocity information, aiding in attitude determination.

1.3.2 Actuators

1. Reaction Wheels:

- Description: These are flywheels mounted on the spacecraft that can be spun up or down to produce torque.
- Function: They allow precise control of orientation without using propellant, ideal for fine-tuning attitude.

2. Control Moment Gyroscopes (CMGs):

- Description: Similar to reaction wheels, but they use the precession of spinning masses to generate torque.
- Function: They provide rapid and large changes in attitude, often used in larger spacecraft.

3. Thrusters:

- Description: Small rocket engines that expel gas to produce thrust. Cold gas jet, monopropellant and bi-propellant jet, ion engine, gas-liquid equilibrium thruster are different variants widely used in the industry.
- Function: They can be used for larger attitude adjustments or maneuvers, especially for spacecraft in low-gravity environments.

4. Magnetic Torquers:

- Description: Electromagnetic coils that interact with Earth's magnetic field.
- Function: They create torque to change the spacecraft's orientation, useful for small adjustments.

5. Gimbaled Engines:

- Description: Engines that can pivot to direct thrust in various directions.
- Function: Used in larger spacecraft for maneuvering and attitude control during propulsion phases.

The combination of these sensors and actuators enables spacecraft to maintain stability, navigate accurately, and respond to various mission requirements, ensuring successful operations in the challenging environment of space.

A spacecraft can have several feedback control systems. In many spacecrafts similar three-axis feedback control is also required to point the communications antenna, science platforms and instruments, solar arrays and other sensors. An open-loop control system is one where the desired position is commanded with no feedback to perform the commanded action. This method is used where low precision is required.

CHAPTER 2: Literature Survey

This thesis work includes a survey of some available scientific literature on attitude control of spacecrafts consisting of some similar techniques used in the course of this thesis work or the control techniques more popular in the industry. The literature survey is separated in two different sections, one on the progress of space technology with nano and micro-satellites and the other section discusses different control approaches of attitude control in satellites.

2.1. Literature survey of Micro/Nano-Satellites:

In the literature survey, this thesis provides a comprehensive review in two main areas: advancements in micro and nano satellite technology and an exploration of control strategies for satellite attitude control. The first part examines the evolution of micro and nano satellites, divided into two sections: one focusing on technological advancements in instrumentation and utility, and the other on attitude control techniques specifically tailored for these small-scale platforms. The second part of the survey covers a range of control approaches used in satellite attitude control, evaluating methodologies in terms of stability, robustness, and adaptability to disturbances. This dual focus aims to build a strong foundation for understanding both the specific challenges of micro and nano satellite control and the broader context of attitude control strategies for satellites.

2.1.1. Introduction to Micro and Nano Satellites

Micro and nano satellites have revolutionized space exploration and satellite technology due to their reduced size, cost, and increased flexibility. These small satellites, typically weighing between 1 kg to 100 kg, have enabled a range of applications from Earth observation to deep space exploration. Their development began in the late 20th century with significant advancements in miniaturization of technology and a growing interest in cost-effective space missions.

2.1.2. Historical Overview:

The concept of small satellites dates back to the 1960s with the launch of experimental satellites like OSCAR 1, the first amateur radio satellite, the result of American space endeavour Project OSCAR. Although all the satellites in earlier period of space technology were small in size and mass due to payload constraints of available propulsion system. With bigger rockets and boosters, larger satellites came in picture which can execute multiple projects with numerous modules installed in the same body. In recent days the smaller satellites are getting prioritized mainly because of the reason that larger satellites are prone to put down

multiple project investments for a single breakdown in the satellite. Also, the smaller satellites are more economically viable options besides involving lower risk to investments.

Name	Launch date	Mass (kg)	Perigee (km)	Apogee (km)	Country
Vanguard-1	17-Mar-58	1.47	652	3961	United States
Pioneer-3	06-Dec-58	5.88	0	1,02,300	United States
Pioneer-4	03-Mar-59	5.88	Lunar Flyby	Lunar Flyby	United States
Explorer-9	16-Feb-61	7	636	2582	United States
OSCAR-1	12-Dec-61	4.5	235	415	United States
OSCAR-2	06-Feb-62	4.5	208	386	United States
Flashing Light	15-May-63	5	161	267	United States
ERS-9	19-Jul-63	1.5	3,662	3731	United States
ERS-12	17-Oct-63	2.1	208	1,03,830	United States
Explorer-19	19-Dec-63	7	589	2393	United States
ERS-13	17-Jul-64	2.1	193	1,04,400	United States
Explorer-24	21-Nov-64	9	334	1551	United States
ERS-17	20-Jul-65	5.4	208	1,12,184	United States
ERS-16	09-Jun-66	5	180	3622	United States
ERS-15	19-Aug-66	5	3,669	3701	United States
ERS-18	28-Apr-67	9	8,619	1,11,530	United States
ERS-9	19-Jul-63	1.5	3,662	3731	United States
ERS-20	28-Apr-67	8.6	8,619	1,11,530	United States
ERS-27	28-Apr-67	6	8,619	1,11,530	United States

Explorer-39	08-Aug-68	9.4	673	2533	United States
ERS-28	26-Sep-68	10	175	35,724	United States
ERS-26	23-May-69	10	59,543	69,011	United States

Table 1: Nanosatellites during early space age [2]

After OSCAR-1 different small satellites were used for various missions, However, the term "micro satellite" gained prominence in the 1990s, with missions such as CUBE-SAT (launched in 2000), which set a precedent for small satellite design and deployment. Although before the inception of the conceptualisation of Cubesat, several small satellite missions were experimented. NASA developed DOVE satellites in 1990s and ESA (European Space Agency) began experimenting with small satellite technologies, leading to developments in lightweight materials and compact instruments. Later different nano and micro satellite missions were carried out as a consequence of success of its predecessors. A few mentionable of such satellites belong from AMSAT, UoSat satellite family, SAMPEX, TRACE etc.

Continued advancements in technology led to further miniaturization of components, such as sensors, processors, and communication systems, making it feasible to pack more functionality into smaller satellites.The rise of private companies interested in small satellite technology began to reshape the landscape, with companies like Planet Labs launching fleets of small satellites for Earth observation. By late 2000s and 2010s micro and nano satellites were used for a variety of applications, including Earth observation, scientific research, and technology demonstration. The concept of satellite constellations gained traction, with companies and organizations proposing networks of small satellites for global communications and monitoring.

The introduction of dedicated small satellite launch vehicles, like Rocket Lab's Electron, has significantly reduced launch costs and increased access to space for small satellites. Modern nano and micro satellites are equipped with advanced technologies, enabling sophisticated missions such as remote sensing, communications, and space exploration.

2.1.3. Technological advancements of micro/nano-satellites:

The major challenge of designing a micro/nano-satellite was accommodating all the hardware of such multi-functionary sophisticated device in such small size. Initially the functionalities of small

satellites were very simplified for that reason. The first Swedish nano-satellite 'MUNIN' was designed and fabricated by Swedish Institute of Space Physics to collect data on auroral activity in both northern and southern hemisphere, such that the data related to current magnetospheric activity can be made available on-line [3]. This data is then used in prediction of space weather. This is cubesat with side length of 21 cm and has weight of 6kg with combined electron and ion spectrometer, solid state detector, miniature CCD camera, silicon solar array on all sides and a Li-ion battery. It uses a magnetic attitude control system which consists of a permanent magnet and a hysteresis rod as a damper. A very precise attitude control system was not needed for the mission as it was not going to use any complex rotation endeavour. The motive was to make the ACS as cheap as possible from both economic and energy perspective. The permanent magnet provides the necessary restoring torque to align the orientation of MUNIN with earth's magnetic field vector. The damping rod ensures the transient dies out. Damping rod is manufactured from a soft-magnetic material and re-magnetized in geomagnetic field under satellite rotation relative to a force line of this field, so it can generate a damping torque.

With advancements in the field of electronics engineering and miniaturisation of hardware micro and nanosatellites were being launched with various purposes like earth observation, geological applications, solar and space weather monitoring etc. The invention of CMOS cameras, ARM7 microcontrollers etc influenced nanosatellites like O/OREOS, CXBN, BRITE during the 2000's decade.

Later constellation of nanosatellites came into picture with missions like OneWeb to provide to provide broadband connectivity all over the globe with a constellation of 2000 nanosatellites [4]. The Dutch nanosatellite constellation HIBER is aiming to provide IoT based services in domains like agriculture, soil and rain sensors, tank and silo monitoring, snow and ice cap monitoring, transportation and logistics over 90% of earth's surface.

Notable mentions of various nanosatellites categorised according to their functions is given below [5].

Sr. No.	**Functionality**	**Nanosatellites.**
1	Earth Imager	M-Cubed-2/ COVE, SwissCube, AArest
2	X-Ray Detectors	MinXSS, HALOSAT, HERMES,MiSolFA
3	Spectrometers	SOLSTICE, OPAL, BIRCHES, GRIFEX
4	Photometers	XPS, ExoPlanet, ASTERIA
5	GNSS Recievers	CYGNSS, CADRE, CAT-2
6	Micro Bolometers	CSIM

7	Radiometers	TEMPEST
8	RADAR system	RAX, Radar Altimeters & SAR, 3SRI-CIRES
9	Particle Detectors	REPTILE, EPISEM, FIRE
10	Plasma Wave Analyser	CADRE / WINCS, DICE, INSPIRE / CVHM

Table 2: Notable Nanosatellites Categorised on Functionality

2.1.4. Attitude Control Techniques for Micro and Nano Satellites

Attitude control in small satellites presents unique challenges and opportunities due to their size constraints and operational environment. Here, we survey the prominent methods and approaches:

The most used attitude control methods with magnetic control were discussed in [6] by M. Yu Ovchinnikov and D. S. Roldugin on 3 premises of simple angular velocity damping, combined operation with other actuators and some passive stabilization methods. Approaches like angular velocity damping has been in use since the preliminary days of space exploration and still in use for its simplicity, energy efficiency and size advantage. Although the study shows for three-axis magnetic control secondary actuation method is necessary in some case, that is where newer control approaches like sliding mode, model predictive control and global optimization performs better.

A study [7] by C. Hajiyev and D. C. Guler discusses the attitude control approach of gyroscopic sensor-less microsatellites using estimation methods. Two types of gyroless satellite attitude determination methods were reviewed in this study: single-frame attitude determination methods based on vector measurements and attitude estimation methods based on Kalman filter. Two types of Kalman filter algorithms were taken into consideration as a traditional approach based on nonlinear measurements and nontraditional approach based on linear measurements. Comparison of different approaches shows that SVD based method shows maximum robustness, while Quaternion Estimation (QUEST) requires least computational burden, and in Kalman Filter based estimation Unscented Kalman Filter showed most superior result in accuracy and convergence speed.

[8] by Liang He et. al. has presented a survey of recent development in the field of attitude control of microsatellites including the significant improvement of high precision attitude control with the inception of miniaturised star sensor, Commercial-Off-The-Shelf (COTS) reaction wheels and Control moment Gyroscopes (CMG). The study

showed conventional control methods face challenges in reducing complex non-linear alignment error due to low redundancy in small spacecrafts. Although Deep Neural Network (DNN) strategies showed great results in similar cases, hence, possessing better possibility of this approach in similar cases.

2.1.5. Conclusion

The field of attitude control for micro and nano satellites continues to evolve, driven by advancements in control algorithms, miniaturization of hardware, and innovative mission profiles. Classical methods like PID control still play a significant role, while adaptive, predictive, and emerging techniques offer enhanced capabilities for handling the complexities of small satellite missions.

2.2. Literature Survey of Various Attitude Control Techniques of Satellite:

Attitude control is critical in the operation of satellites for maintaining the desired orientation (attitude) with respect to an inertial or reference frame. The attitude of a satellite can significantly affect its communication, imaging, scientific experiments, and overall mission success. The 2nd part of this survey highlights key algorithms developed over the years for satellite attitude control, focusing on recent advancements and typical classification schemes for such algorithms.

Magnetic coils have been used for attitude control action from the earliest years of satellite missions, hence, those have become a subject of extended study (see Stickler & Alfriend (1976) [9] and the references therein). The major drawback of this problem was the control torque to the satellite cannot be provided along the direction of earth's magnetic field lines. Later it was proved that three-axis stabilization is possible, only if the particular orbit of the satellite observes a time variation in magnetic field sufficient to guarantee stabilizability of the satellite in [10] by Bhat & Dham, 2003). Before this finding it was assumed initially that three independent control torques can be applied to the satellite and that, on the basis of this assumption, a conventional PD control law (which guarantees attitude regulation in the case of three controls, as per [11] by Wen & Kreutz-Delgado, 1991) had been designed. Therefore, as long as the closed-loop dynamics is sufficiently slow, the stability of the time-varying closed-loop system can be approximately studied on the basis of its time-invariant approximations. Hence, other classical control approaches were used as well. Assuming that the periodic approximation for the geomagnetic field is satisfactory, the resulting periodic dynamics for the spacecraft can be stabilized

either by state or output periodic feedback. A number of contributions have been given in the literature to the analysis of the LQ magnetic attitude control problem. In [12] by Pittelkau, both output feedback stabilization and disturbance attenuation for a momentum biased spacecraft have been analyzed; in particular, the disturbance issue has been addressed by means of an internal model principle approach. In order to avoid the difficulties in the solution of the LQ problems due to the presence of uncontrollable modes with poles on the imaginary axis, the secular and cyclic components of the external disturbances have been modeled with stable models (first order with a large time constant for the secular part and second order with small damping for the cyclic part). This gives rise to a time periodic filter and a time periodic state feedback. In [13] by Lovera et al. and [14] by De Marchi et al. the problem is analyzed in a similar fashion, by using an extension of the periodic LQ control problem (initially proposed in [15] by Arcara et al.), by which it is possible to include marginally stable disturbance models in the plant description. The resulting control design method is applied in a simulation study for the Italian spacecraft MITA. A similar approach has been also proposed in [16] by Wisniewski (1996), [17] by Wisniewski and Blanke (1999) and [18] by Wisniewski and Markley (1999), where the sole state feedback problem is considered. An LMI approach to the design of H_2 -optimal periodic controllers was proposed in [19] by Wisniewski & Stoustrup (2002). The H_∞ approach to the problem has been first proposed in [20] for the design of state feedback attitude controllers and in [21] for the implementation of momentum management control laws based on magnetic actuators.

A novel approach in the domain of predictive control is used in [22] for attitude stabilization of a spacecraft. Furthermore, classical LQ and H_∞ periodic control and nonlinear control have been discussed with an aim of robustness of the control law in presence of different disturbances and a satisfactory solution is proposed.

Sliding mode controller offers low complexity, low computational burden control method which can make the output converge in finite time. Hence, it is very suitable for attitude stabilization of orbital spacecrafts. This [23] paper from 1997 discusses a new Terminal Sliding Mode (TSM) control scheme which operates on a multiple input multiple output linear system. It is shown, by using this controller the system goes to origin in finite time and attains infinity stability on the terminal sliding mode. In 2002, this paper [24] proposed the way to overcome the singularity problem associated with the conventional TSM control scheme, ensuring finite reaching time for every initial condition. [25] shows a non-linear system can asymptotically track a desired output trajectory when controlled by an SMC in closed loop. As it accomplishes

precise attitude control despite present uncertainties, the robustness offered by SMC is also observed. This paper [26] uses sliding mode control for a spacecraft that performs large angle manoeuvres. But SMC causes chattering effect generated from its switching function, this causes harm to the actuator in long term. To solve this issue, using fuzzy sliding mode controlled seemed like an improvement. But fixed fuzzy rules are observed to cause instability in the system. So, this paper [27] presents the detailed procedure to design an Adaptive Fuzzy Sliding Mode Controller (AFSMC) and shows that it eliminates the chattering effect while keeping the system stability undisturbed. The major drawback of AFSMC is its high computational burden, which is not at all desired in smaller spacecrafts. An energy efficient way is suggested here [28], naming Minimum Sliding Mode Error Feedback Control (MSMEFC). Although it is energy efficient, eliminates chattering and robust enough, the performance degrades steeply under large perturbations or in an effort to track sharp turns in trajectory. Another widely used variation of SMC is Integral Sliding Mode Controller (ISMC).

CHAPTER 3: Derivation of Mathematic Models

Mathematical modelling of a satellite or a spacecraft in general can be done in various methods. In this thesis work derivation of 3 type of mathematical model is presented and an effort has been made to explain every modelling in the simplest way possible with detailed derivation process.

3.1. Derivation of Euler Angle-based Mathematical Model:

For developing the mathematical model of the spacecraft attitude dynamics, rigid body rotational dynamics and kinematics are to be understood fast.

3.1.1. Rigid Body Rotational Kinematics and Dynamics:

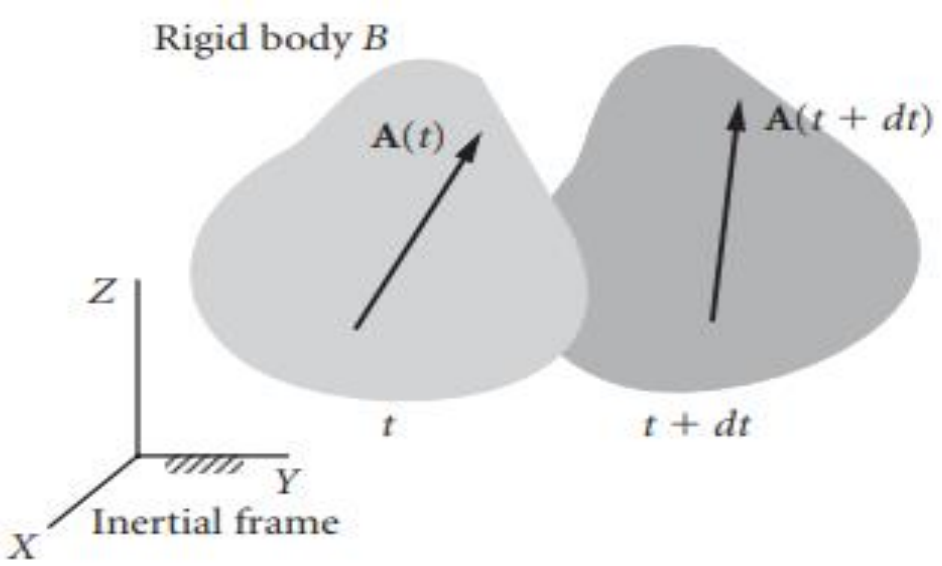

Figure 3: Rigid Body Rotation [29]

Suppose the shown rigid body is rotating with an angular velocity $\vec{\omega}$ with respected to the fixed/inertial frame. Assume a vector $\vec{A}(t)$ inscribed in the rigid body which will go under the similar rotation with angular velocity $\vec{\omega}$. Say after a small time *dt* the vector inscribed in the rigid body becomes $\vec{A}(t + dt)$. If the change in the vector is said to be $\overrightarrow{dA}$, then from the triangle law of vector we can say,

$$\vec{A}(t + dt) - \vec{A}(t) = \overrightarrow{dA}$$

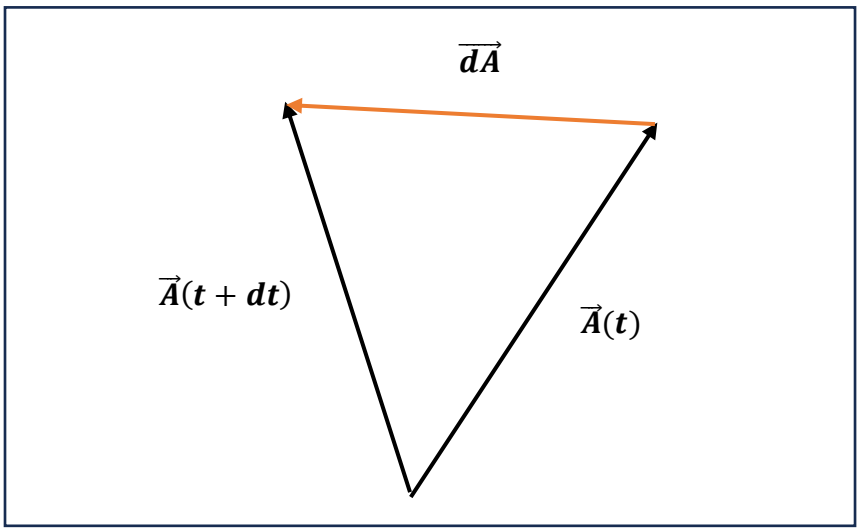

Which can be written as

$$\overrightarrow{dA} = [|\vec{A}|\sin\varphi \; d\theta]\,\hat{n} \qquad \textbf{(1)}$$

$\hat{n}$ is the unit vector in the normal direction of the plane of rotation of $\vec{A}(t)$ vector. φ is the angle between the vector $\vec{A}(t)$ and angular velocity vector $\vec{\omega}$. We know that if a vector/line of length R is rotated with elemental angle dθ then the elemental length difference is R$d\theta$. But here the vector and its angular velocity vector is not perpendicular, so only the perpendicular component of $\vec{A}(t)$ will be rotated with angle $d\theta$. The component that is coincident with $\vec{\omega}$ will not go through any rotation, as we can clearly understand. The length of the perpendicular component being $|\vec{A}|\sin\varphi$, the length of $\overrightarrow{dA}$ is should be $|\vec{A}|\sin\varphi \; d\theta$, which is stated in equation (1).

Now, we know,

$$\frac{d\theta}{dt} = |\vec{\omega}|$$

$$d\theta = |\vec{\omega}|dt$$

Using this in equation (1) we get,

$$d\vec{A} = [(|\vec{\omega}|dt)|\vec{A}|\sin\emptyset]\,\hat{n} \quad \textbf{(2)}$$

$$\boxed{\frac{d\vec{A}}{dt} = \vec{\omega} \times \vec{A}} \quad \textbf{(3)}$$

Equation (3) will be useful in the next part when we try to differentiate a vector described in the body reference frame with respect to inertial frame.

3.1.2. Dynamics of Spacecraft:

Suppose the angular momentum of a rigid body is,

$$\vec{H} = H_x\hat{\imath} + H_y\hat{\jmath} + H_z\hat{k}$$

Where the unit vectors with lower case is the unit cartesian vectors w.r.t. moving body frame and the set with upper case unit cartesian vectors are w.r.t. inertial frame.

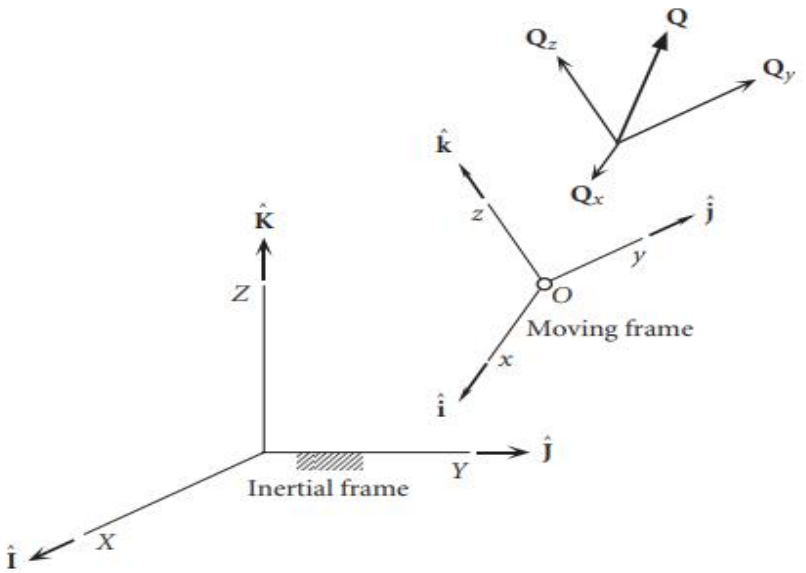

Figure 3: Inertial frame and moving frame [29]

Differentiating $\vec{H}$ with respect to inertial frame we get,

$$\frac{d\vec{H}}{dt} = \left(\frac{dH_x}{dt}\hat{\imath} + \frac{dH_y}{dt}\hat{\jmath} + \frac{dH_z}{dt}\hat{k}\right) + \left(H_x\frac{d\hat{\imath}}{dt} + H_y\frac{d\hat{\jmath}}{dt} + H_z\frac{d\hat{k}}{dt}\right) \quad \textbf{(4)}$$

The unit vectors of the moving frame are to be differentiated as well, as they are moving with the frame and hence not a constant.
Using equation (3) we can write,
$\frac{d\hat{\imath}}{dt} = \overrightarrow{\omega} \times \hat{\imath}$ and so on. So, we can write,

$$\frac{d\vec{H}}{dt} = \left(\frac{dH_x}{dt}\hat{\imath} + \frac{dH_y}{dt}\hat{\jmath} + \frac{dH_z}{dt}\hat{k}\right) + \overrightarrow{\omega} \times (H_x\hat{\imath} + H_y\hat{\jmath} + H_z\hat{k})$$

$$\boxed{\frac{d\vec{H}}{dt} = \frac{d\vec{H}}{dt}\Big|_{rel} + \overrightarrow{\omega} \times} \quad \textbf{(5)}$$

$\frac{d\vec{H}}{dt}$ → differentiation of $\vec{H}$ w.r.t. fixed inertial frame
$\frac{d\vec{H}}{dt}|_{rel}$ → differentiation of $\vec{H}$ w.r.t. moving body frame
Now consider a spacecraft which has moment of inertia I, the angular velocity and angular momentum with respect to moving body frame are $\overrightarrow{\omega}$ and $\vec{H}$.
So, $\vec{H} = I\overrightarrow{\omega}$.
From Newton's second law we can write,
$\frac{d\vec{H}}{dt} = \vec{\tau}$, where τ is the total moment of all the forces applied about the CoM of spacecraft.

$\frac{d\vec{H}}{dt}|_{rel} = I\dot{\vec{\omega}}$. By using the relation in equation (5), we can write,

$$\vec{\tau} = \frac{d\vec{H}}{dt}\Big|_{rel} + \overrightarrow{\omega} \times \vec{H}$$

$$\vec{\tau} = I\dot{\vec{\omega}} + \overrightarrow{\omega} \times I\overrightarrow{\omega}$$

$$\boxed{I\dot{\vec{\omega}} = \vec{\tau} - \overrightarrow{\omega} \times I\overrightarrow{\omega}} \quad \textbf{(6)}$$

This result is supported by reference [1].

$$\dot{\vec{\omega}} = I^{-1}\left(-\left(\overrightarrow{\omega} \times I\overrightarrow{\omega}\right) + \vec{\tau}\right) \quad \textbf{(7)}$$

Now this vector equation can be written in matrix form. Suppose the moment of inertia matrix $\boldsymbol{I} = diag\,(I_x, I_y, I_z)$, and angular velocity vector $\boldsymbol{\omega} = [p, q, r]^T$. $p, q\ and\ r$ represents the roll, pitch and yaw rates respectively. They are certainly w.r.t. body frame axes as $\overrightarrow{\boldsymbol{\omega}}$ was defined in the same reference frame.

$I\overrightarrow{\boldsymbol{\omega}} = [I_x p, , I_y q, I_z r]^{\boldsymbol{T}}$

So, $\overrightarrow{\boldsymbol{\omega}} \times I\overrightarrow{\boldsymbol{\omega}} = \begin{bmatrix} \hat{\boldsymbol{\imath}} & \hat{\boldsymbol{\jmath}} & \hat{\boldsymbol{k}} \\ p & q & r \\ I_x p & I_y q & I_z r \end{bmatrix} = -[(I_y - I_z)qr\ \hat{\boldsymbol{\imath}} + (I_z - I_x)rp\ \hat{\boldsymbol{\jmath}} + (I_x - I_y)pq\ \hat{\boldsymbol{k}}]$

So, in matrix form we can write equation (7) as,

$$\begin{bmatrix} \dot{p} \\ \dot{q} \\ \dot{r} \end{bmatrix} = \begin{bmatrix} I_x^{-1} & 0 & 0 \\ 0 & I_y^{-1} & 0 \\ 0 & 0 & I_z^{-1} \end{bmatrix} \begin{bmatrix} w_1 \\ w_2 \\ w_3 \end{bmatrix} - \begin{bmatrix} I_x^{-1} & 0 & 0 \\ 0 & I_y^{-1} & 0 \\ 0 & 0 & I_z^{-1} \end{bmatrix} \begin{bmatrix} -(I_y - I_z)qr \\ -(I_z - I_x)rp \\ -(I_x - I_y)pq \end{bmatrix}$$

$$\begin{bmatrix} \dot{p} \\ \dot{q} \\ \dot{r} \end{bmatrix} = \begin{bmatrix} I_x^{-1} & 0 & 0 \\ 0 & I_y^{-1} & 0 \\ 0 & 0 & I_z^{-1} \end{bmatrix} \begin{bmatrix} w_1 \\ w_2 \\ w_3 \end{bmatrix} + \begin{bmatrix} I_x^{-1} & 0 & 0 \\ 0 & I_y^{-1} & 0 \\ 0 & 0 & I_z^{-1} \end{bmatrix} \begin{bmatrix} (I_y - I_z)qr \\ (I_z - I_x)rp \\ (I_x - I_y)pq \end{bmatrix} \quad \textbf{(8)}$$

The Euler's angles are denoted as φ, θ, ψ as roll, pitch and yaw angle w.r.t earth inertial frame. $\vec{\boldsymbol{\tau}} = w_1\hat{\boldsymbol{\imath}} + w_2\hat{\boldsymbol{\jmath}} + w_3\hat{\boldsymbol{k}}$.

3.1.3. Kinematics of Spacecraft:

First the basic rotation matrices for Euler axes are defined.

Say, the rotation matrix for a rotation of angle $\varphi, \theta\ and\ \psi$ along roll, pitch and yaw axis respectively and separately are $C_\varphi, C_\theta\ and\ C_\psi$.

Their values are as shown below,

$$C_\varphi = \begin{bmatrix} 1 & 0 & 0 \\ 0 & \cos\varphi & \sin\varphi \\ 0 & -\sin\varphi & \cos\varphi \end{bmatrix}$$

$$C_\theta = \begin{bmatrix} \cos\theta & 0 & -\sin\theta \\ 0 & 1 & 0 \\ \sin\theta & 0 & \cos\theta \end{bmatrix}$$

$$C_{\psi} = \begin{bmatrix} \cos\psi & \sin\psi & 0 \\ -\sin\psi & \cos\psi & 0 \\ 0 & 0 & 1 \end{bmatrix}$$

The basic rotation matrices are found by rotating a frame with respect to one fixed axis by a certain angle. So, the directions of other 2 axes change. The rotational transformation matrix for this transformation is called the basic rotation matrix.

We set the convention as, the body fixed frame follows a *frd* (front-right-down) coordinate system and a *ned* (north-east-down) system is taken in reference frame. A yaw-pitch-roll Euler angle sequence is taken for the rotational conversion of frame. So, the transformation of angular rates from *ned* to *frd* can be shown as,

$$\begin{bmatrix} p \\ q \\ r \end{bmatrix} = \begin{bmatrix} \dot{\varphi} \\ 0 \\ 0 \end{bmatrix} + C_{\varphi}\left(\begin{bmatrix} 0 \\ \dot{\theta} \\ 0 \end{bmatrix} + C_{\theta}\begin{bmatrix} 0 \\ 0 \\ \dot{\psi} \end{bmatrix}\right)$$

$$\begin{bmatrix} p \\ q \\ r \end{bmatrix} = \begin{bmatrix} \dot{\varphi} \\ 0 \\ 0 \end{bmatrix} + \begin{bmatrix} 1 & 0 & 0 \\ 0 & \cos\varphi & \sin\varphi \\ 0 & -\sin\varphi & \cos\varphi \end{bmatrix}\left(\begin{bmatrix} 0 \\ \dot{\theta} \\ 0 \end{bmatrix} + \begin{bmatrix} \cos\theta & 0 & -\sin\theta \\ 0 & 1 & 0 \\ \sin\theta & 0 & \cos\theta \end{bmatrix}\begin{bmatrix} 0 \\ 0 \\ \dot{\psi} \end{bmatrix}\right)$$

$$\begin{bmatrix} p \\ q \\ r \end{bmatrix} = \begin{bmatrix} \dot{\varphi} \\ 0 \\ 0 \end{bmatrix} + \begin{bmatrix} 1 & 0 & 0 \\ 0 & \cos\varphi & \sin\varphi \\ 0 & -\sin\varphi & \cos\varphi \end{bmatrix}\left(\begin{bmatrix} 0 \\ \dot{\theta} \\ 0 \end{bmatrix} + \begin{bmatrix} -\dot{\psi}\sin\theta \\ 0 \\ \dot{\psi}\cos\theta \end{bmatrix}\right)$$

$$\begin{bmatrix} p \\ q \\ r \end{bmatrix} = \begin{bmatrix} \dot{\varphi} \\ 0 \\ 0 \end{bmatrix} + \begin{bmatrix} 1 & 0 & 0 \\ 0 & \cos\varphi & \sin\varphi \\ 0 & -\sin\varphi & \cos\varphi \end{bmatrix}\left(\begin{bmatrix} -\dot{\psi}\sin\theta \\ \dot{\theta} \\ \dot{\psi}\cos\theta \end{bmatrix}\right)$$

$$\begin{bmatrix} p \\ q \\ r \end{bmatrix} = \begin{bmatrix} \dot{\varphi} \\ 0 \\ 0 \end{bmatrix} + \begin{bmatrix} -\dot{\psi}\sin\theta \\ \dot{\theta}\cos\varphi + \dot{\psi}\cos\theta\sin\varphi \\ -\dot{\theta}\sin\varphi + \dot{\psi}\cos\theta\cos\varphi \end{bmatrix}$$

$$\begin{bmatrix} p \\ q \\ r \end{bmatrix} = \begin{bmatrix} \dot{\varphi} - \dot{\psi}\sin\theta \\ \dot{\theta}\cos\varphi + \dot{\psi}\cos\theta\sin\varphi \\ -\dot{\theta}\sin\varphi + \dot{\psi}\cos\theta\cos\varphi \end{bmatrix}$$

$$\begin{bmatrix} p \\ q \\ r \end{bmatrix} = \begin{bmatrix} 1 & 0 & \sin\theta \\ 0 & \cos\varphi & \cos\theta\sin\varphi \\ 0 & -\sin\varphi & \cos\theta\cos\varphi \end{bmatrix}\begin{bmatrix} \dot{\varphi} \\ \dot{\theta} \\ \dot{\psi} \end{bmatrix}$$

For expressing the angular rates about the *ned* frame with respect to *frd* frame, we have to take the inverse of the rotation matrix (transforming *frd* →*ned*)

Determinant = $\cos\theta$

Co-factor matrix = $\begin{bmatrix} \cos\theta & 0 & 0 \\ \sin\theta\sin\varphi & \cos\theta\cos\varphi & \sin\varphi \\ \sin\theta\cos\varphi & -\cos\theta\sin\varphi & \cos\varphi \end{bmatrix}$

Adjoint matrix = $\begin{bmatrix} \cos\theta & \sin\theta\sin\varphi & \sin\theta\cos\varphi \\ 0 & \cos\theta\cos\varphi & -\cos\theta\sin\varphi \\ 0 & \sin\varphi & \cos\varphi \end{bmatrix}$

So, we can write the final transformation as,

$$\begin{bmatrix} \dot{\varphi} \\ \dot{\theta} \\ \dot{\psi} \end{bmatrix} = \begin{bmatrix} 1 & \sin\varphi\tan\theta & \cos\varphi\tan\theta \\ 0 & \cos\varphi & -\sin\varphi \\ 0 & \sin\varphi/\cos\theta & \cos\varphi/\cos\theta \end{bmatrix} \begin{bmatrix} p \\ q \\ r \end{bmatrix} \quad \textbf{(9)}$$

From equation (8) and (9), we can state the spacecraft attitude dynamics if we take the states as $X = [x_1, x_2, x_3, x_4, x_5, x_6]^T$, where,

The state-space dynamics of the system is,

$x_1 = p$ $\quad$ $x_4 = \varphi$

$x_2 = q$ $\quad$ $x_5 = \theta$

$x_3 = r$ $\quad$ $x_6 = \psi$

$$\dot{\boldsymbol{x_1}} = \boldsymbol{I_x^{-1}}\left[\left(\boldsymbol{I_y} - \boldsymbol{I_z}\right)\boldsymbol{x_2}\boldsymbol{x_3} + \boldsymbol{w_1}\right]$$

$$\dot{\boldsymbol{x_2}} = \boldsymbol{I_y^{-1}}\left[\left(\boldsymbol{I_z} - \boldsymbol{I_x}\right)\boldsymbol{x_3}\boldsymbol{x_1} + \boldsymbol{w_2}\right]$$

$$\dot{\boldsymbol{x_3}} = \boldsymbol{I_z^{-1}}\left[\left(\boldsymbol{I_x} - \boldsymbol{I_y}\right)\boldsymbol{x_1}\boldsymbol{x_2} + \boldsymbol{w_3}\right]$$

$$\dot{\boldsymbol{x_4}} = \boldsymbol{x_1} + (\sin\boldsymbol{x_4})(\tan\boldsymbol{x_5})\boldsymbol{x_2} + (\cos\boldsymbol{x_4})(\tan\boldsymbol{x_5})\boldsymbol{x_3}$$

$$\dot{\boldsymbol{x_5}} = (\cos\boldsymbol{x_4})\boldsymbol{x_2} - (\sin\boldsymbol{x_4})\boldsymbol{x_3}$$

$$\dot{\boldsymbol{x_6}} = \frac{\sin\boldsymbol{x_4}}{\cos\boldsymbol{x_5}}\boldsymbol{x_2} + \frac{\cos\boldsymbol{x_4}}{\cos\boldsymbol{x_5}}\boldsymbol{x_3}$$

NOTE:

This model is applied only when the moment of inertia matrix of the spacecraft is diagonal, which happens only when the spacecraft is symmetric about the xy, yz and zx plane, where the body axes system is OXYZ.

It is very common case for a lot of spacecrafts, although there are few whose moment of inertia matrix is **not diagonal** and just carries the symmetric property. In such cases the model cannot be simplified as above. We have to use the state equations as,

Dynamic Equation:

$\dot{\omega} = I^{-1}(-\omega^{\times} I\omega + \tau)$ where $\omega^{\times} = \begin{bmatrix} 0 & -r & q \\ r & 0 & -p \\ -q & p & 0 \end{bmatrix}$, $\omega = \begin{bmatrix} p \\ q \\ r \end{bmatrix}$

Kinematic Equation:

$$\begin{bmatrix} \dot{\varphi} \\ \dot{\theta} \\ \dot{\psi} \end{bmatrix} = \begin{bmatrix} 1 & \sin\varphi \tan\theta & \cos\varphi \tan\theta \\ 0 & \cos\varphi & -\sin\varphi \\ 0 & \sin\varphi / \cos\theta & \cos\varphi / \cos\theta \end{bmatrix} \begin{bmatrix} p \\ q \\ r \end{bmatrix}$$

3.2. Derivation of Quaternion-based Mathematical Model:

3.2.1. What is Quaternion?

W.R. Hamilton introduced the term quaternion in an attempt to generalize complex numbers from a plane to three dimensions in 1943. The quaternion described by him has the form,

$$q = q_0 + q_1 i + q_2 j + q_3 k$$

Where the imaginary operators are given by,

$$i^2 = j^2 = k^2 = -1$$

$$ij = k = -ji$$

$$jk = i = -kj$$

$$ki = j = -ik$$

Quaternions follow the basic laws of algebra, except the multiplication is not commutative for the last 3 operations shown above. That is why it is a good idea to express a quaternion where we assume it is a combination of a scalar and a vector part. The vector part being $\vec{q} = q_1 i + q_2 j + q_3 k$. It can be expressed in the below stated form

$$q = \begin{bmatrix} q_0 \\ q_1 \\ q_2 \\ q_3 \end{bmatrix} = \begin{bmatrix} q_0 \\ \vec{q} \end{bmatrix}$$

3.2.2. Why quaternion-based model

- Quaternions are introduced here because of their "all-attitude" capability.
- It is free from the singularity that Euler angle-based model has at pitch angle 90º.
- Quaternion model has some computational advantages in simulation over other available models of attitude dynamics.

3.2.3. Quaternion Multiplication

Say $p = p_0 + \vec{p}$ and $q = q_0 + \vec{q}$, then their multiplication operation $(*)$ will be,

$$p * q = (p_0 + \vec{p}) * (q_0 + \vec{q})$$

$$\Rightarrow p * q = p_0 q_0 + p_0 \vec{q} + q_0 \vec{p} + (\vec{p} \times \vec{q}) - \vec{p} \cdot \vec{q}$$

So, the scalar part of the expression is $(p_0 q_0 - \vec{p} \cdot \vec{q})$ and the vector part is $(p_0 \vec{q} + q_0 \vec{p} + (\vec{p} \times \vec{q}))$

In quaternion form we can write,

$$p * q = \begin{bmatrix} p_0 \\ \vec{p} \end{bmatrix} * \begin{bmatrix} q_0 \\ \vec{q} \end{bmatrix} = \begin{bmatrix} p_0 q_0 - \vec{p} \cdot \vec{q} \\ p_0 \vec{q} + q_0 \vec{p} + (\vec{p} \times \vec{q}) \end{bmatrix}$$

Consider the following product

$$\begin{bmatrix} q_0 \\ \vec{q} \end{bmatrix} * \begin{bmatrix} q_0 \\ -\vec{q} \end{bmatrix} = \begin{bmatrix} q_0^2 - (\vec{q} \cdot (-\vec{q})) \\ q_0 \vec{q} - q_0 \vec{q} + (\vec{q} \times (-\vec{q})) \end{bmatrix}$$

$$\Rightarrow \begin{bmatrix} q_0 \\ \vec{q} \end{bmatrix} * \begin{bmatrix} q_0 \\ -\vec{q} \end{bmatrix} = \begin{bmatrix} q_0^2 + (\vec{q} \cdot \vec{q}) \\ 0 \end{bmatrix}$$

$$\Rightarrow \begin{bmatrix} q_0 \\ \vec{q} \end{bmatrix} * \begin{bmatrix} q_0 \\ -\vec{q} \end{bmatrix} = \begin{bmatrix} norm(q) \\ 0 \end{bmatrix}$$

From this result we can have inverse of a quaternion as,

$$\boxed{\begin{bmatrix} q_0 \\ \vec{q} \end{bmatrix}^{-1} = \frac{1}{norm(q)} \begin{bmatrix} q_0 \\ -\vec{q} \end{bmatrix}}$$

3.2.4. Co-ordinate Transformation by Quaternions:

A quaternion can be used to rotate a Euclidean vector in the same manner as the rotation formula by rotation matrices, and the quaternion rotation is much simpler in form. The vector part of the quaternion is used to define the rotation axis and the scalar part to define the angle of rotation. The rotation axis is specified by its direction cosines in the reference coordinate system, and it is convenient to impose a **unity norm** constraint on the quaternion. Therefore, if the direction angles of the axis are α, β, γ and a measure of the rotation angle is δ, the rotation quaternion is written as

$$q = \begin{bmatrix} \cos\delta \\ \sin\delta\cos\alpha \\ \sin\delta\cos\beta \\ \sin\delta\cos\gamma \end{bmatrix} = \begin{bmatrix} \cos\delta \\ \sin\delta\,\widehat{\boldsymbol{n}^{\boldsymbol{r}}} \end{bmatrix}$$

The r in superscript refers that the vector is in the reference frame.

To operate the transformation on a vector the vector needs to be expressed in quaternion form first. The standard way to do this is to express the vector as,

$$u = \begin{bmatrix} 0 \\ \vec{u} \end{bmatrix}$$

The result of the rotation must also be a quaternion with a scalar part of zero, the transformation must be reversible by means of the quaternion inverse, and Euclidean length must be preserved. The transformation $v = q * u$ obviously does not satisfy the first of these requirements. Therefore, we consider the transformation,

$$v = q^{-1} * u * q$$

$$\Rightarrow v = \frac{1}{norm(q)}\begin{bmatrix} q_0 \\ -\vec{q} \end{bmatrix} * \begin{bmatrix} 0 \\ \vec{u} \end{bmatrix} * \begin{bmatrix} q_0 \\ \vec{q} \end{bmatrix}$$

$$\Rightarrow v = \frac{1}{norm(q)}\begin{bmatrix} \vec{q}\cdot\vec{u} \\ q_0\vec{u} + ((-\vec{q})\times\vec{u}) \end{bmatrix} * \begin{bmatrix} q_0 \\ \vec{q} \end{bmatrix}$$

$$\Rightarrow v = \frac{1}{norm(q)}\begin{bmatrix} q_0(\vec{q}\cdot\vec{u}) - (q_0\vec{u} + ((-\vec{q})\times\vec{u}))\cdot\vec{q} \\ (\vec{q}\cdot\vec{u})\vec{q} + q_0(q_0\vec{u} + ((-\vec{q})\times\vec{u})) + (q_0\vec{u} + ((-\vec{q})\times\vec{u}))\times\vec{q} \end{bmatrix}$$

$$\Rightarrow v = \frac{1}{norm(q)}\begin{bmatrix} q_0(\vec{q}\cdot\vec{u}) - q_0(\vec{u}\cdot\vec{q}) \\ (\vec{q}\cdot\vec{u})\vec{q} + q_0^2\vec{u} + q_0(\vec{u}\times\vec{q}) + q_0(\vec{u}\times\vec{q}) + (\vec{u}\times\vec{q})\times\vec{q} \end{bmatrix}$$ [$\because$ $\vec{q}\ and\ (-\vec{q})\times\vec{u})$ are perpendicular to each other]

$$\Rightarrow v = \frac{1}{norm(q)}\begin{bmatrix} 0 \\ (\vec{q}\cdot\vec{u})\vec{q} + q_0^2\vec{u} + 2q_0(\vec{u}\times\vec{q}) - \vec{q}\times(\vec{u}\times\vec{q}) \end{bmatrix}$$

$$\Rightarrow v = \frac{1}{norm(q)}\begin{bmatrix} 0 \\ (\vec{q}\cdot\vec{u})\vec{q} + q_0^2\vec{u} + 2q_0(\vec{u}\times\vec{q}) - \vec{u}(\vec{q}\cdot\vec{q}) + \vec{q}(\vec{u}\cdot\vec{q}) \end{bmatrix}$$

$[\because \vec{a}\times(\vec{b}\times\vec{c}) = \vec{b}(\vec{c}.\vec{a}) - \overrightarrow{c}(\vec{a}\cdot\vec{b})]$

$$\Rightarrow v = \frac{1}{norm(q)}\begin{bmatrix} 0 \\ 2(\vec{q}\cdot\vec{u})\vec{q} + (q_0^2 - \vec{q}\cdot\vec{q})\vec{u} + 2q_0(\vec{u}\times\vec{q}) \end{bmatrix}$$

Now if q is chosen to be,

$$q = \begin{bmatrix} \cos\delta \\ \sin\delta\cos\alpha \\ \sin\delta\cos\beta \\ \sin\delta\cos\gamma \end{bmatrix} = \begin{bmatrix} \cos\delta \\ \sin\delta\,\vec{\boldsymbol{n}} \end{bmatrix}$$

$$2(\vec{q}\cdot\vec{u})\vec{q} = 2\sin^2\delta\,(\vec{n}\cdot\vec{u})\vec{n} = (1 - \cos\mu)(\vec{n}\cdot\vec{u})\vec{n}$$

$$(q_0^2 - \vec{q}\cdot\vec{q})\vec{u} = (\cos^2\delta - \sin^2\delta)\vec{u} = \cos\mu\ \vec{u}$$ (If we assume $\mu = 2\delta$)

$$2q_0(\vec{u}\times\vec{q}) = 2\sin\delta\cos\delta\,(\vec{u}\times\vec{n}) = \sin\mu\,(\vec{u}\times\vec{n})$$

The quaternion can be expressed as,

$$q = \begin{bmatrix} \cos\frac{\mu}{2} \\ \sin\frac{\mu}{2}\vec{\boldsymbol{n}} \end{bmatrix}$$

For this quaternion (where norm(q) is unity), the transformed vector becomes,

$$v = q^{-1} * u * q = \begin{bmatrix} 0 \\ (1 - \cos\mu)(\vec{n}\cdot\vec{u})\vec{n} + \cos\mu\ \vec{u} + \sin\mu\,(\vec{u}\times\vec{n}) \end{bmatrix}$$

We will define the quaternion that performs the coordinate rotation to system *b* from system *a* to be $q_{b/a}$; therefore,

$$q_{b/a} = \begin{bmatrix} \cos\frac{\mu}{2} \\ \sin\frac{\mu}{2}\vec{\boldsymbol{n}} \end{bmatrix}$$

And the co-ordinate transformation is,

$$u_b = {q_{b/a}}^{-1} * u_a * q_{b/a}$$

A few properties of this coordinate transformation using quaternions are,

- $q_{b/a} = {q_{a/b}}^{-1}$
- $q_{c/a} = q_{b/a} * q_{c/b}$

3.2.5. Quaternion Kinematic Equation:

With the goal of finding an expression for the derivative of a time-varying quaternion, and hence obtaining a state equation for spacecraft attitude, we will derive an expression for an incremental increase *q(t + δt)* from an existing state *q(t)* in response to a nonzero angular velocity vector. Following the order of Equation for multiplication of two "forward" quaternions as stated in the 2nd property of the quaternion coordinate transform, we have,

$q(t + \delta t) = q(t) * \delta q(\delta t)$, where the quaternions $q(t) = \begin{bmatrix} \cos\frac{\mu}{2} \\ \sin\frac{\mu}{2}\vec{\boldsymbol{n}} \end{bmatrix}$ and $\delta q(\delta t) = \begin{bmatrix} \cos\frac{\delta\mu}{2} \\ \sin\frac{\delta\mu}{2}\vec{\boldsymbol{n}} \end{bmatrix} \cong \begin{bmatrix} 1 \\ \frac{\delta\mu}{2}\vec{\boldsymbol{n}} \end{bmatrix}$. Hence,

$$q(t + \delta t) = \begin{bmatrix} \cos\frac{\mu}{2} \\ \sin\frac{\mu}{2}\vec{\boldsymbol{n}} \end{bmatrix} * \begin{bmatrix} 1 \\ \frac{\delta\mu}{2}\vec{\boldsymbol{n}} \end{bmatrix} = \begin{bmatrix} \cos\frac{\mu}{2} - \frac{\delta\mu}{2}\sin\frac{\mu}{2} \\ \left(\frac{\delta\mu}{2}\cos\frac{\mu}{2} + \sin\frac{\mu}{2}\right)\vec{\boldsymbol{n}} \end{bmatrix}$$

$$q(t + \delta t) - q(t) = \begin{bmatrix} \cos\frac{\mu}{2} - \frac{\delta\mu}{2}\sin\frac{\mu}{2} \\ \left(\frac{\delta\mu}{2}\cos\frac{\mu}{2} + \sin\frac{\mu}{2}\right)\vec{\boldsymbol{n}} \end{bmatrix} - \begin{bmatrix} \cos\frac{\mu}{2} \\ \sin\frac{\mu}{2}\vec{\boldsymbol{n}} \end{bmatrix} = \begin{bmatrix} -\frac{\delta\mu}{2}\sin\frac{\mu}{2} \\ \frac{\delta\mu}{2}\cos\frac{\mu}{2}\vec{\boldsymbol{n}} \end{bmatrix}$$

$$q(t) * \begin{bmatrix} 0 \\ \frac{\delta\mu}{2}\vec{\boldsymbol{n}} \end{bmatrix} = \begin{bmatrix} \cos\frac{\mu}{2} \\ \sin\frac{\mu}{2}\vec{\boldsymbol{n}} \end{bmatrix} * \begin{bmatrix} 0 \\ \frac{\delta\mu}{2}\vec{\boldsymbol{n}} \end{bmatrix} = \begin{bmatrix} -\frac{\delta\mu}{2}\sin\frac{\mu}{2} \\ \frac{\delta\mu}{2}\cos\frac{\mu}{2}\vec{\boldsymbol{n}} \end{bmatrix}$$

so, $q(t+\delta t) - q(t) = q(t) * \begin{bmatrix} 0 \\ \frac{\delta\mu}{2}\vec{\boldsymbol{n}} \end{bmatrix}$

Now, the differentiation of q(t) is

$$\frac{dq}{dt} = \lim_{\delta t \to 0} \frac{q(t+\delta t) - q(t)}{\delta t} = \frac{q(t) * \begin{bmatrix} 0 \\ \frac{\delta\mu}{2}\vec{\boldsymbol{n}} \end{bmatrix}}{\delta t} = \frac{1}{2} q(t) * \begin{bmatrix} 0 \\ \frac{\delta\mu}{\delta t}\vec{\boldsymbol{n}} \end{bmatrix}$$

$$\Rightarrow \dot{q} = \frac{1}{2} q(t) * \begin{bmatrix} 0 \\ \vec{\boldsymbol{\omega}} \end{bmatrix}$$

$$\Rightarrow \begin{bmatrix} \dot{q}_0 \\ \dot{q}_v \end{bmatrix} = \frac{1}{2} \begin{bmatrix} q_0 \\ \overrightarrow{\boldsymbol{q_v}} \end{bmatrix} * \begin{bmatrix} 0 \\ \vec{\boldsymbol{\omega}} \end{bmatrix}$$

$$\Rightarrow \begin{bmatrix} \dot{q}_0 \\ \dot{q}_v \end{bmatrix} = \frac{1}{2} \begin{bmatrix} -\overrightarrow{\boldsymbol{q_v}} \cdot \vec{\boldsymbol{\omega}} \\ q_0\vec{\boldsymbol{\omega}} + \overrightarrow{\boldsymbol{q_v}} \times \vec{\boldsymbol{\omega}} \end{bmatrix} \quad \ldots (1)$$

This relation is in vector form. For deriving the state space model of attitude dynamics, we need to convert this in matrix from completely. In matrix form dot product of 2 vectors can be substituted by transposed product of the vectors. In case of cross product of 2 vectors, the pre-multiplier can be expressed as an equivalent square matrix to make the matrix product feasible. For an example, if a vector $m = [m_1\ m_2\ m_3]^T$, then the corresponding cross multiplication equivalent will be,

$$m^{\times} = \begin{bmatrix} 0 & -m_3 & m_2 \\ m_3 & 0 & -m_1 \\ -m_2 & m_1 & 0 \end{bmatrix}$$

Equation (1) can be expressed as 2 equations in matrix form,

$$\boldsymbol{\dot{q}_0 = -\frac{1}{2} q_v^T \omega}$$

$$\boldsymbol{\dot{q}_v = \frac{1}{2}(q_0 I_{3\times 3} + q_v^{\times})\omega} \quad (a)$$

This is the quaternion kinematic equation.

3.2.6. Quaternion Dynamic Equation:

The dynamic equation of a rigid body does not involve any quaternion. It is same as the one derived in Euler angle-based attitude dynamics model, sent previously. So, without derivation the matrix equation is used here.

$$\boxed{\dot{\boldsymbol{\omega}} = \boldsymbol{I}^{-1}(-\boldsymbol{\omega}^{\times}\boldsymbol{I}\boldsymbol{\omega} + \boldsymbol{\tau}(\boldsymbol{t}) + \boldsymbol{d}(\boldsymbol{t}))} \quad \text{(b)}$$

There 7 differential equations, considering (a) and (b). Although for a 3-DoF attitude dynamics there should be 6 states, hence 6 differential equations. That happens because we have used unit quaternion and all 4 entries of a unit quaternion are not independent of each other. This mutual dependence increases the number of differential equations. Their mutual dependance is expressed by the equation,

$$q_0^2 + q_v^T q_v = 1$$

3.3. Derivation of Error Quaternion Based Mathematical Model:

Previously we have found out (conversion from vector form to matrix from),

$$v = \begin{bmatrix} 0 \\ 2(\vec{q}\cdot\vec{u})\vec{q} + (q_0^2 - \vec{q}\cdot\vec{q})\vec{u} + 2q_0(\vec{u}\times\vec{q}) \end{bmatrix}$$

(Where q is unit quaternion and v is the vector, we get after rotating u with q)

$$(1)\quad 2(\vec{q}\cdot\vec{u})\vec{q} = 2(q_1u_1 + q_2v_2 + q_3v_3)\begin{bmatrix} q_1 \\ q_2 \\ q_3 \end{bmatrix}$$

$$\Rightarrow 2(\vec{q}\cdot\vec{u})\vec{q} = 2\begin{bmatrix} q_1^2u_1 + q_1q_2u_2 + q_1q_3u_3 \\ q_1q_2u_1 + q_2^2u_2 + q_2q_3u_3 \\ q_1q_3u_1 + q_2q_3u_2 + q_3^2u_3 \end{bmatrix}$$

$$\Rightarrow 2(\vec{q}\cdot\vec{u})\vec{q} = 2\begin{bmatrix} q_1^2 & q_1q_2 & q_1q_3 \\ q_1q_2 & q_2^2 & q_2q_3 \\ q_1q_3 & q_2q_3 & q_3^2 \end{bmatrix}\begin{bmatrix} u_1 \\ u_2 \\ u_3 \end{bmatrix}$$

$$\Rightarrow 2(\vec{q}\cdot\vec{u})\vec{q} = 2(qq^T)u$$

(2) $(q_0^2 - \vec{q}\cdot\vec{q})\vec{u} = (q_0^2 - q^Tq)u$

(3) $2q_0(\vec{u}\times\vec{q}) = 2q_0\begin{bmatrix} u_2q_3 - u_3q_2 \\ u_3q_1 - u_1q_3 \\ u_1q_2 - u_2q_1 \end{bmatrix}$

$$\Rightarrow 2q_0(\vec{u}\times\vec{q}) = 2\begin{bmatrix} u_2q_0q_3 - u_3q_0q_2 \\ u_3q_0q_1 - u_1q_0q_3 \\ u_1q_0q_2 - u_2q_0q_1 \end{bmatrix}$$

$$\Rightarrow 2q_0(\vec{u}\times\vec{q}) = 2\begin{bmatrix} 0 & q_0q_3 & -q_0q_2 \\ -q_0q_3 & 0 & q_0q_1 \\ q_0q_2 & -q_0q_1 & 0 \end{bmatrix}\begin{bmatrix} u_1 \\ u_2 \\ u_3 \end{bmatrix}$$

$$\Rightarrow 2q_0(\vec{u}\times\vec{q}) = 2q_0\begin{bmatrix} 0 & q_3 & -q_2 \\ -q_3 & 0 & q_1 \\ q_2 & -q_1 & 0 \end{bmatrix}\begin{bmatrix} u_1 \\ u_2 \\ u_3 \end{bmatrix}$$

$$\Rightarrow 2q_0(\vec{u}\times\vec{q}) = 2q_0(-q^\times)u = -2q_0q^\times u$$

So, the rotation of a vector $\vec{u}$ with the quaternion q gives us (in matrix form),

$$v = 2(\vec{q}\cdot\vec{u})\vec{q} + (q_0^2 - \vec{q}\cdot\vec{q})\vec{u} + 2q_0(\vec{u}\times\vec{q})$$
$$= 2(qq^T)u + (q_0^2 - q^Tq)u - 2q_0q^\times u$$

$$\Rightarrow v = [2(qq^T) + (q_0^2 - q^Tq)I - 2q_0q^\times]u = Cu$$

Where $C = [2(qq^T) + (q_0^2 - q^Tq)I - 2q_0q^\times]$ which Is the rotation cosine matrix. This formula can be used to interconvert rotation cosine matrix from quaternion.

Coming to error quaternion dynamics calculation, say the desired quaternion is q_d and the actual quaternion is q. We define the error quaternion to be q_e. Now, quaternion gives us the unit vector along the direction of rotation and the cosine of the angle of rotation. If our quaternion is not our desired quaternion, then we can perform another rotation along the error rotation axis $\overrightarrow{q_{ev}}$ with an angle of $\cos^{-1}(q_{e0})$, which can be described by the error quaternion at once. This composite rotation gives us,

$$q = q_d * q_e$$

$$q_e = {q_d}^{-1} * q$$

$$\begin{bmatrix} q_{e0} \\ q_{ev} \end{bmatrix} = \begin{bmatrix} q_{d0} \\ -q_{dv} \end{bmatrix} * \begin{bmatrix} q_0 \\ q_v \end{bmatrix}$$

Which gives us,

$$q_{e0} = q_{d0}q_0 + {q_{dv}}^T q_v$$

$$q_{ev} = q_{d0}q_v - q_0 q_{dv} - {q_{dv}}^{\times} q_v$$

As angular velocity vector is always expressed with reference to the rotating frame, before finding out error angular velocity vector, we have to use the rotational matrix C. The relation is as shown below,

$$\omega_e = \omega - C\omega_d$$

Where $C = 2\left(q_{ev}{q^T}_{ev}\right) + \left(q_{e0}^2 - {q^T}_e q_e\right)I - 2q_{e0}{q^{\times}}_{ev}$ (because the rotational matrix relating the desired frame and actual frame is the error rotation matrix, hence error quaternion is used.) and $\dot{C} = -\omega_e^{\times} C$ from basic property of rotational matrices.

Differentiating the above equation w.r.t. time,

$$\dot{\omega_e} = \dot{\omega} - \dot{C}\omega_d - C\dot{\omega_d}$$

$$\Rightarrow \dot{\omega_e} = I^{-1}(-\omega^{\times} I\omega + \tau(t) + d(t)) - (-\omega_e^{\times} C)\omega_d - C\dot{\omega_d}$$

$$\Rightarrow \dot{\omega_e} = I^{-1}\left(-(\omega_e + C\omega_d)^{\times} I(\omega_e + C\omega_d) + \tau(t) + d(t)\right) + \omega_e^{\times} C\omega_d - C\dot{\omega_d}$$

$$\Rightarrow \dot{\omega_e} = I^{-1}[\left(-(\omega_e + C\omega_d)^{\times} I(\omega_e + C\omega_d) + \tau(t) + d(t)\right) + I(\omega_e^{\times} C\omega_d - C\dot{\omega_d})]$$

Using these equations, we can state the error dynamics to be,

$$\dot{\boldsymbol{q_{e0}}} = -\frac{1}{2}\boldsymbol{q_{ev}^T \omega_e}$$

$$\dot{\boldsymbol{q_{ev}}} = \frac{1}{2}(\boldsymbol{q_{e0} I_{3\times 3} + q_{ev}^{\times}})\boldsymbol{\omega_e}$$

$$\dot{\boldsymbol{\omega_e}} = \boldsymbol{I^{-1}}[\left(-(\boldsymbol{\omega_e + C\omega_d})^{\times} \boldsymbol{I(\omega_e + C\omega_d)} + \boldsymbol{\tau(t)} + \boldsymbol{d(t)}\right) + \boldsymbol{I(\omega_e^{\times} C\omega_d - C\dot{\omega_d})}]$$

CHAPTER 4: Simulation Summary

4.1. Assumptions of model:

To investigate the proposed mathematical models and their performance with and without controllers, a microsatellite is assumed with following data from [34].

Inertia matrix $= \begin{bmatrix} 19.4 & 0.1 & 3.0 \\ 0.1 & 25.7 & 0.5 \\ 3.0 & 0.5 & 18.4 \end{bmatrix}$ kg-m^2

Disturbance signal $= 0.01 \begin{bmatrix} \sin(0.1t) \\ \sin(0.2t) \\ \sin(0.3t) \end{bmatrix}$ N-m

3 Simulink models are prepared based on the three mathematical models derived in this thesis work. First their Open Loop behaviour is tested against different kind of input signals.

4.2. Open Loop Response of the System (Euler-angle based model):

As it should be clear from the different models derived the system takes a torque vector $\vec{\tau} = \overrightarrow{\tau_x} + \overrightarrow{\tau_y} + \overrightarrow{\tau_z}$ w.r.t. its Body Frame as its input which comes from its ACS actuator. Different disturbance signal, which are basically unwanted torque of small magnitude coming from sources like earth's stray magnetism, gravity gradient, Solar Radiation Pressure (SRP), aerodynamic drag (especially in LEO) or misalignment in the reaction wheels, are also present, although results with and without disturbance will be shown in Open Loop Response. And the Output of the system is its Euler angles/ quaternion/ error quaternion depending on the model, as it is an attitude control problem. However, the angular velocity dynamics will also be studied.

Case 1:

Input $\vec{\tau} = 0\hat{\boldsymbol{\imath}} + u(t-1)\,\hat{\boldsymbol{\jmath}} + 0\hat{\boldsymbol{k}}$

Or a torque is applied on the system whose only non-zero component is along y axis, which is by magnitude a unit step function (with unit delay).

The system behaviour is shown below.

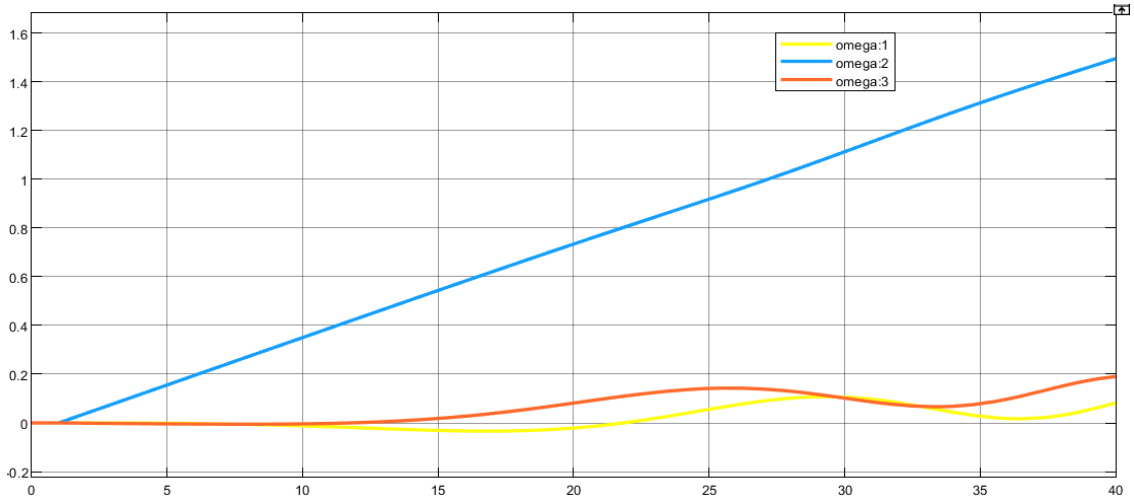

Fig 4: Angular velocity of satellite for unidirectional step input

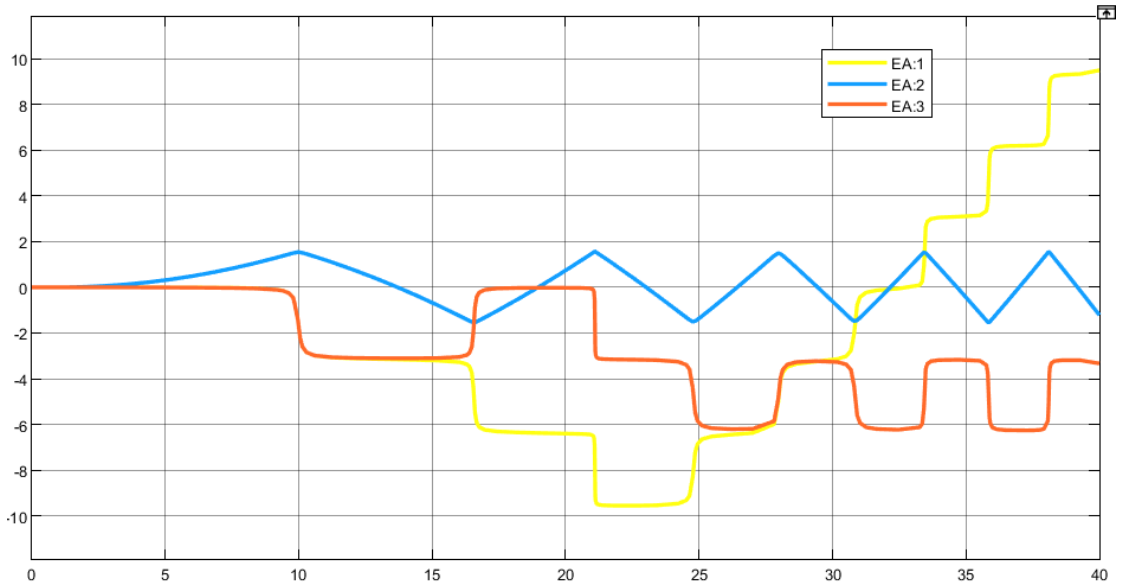

Fig 5: Euler Angles of satellite for unidirectional step input

4.2.1. Concept of Inertial Coupling:

Although the torque is provided in only one direction, it can be seen that the satellite gains angular velocity in all direction, which seems very counter-intuitive. This happens because of the inertial coupling between the axes of the satellite. If we observe the inertia matrix of the satellite, it has non zero $I_{xy}, I_{yz}\ and\ I_{zx}$ terms. This suggests that the satellite body is not symmetric along either of the xy, yz and zx plane. That is why even if torque is applied in only direction, the kinetic energy gets transferred along other axes as well.

To prove this, let us assume another satellite of similar kind, which is symmetric across the xy, yz and zx plane, hence have zero $I_{xy}, I_{yz}\ and\ I_{zx}$ terms, making their inertia matrix diagonal.

In this case the inertia matrix is taken as,

$$\text{Inertia matrix} = \begin{bmatrix} 19.4 & 0 & 0 \\ 0 & 25.7 & 0 \\ 0 & 0 & 18.4 \end{bmatrix} \text{kg-m}^2$$

Same input is provided and the result is shown.

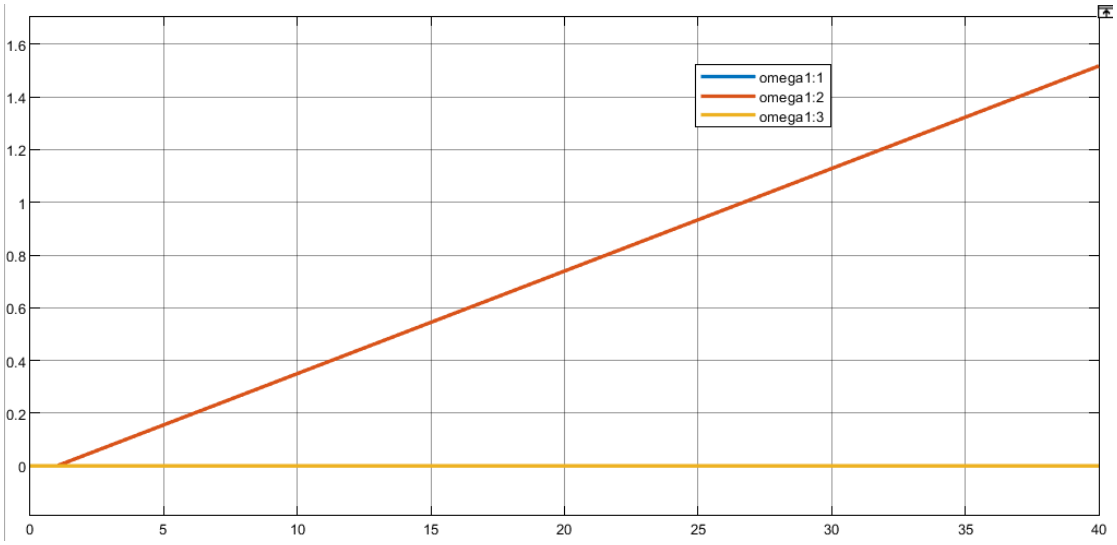

Fig 6: Angular Velocity of symmetric satellite for unidirectional step input

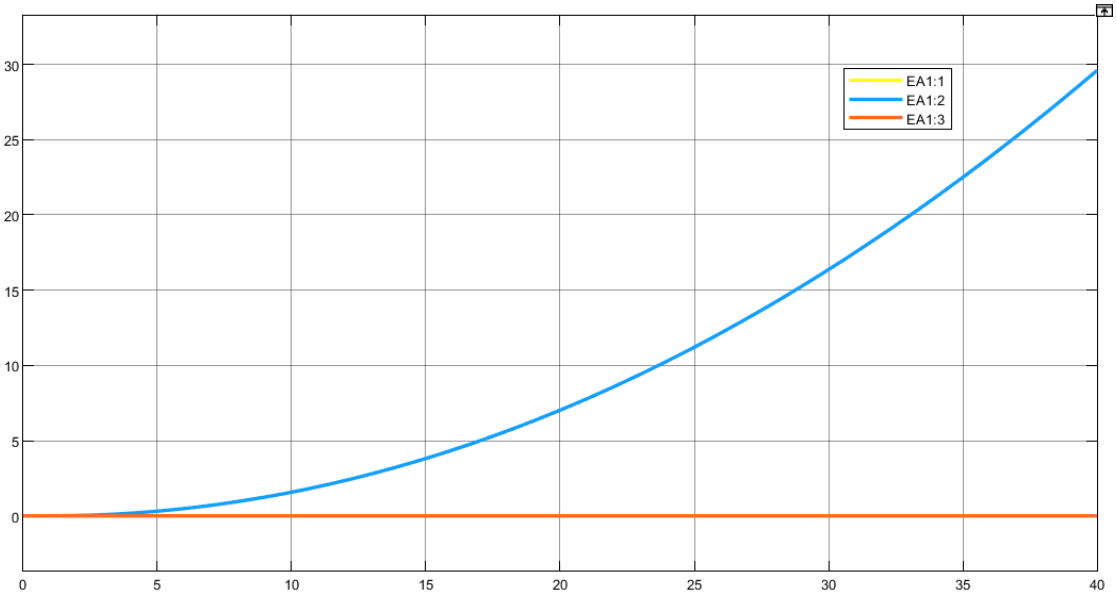

Fig 7: Euler Angles of symmetric satellite for unidirectional step input

In this case, the angular velocity of only y axis increases as a ramp signal for step input along y axis, which is exactly what we expect. Hence, only one Euler angle (pitch angle) gets increase parabolically.

Case 2:

Input $\vec{\tau} = u(t-1)\hat{\boldsymbol{\imath}} + u(t-1)\,\hat{\boldsymbol{\jmath}} + u(t-1)\hat{\boldsymbol{k}}$

If step signal is applied along all direction, the response of the systems comes out as below.

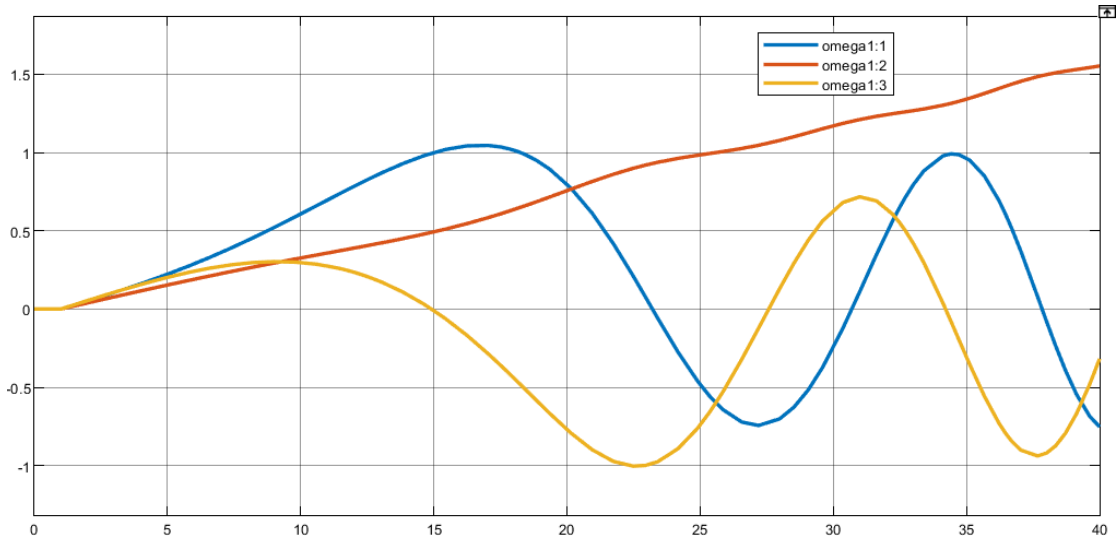

Fig 8: Angular Velocity of Satellite with Diagonal Inertia Matrix for Step Input

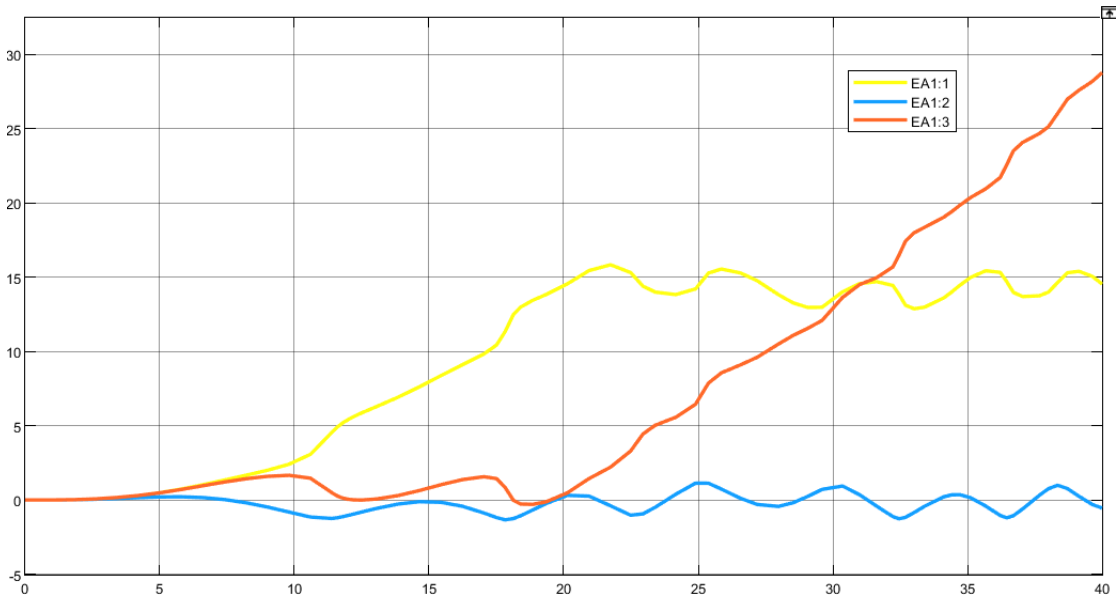

Fig 9: Euler Angle of Satellite with Diagonal Inertia Matrix for Step Input

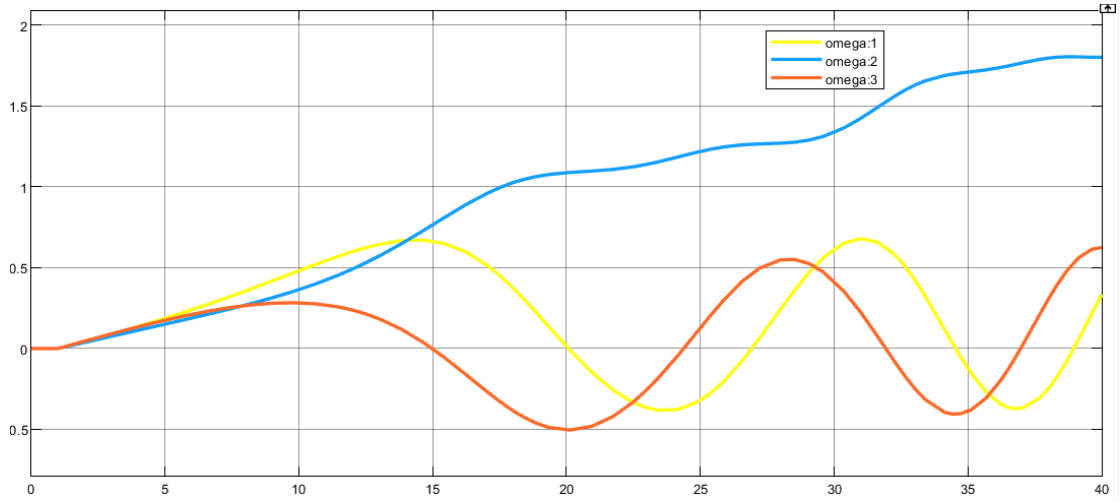

Fig 10: Angular Velocity of Satellite with Non-Diagonal Inertia Matrix for Step Input

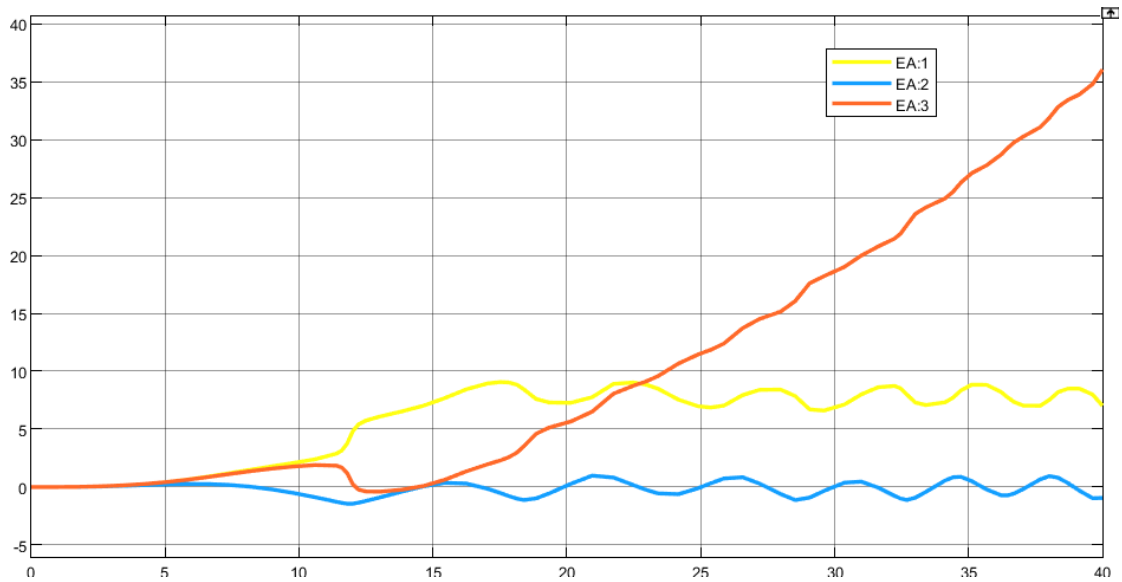

Fig 11: Euler Angle of Satellite with Non-Diagonal Inertia Matrix for Step Input

Observation:

It can be observed that the system is inherently unstable, which could have been predicted as there is no damping element.

Case 3:

Pulse input $\vec{\tau} = P(t)(\hat{\boldsymbol{\imath}} + \hat{\boldsymbol{\jmath}} + \hat{\boldsymbol{k}})$, where $P(t) = 20[u(t) - u(t-1)]$

The response of the system is shown below,

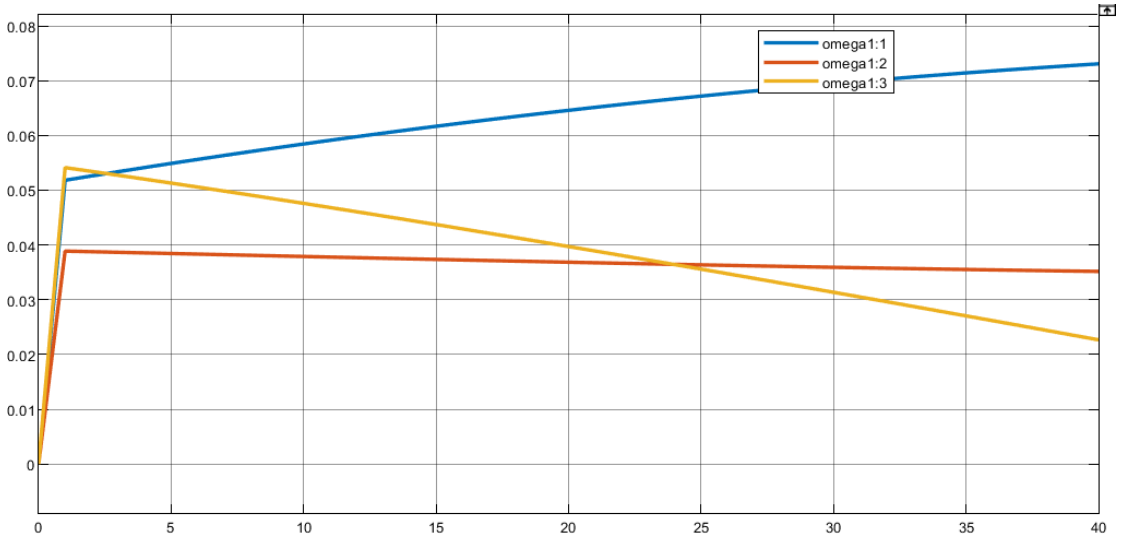

Fig 12: Angular Velocity of Satellite with Diagonal Inertia Matrix for Pulse Input

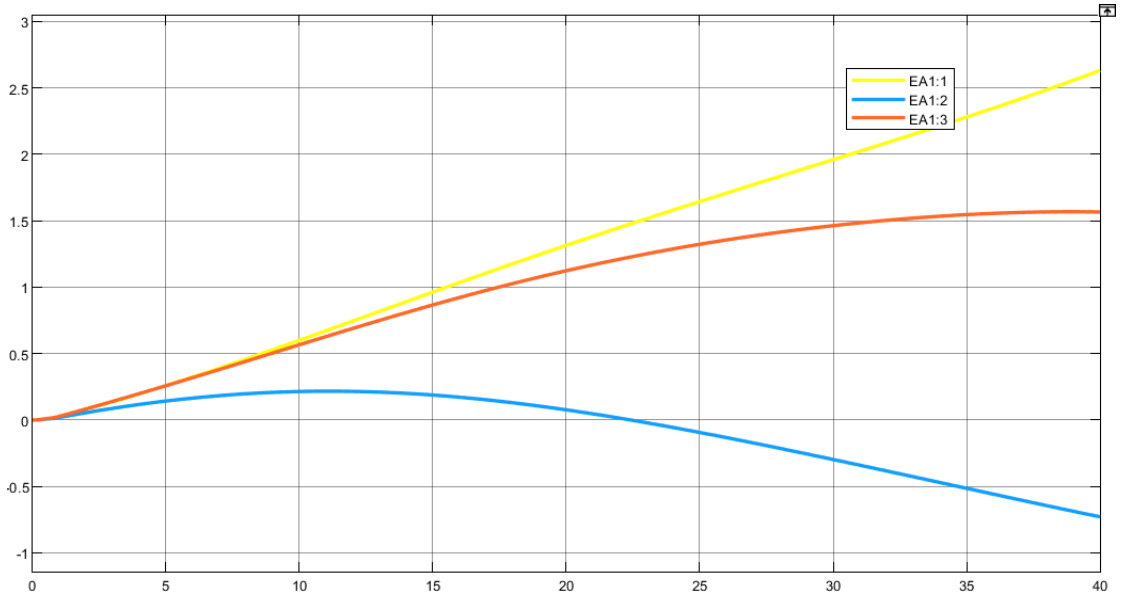

Fig 13: Euler Angle of Satellite with Diagonal Inertia Matrix for Pulse Input

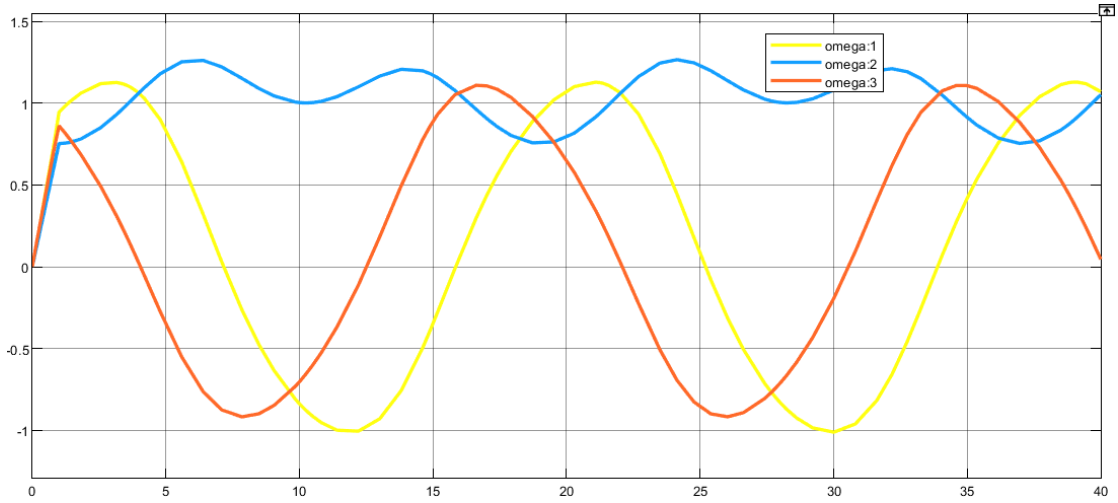

Fig 14: Angular Velocity of Satellite with Non-Diagonal Inertia Matrix for Pulse Input

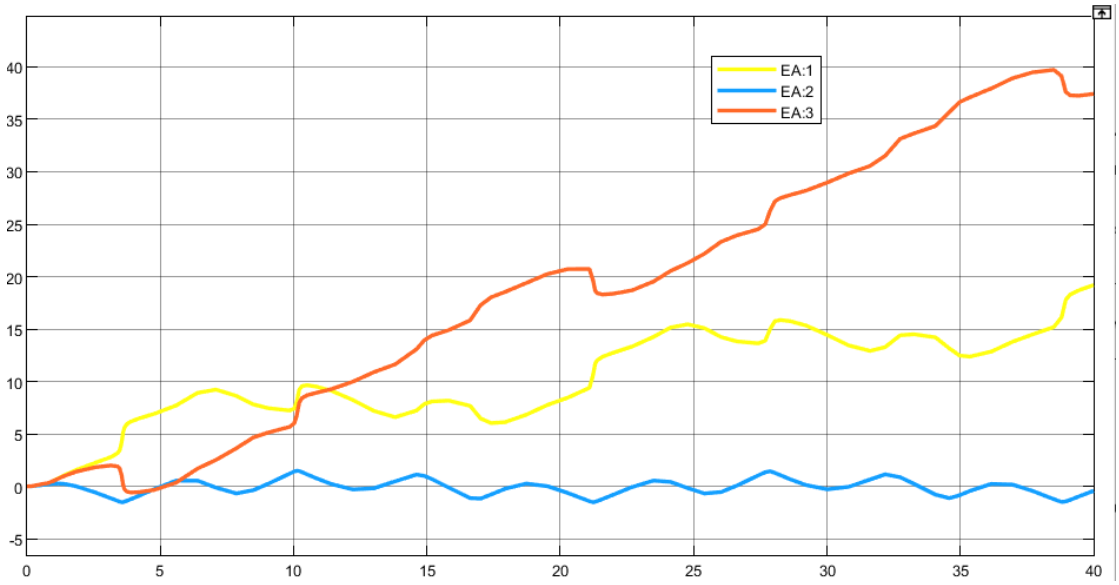

Fig 15: Euler Angle of Satellite with Non-Diagonal Inertia Matrix for Pulse Input

Observation:

From the response shown by both the satellites (diagonal and non-diagonal), it can be understood from the angular velocity graph that the satellites gain kinetic energy till 1 sec as the energy was being supplied to the system by external torque and after that the kinetic energy remains same for absence of any damping/non-conservative force.

Case 4:

Doublet pulse input $\vec{\tau} = D(t)(\hat{\boldsymbol{\imath}} + \hat{\boldsymbol{\jmath}} + \hat{\boldsymbol{k}})$,

where $D(t) = [u(t) - u(t-1)] - [u(t-1) - u(t-2)]$

Doublet is a well-known signal in control engineering, consisting of 2 successive pulses of opposite magnitude, which can emulate the characteristics of Bang Bang Control. System response is shown below.

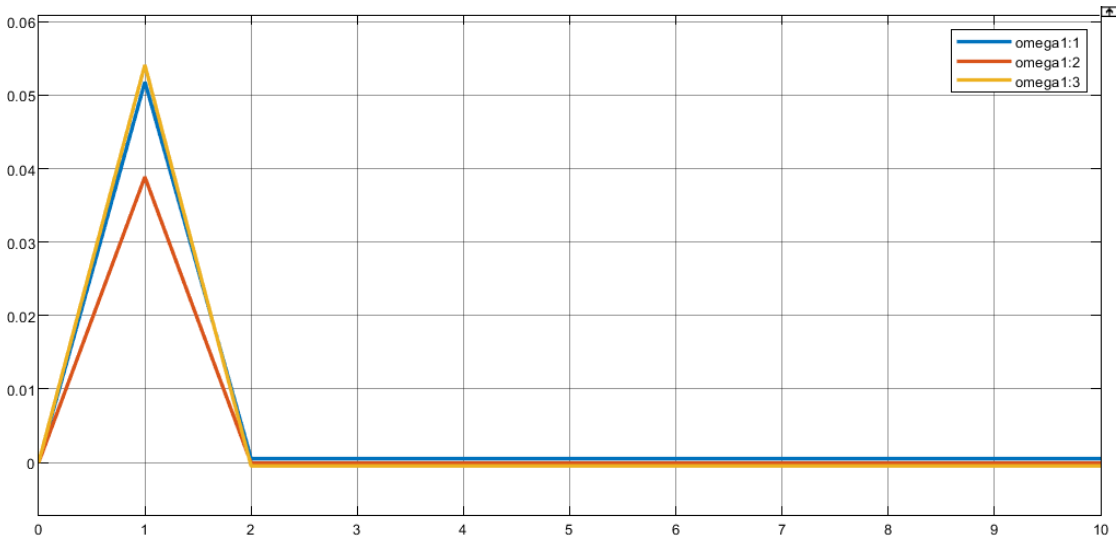

Fig 16: Angular Velocity of Satellite with Diagonal Inertia Matrix for Doublet Input

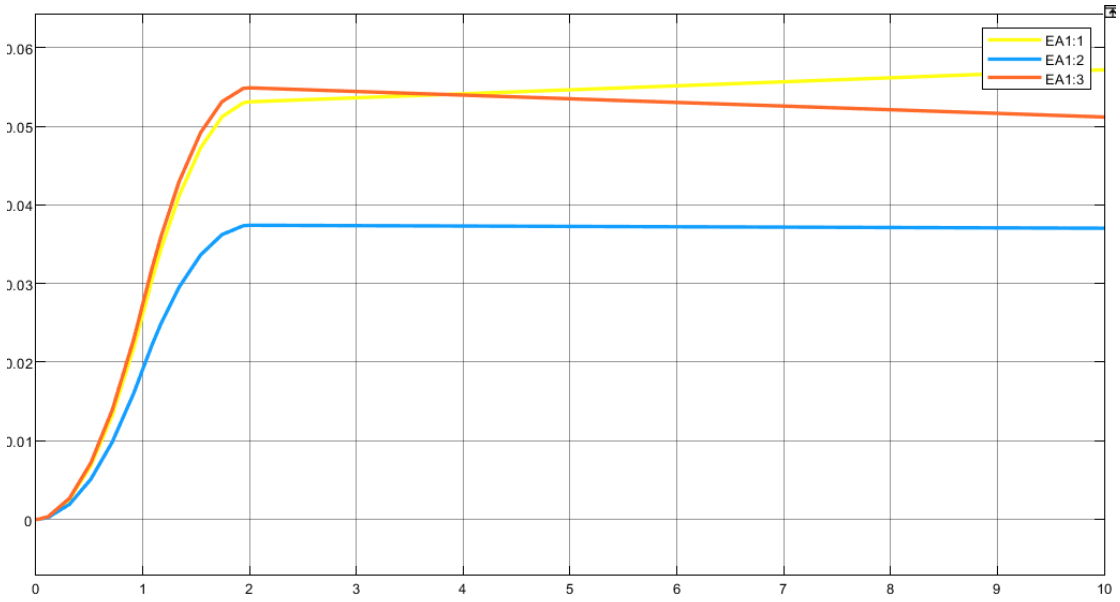

Fig 17: Euler Angle of Satellite with Diagonal Inertia Matrix for Doublet Input

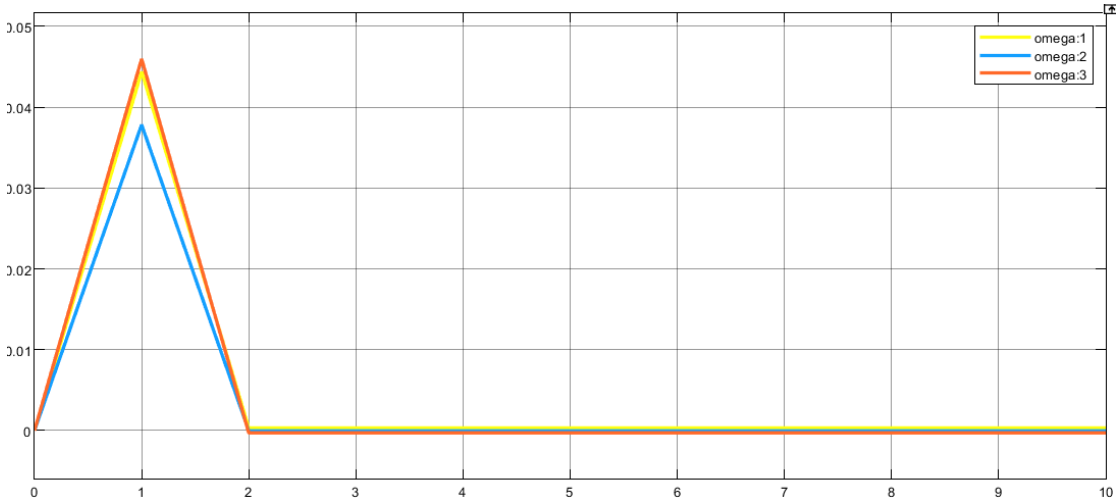

Fig 18: Angular Velocity of Satellite with Non-Diagonal Inertia Matrix for Doublet Input

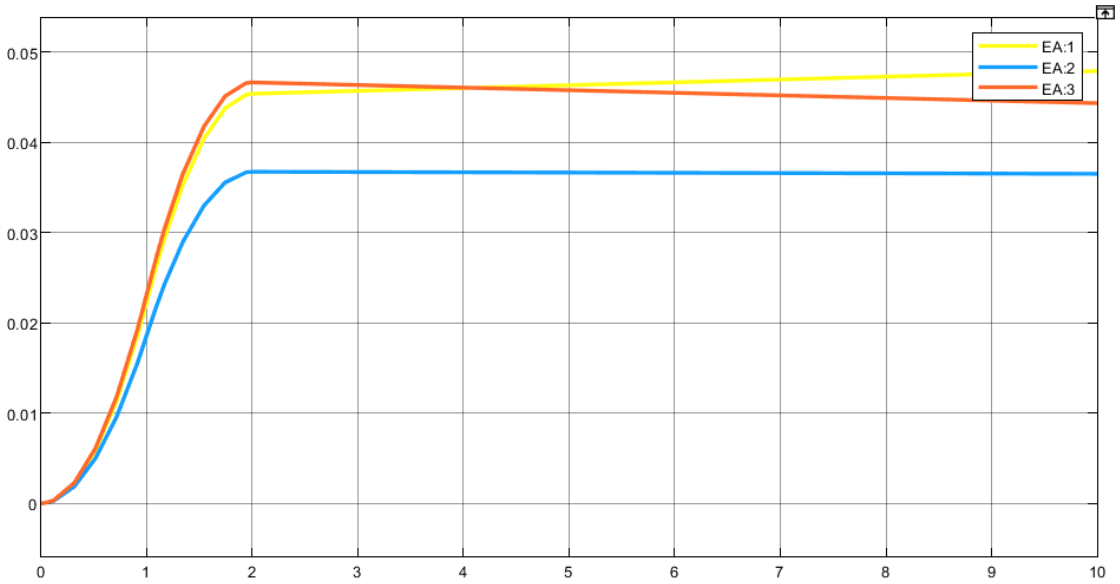

Fig 19: Euler Angle of Satellite with Non-Diagonal Inertia Matrix for Doublet Input

Observation:

A doublet signal is two successive pulses with opposite magnitude, so the system is given kinetic energy for first 1 sec and the next second the applied torque performs negative work done. Hence, the total energy of the system comes nearly to zero for both satellites. It can be confirmed from the angular velocity graph, as all components of angular velocity becomes nearly zero.

But the total kinetic energy cannot be diminished completely in this way as work done $= \int \vec{\tau} \cdot \vec{\omega}\, dt$, and the $\vec{\omega}$ profile is different for 1st and 2nd seconds, making the magnitude of positive and negative work done unequal.

4.2.2 Effect of Disturbance:

Now the effect of introducing disturbance to the system will be shown and discussed for the above cases.

Case 1:

System response without any input.

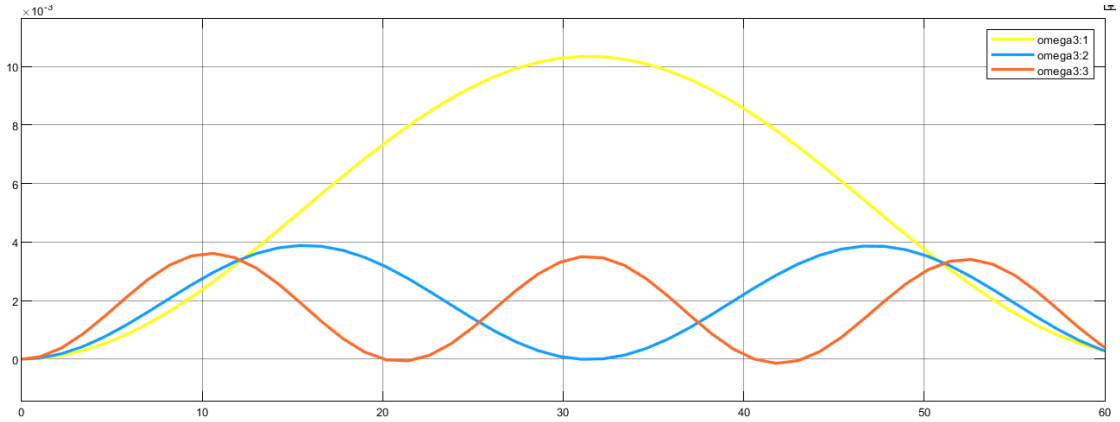

Fig 20: Angular Velocity of Satellite with Diagonal Inertia Matrix for With Disturbance and Without Input

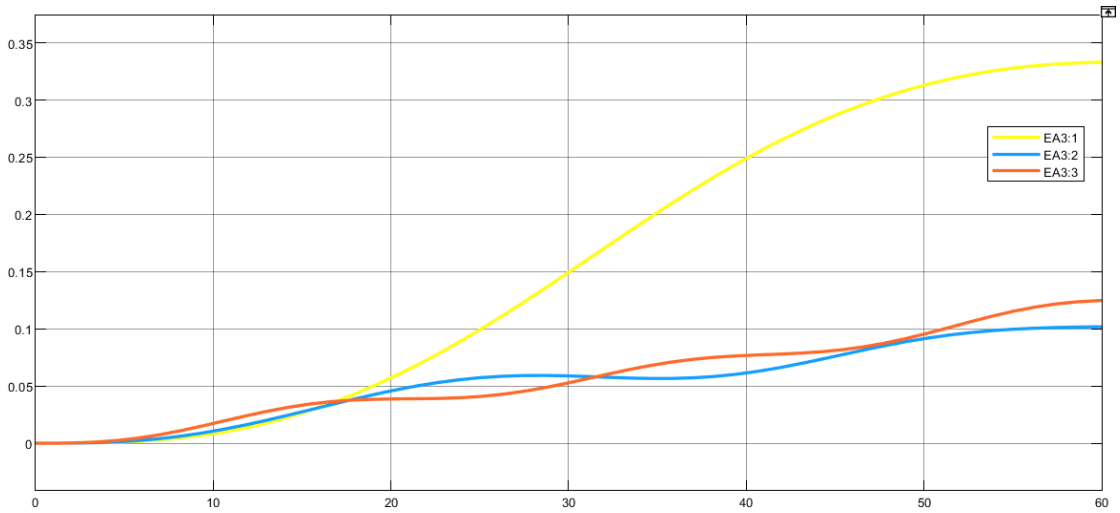

Fig 21: Euler Angle of Satellite with Diagonal Inertia Matrix for With Disturbance and Without Input

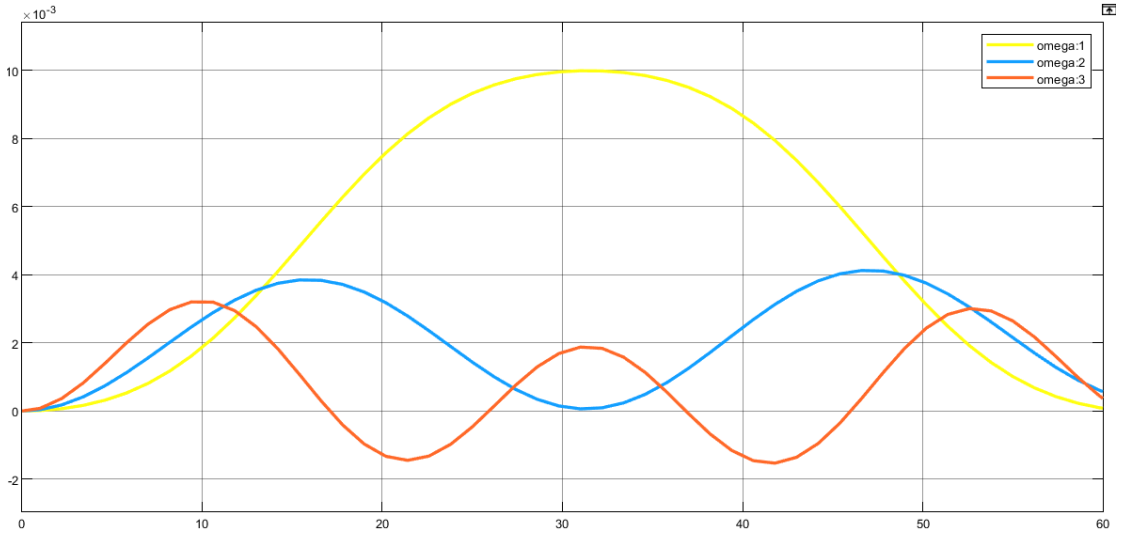

Fig 22: Angular Velocity of Satellite with Non-Diagonal Inertia Matrix for With Disturbance and Without Input

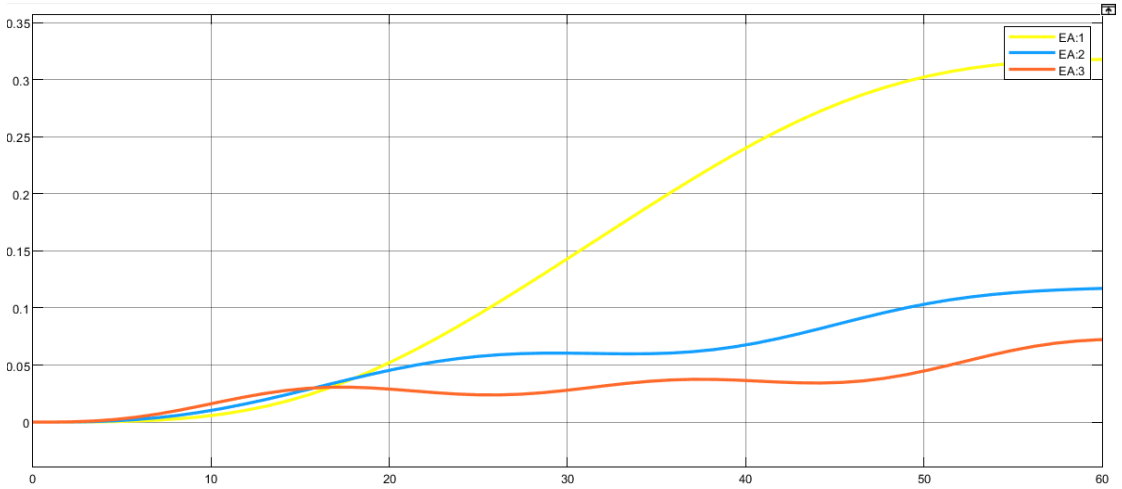

Fig 23: Euler Angle of Satellite with Non-Diagonal Inertia Matrix for With Disturbance and Without Input

Case 2:

System response for step input.

$$\vec{\tau} = u(t-1)\hat{\boldsymbol{\imath}} + u(t-1)\,\hat{\boldsymbol{\jmath}} + u(t-1)\hat{\boldsymbol{k}}$$

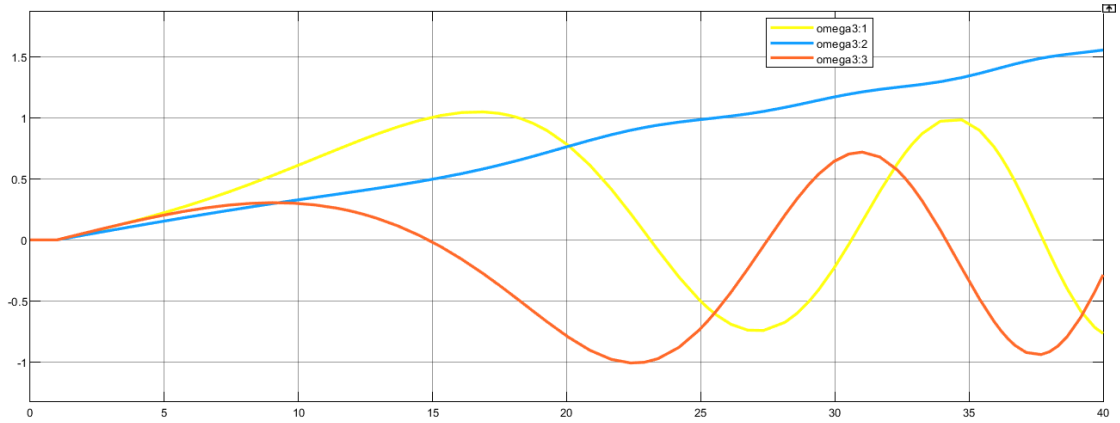

Fig 24: Angular Velocity of Satellite with Diagonal Inertia Matrix for With Disturbance and Step Input

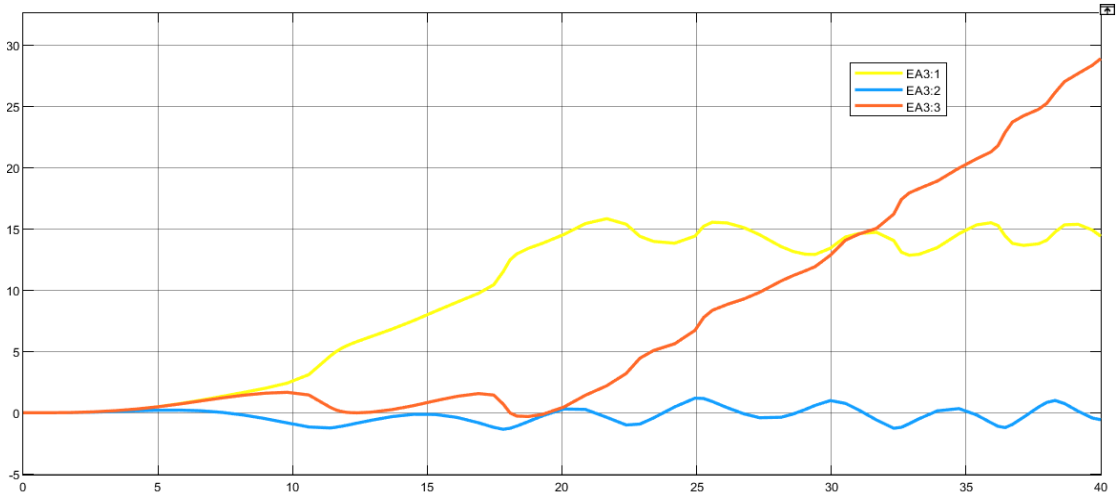

Fig 25: Euler Angle of Satellite with Diagonal Inertia Matrix for With Disturbance and Step Input

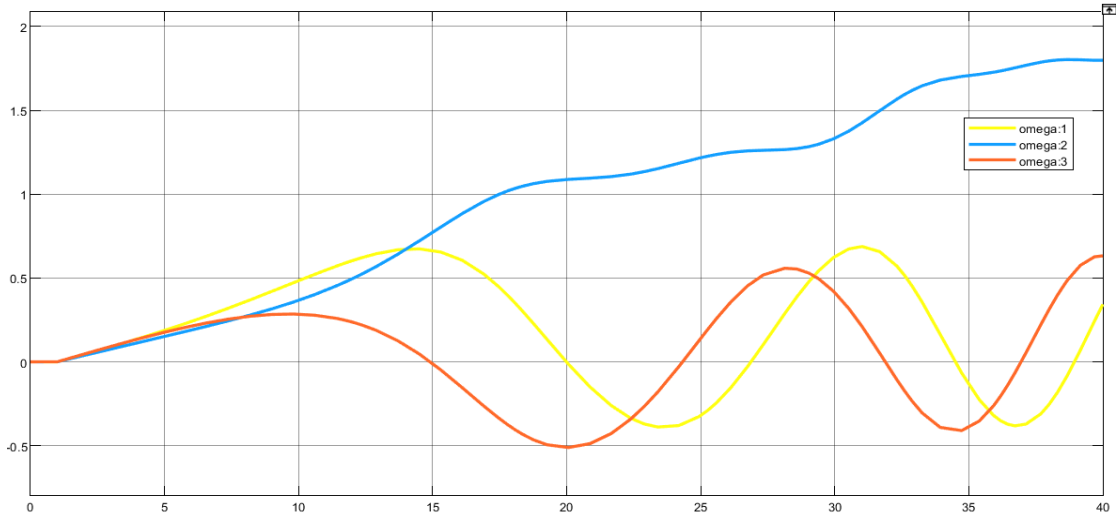

Fig 26: Angular Velocity of Satellite with Non-Diagonal Inertia Matrix for With Disturbance and Step Input

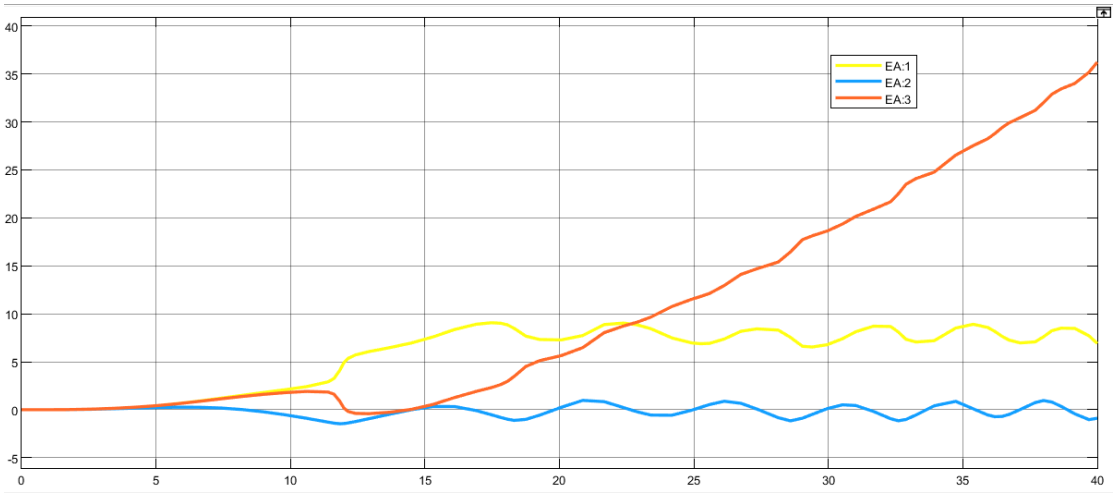

Fig 27: Euler Angle of Satellite with Non-Diagonal Inertia Matrix for With Disturbance and Step Input

Case 3:

Pulse input $\vec{\tau} = P(t)(\hat{\boldsymbol{\imath}} + \hat{\boldsymbol{\jmath}} + \hat{\boldsymbol{k}})$, where $P(t) = 20[u(t) - u(t-1)]$

The response of the system is shown below,

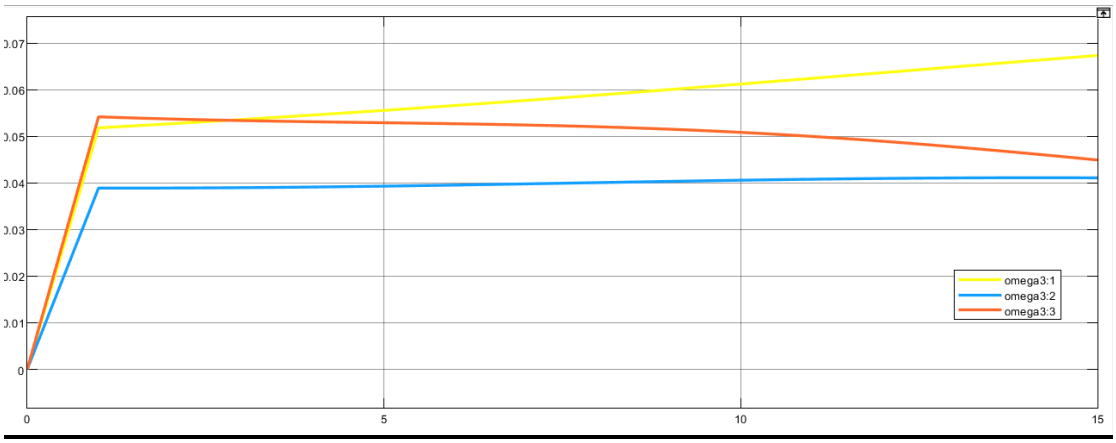

Fig 28: Angular Velocity of Satellite with Diagonal Inertia Matrix for With Disturbance and Pulse Input

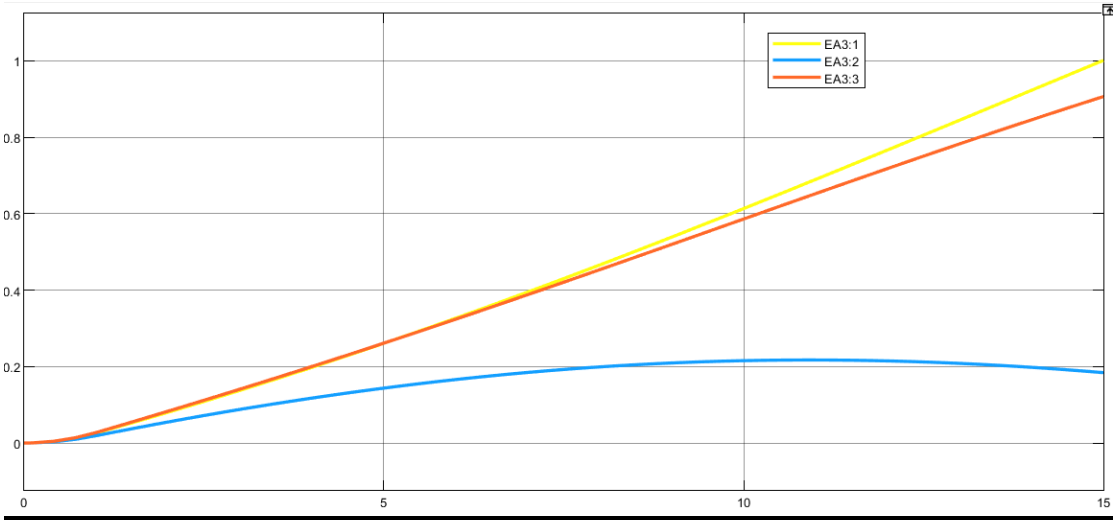

Fig 29: Euler Angle of Satellite with Diagonal Inertia Matrix for With Disturbance and Pulse Input

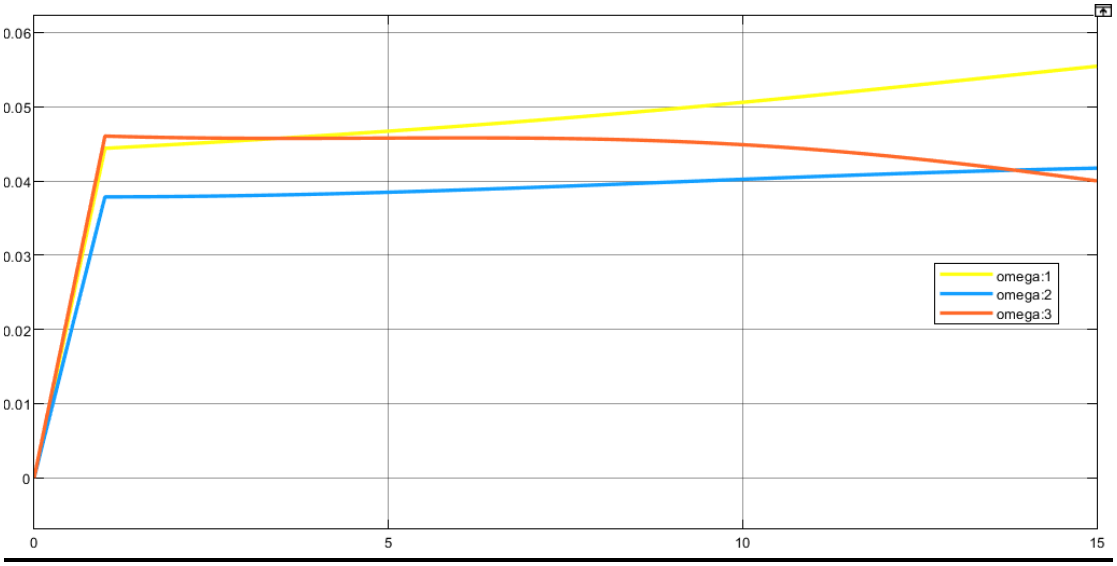

Fig 30: Angular Velocity of Satellite with Non-Diagonal Inertia Matrix for With Disturbance and Pulse Input

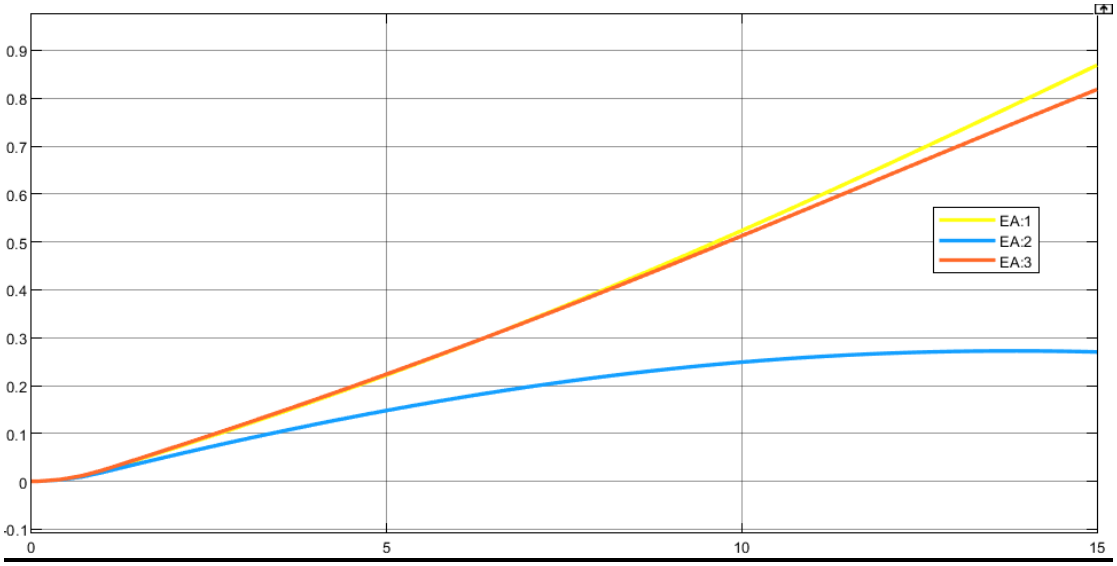

Fig 31: Euler Angle of Satellite with Non-Diagonal Inertia Matrix for With Disturbance and Pulse Input

Case 4:

Doublet pulse input $\vec{\tau} = D(t)(\hat{\boldsymbol{\imath}} + \hat{\boldsymbol{\jmath}} + \hat{\boldsymbol{k}})$,

where $D(t) = [u(t) - u(t-1)] - [u(t-1) - u(t-2)]$

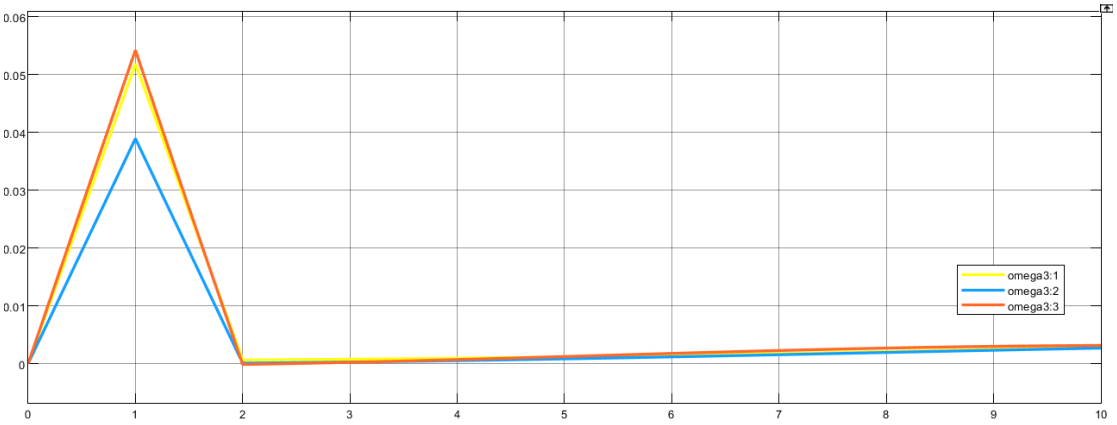

Fig 32: Angular Velocity of Satellite with Diagonal Inertia Matrix for With Disturbance and Doublet Input

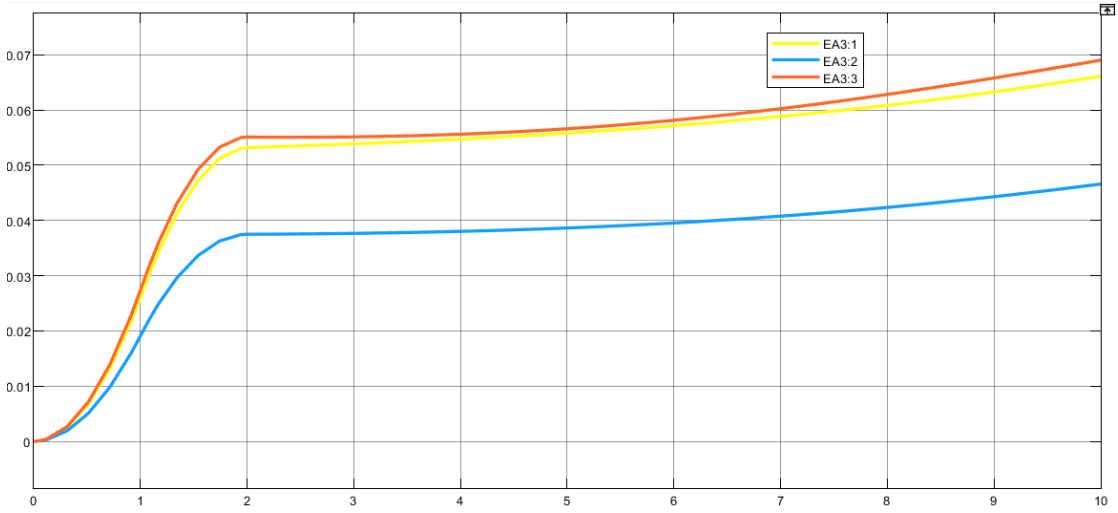

Fig 33: Euler Angle of Satellite with Diagonal Inertia Matrix for With Disturbance and Doublet Input

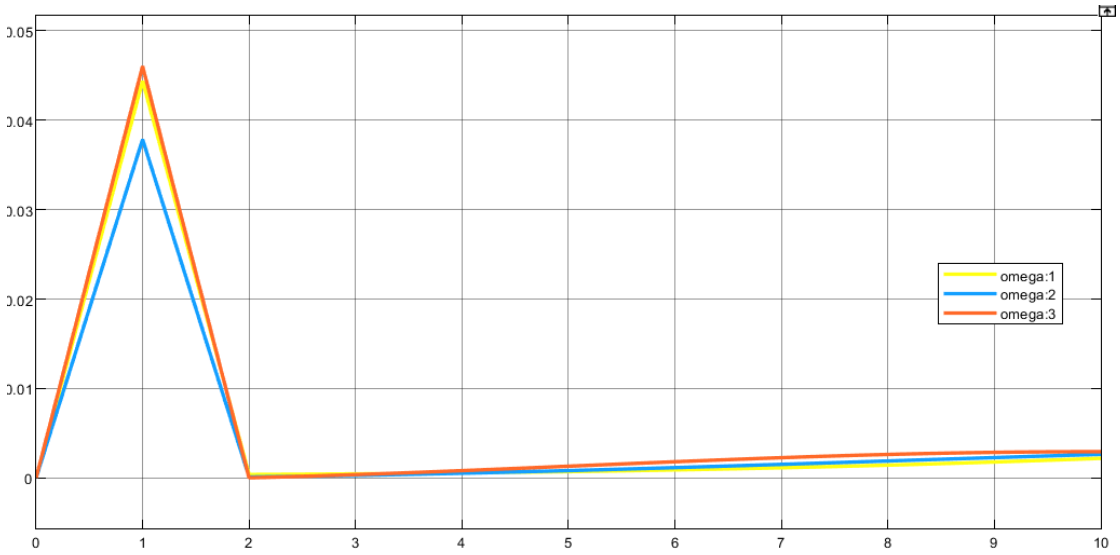

Fig 34: Angular Velocity of Satellite with Non-Diagonal Inertia Matrix for With Disturbance and Doublet Input

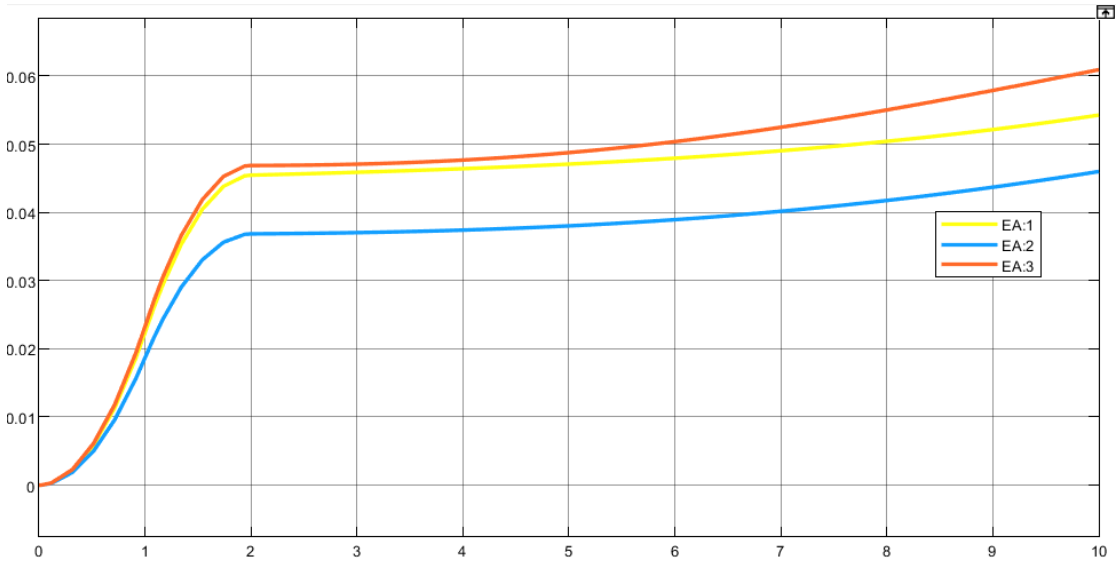

Fig 35: Euler Angle of Satellite with Non-Diagonal Inertia Matrix for With Disturbance and Doublet Input

Observation:

The major observation from the open loop response and the response after introducing disturbance is that the output in both angular velocity and Euler angle got introduced with some sinusoidal harmonics along with its disturbance-less counter-part.

4.3. Open Loop Response of the System (Quaternion based model):

Quaternion is a concept designed specifically for representing orientation. It can be assumed as a vector-like quantity with four parameters who's last three parameters express a direction and the first quantity expresses an angle the subject makes with that direction. In this model as well, the input remains the same, i.e. the torque vector. But output will be the quaternion, although angular velocity changes will be shown as well.

Case 1:

Input $\vec{\tau} = u(t-1)\,\hat{\boldsymbol{\imath}} + 0\hat{\boldsymbol{\jmath}} + 0\hat{\boldsymbol{k}}$

Or a torque is applied on the system whose only non-zero component is along x axis, which is by magnitude a unit step function (with unit delay).

The system behaviour is shown below.

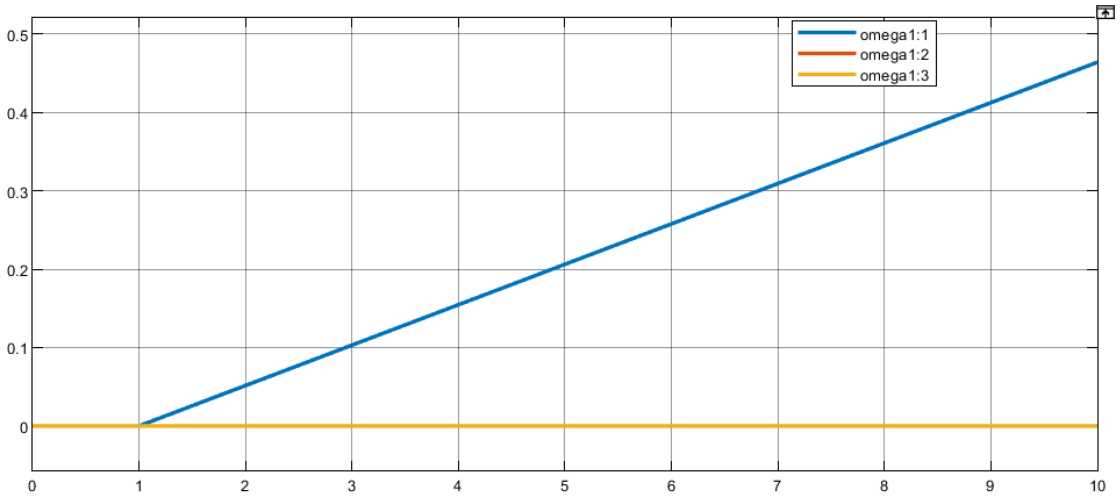

Fig 36: Angular velocity of satellite with Diagonal Inertia Matrix for unidirectional step input

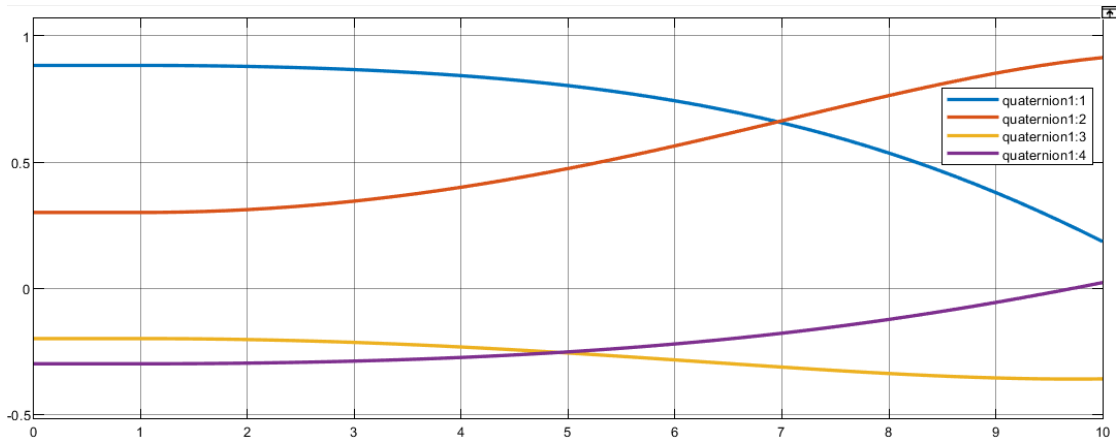

Fig 37: Quaternion of satellite with Diagonal Inertia Matrix for unidirectional step input

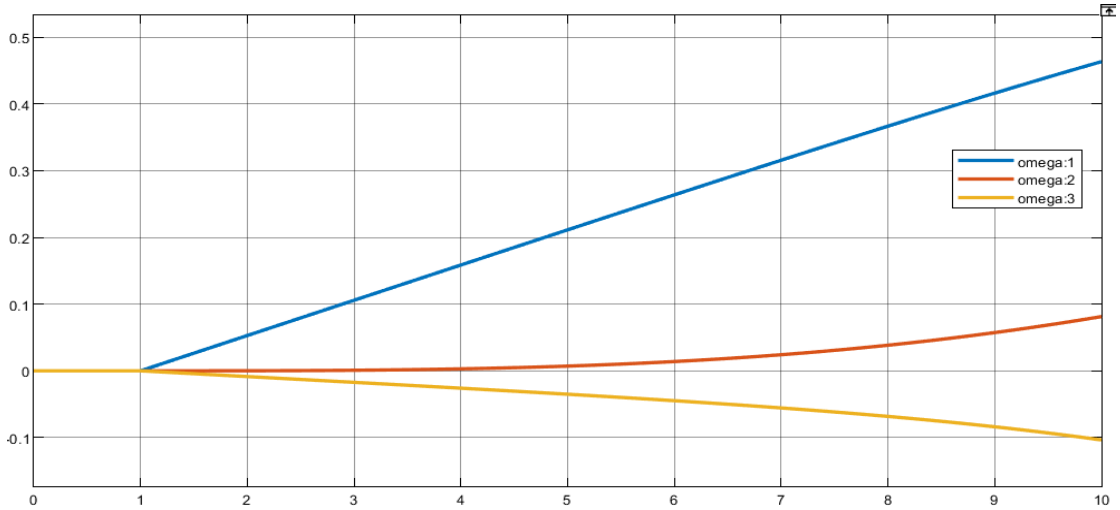

Fig 38: Angular velocity of satellite with Non-Diagonal Inertia Matrix for unidirectional step input

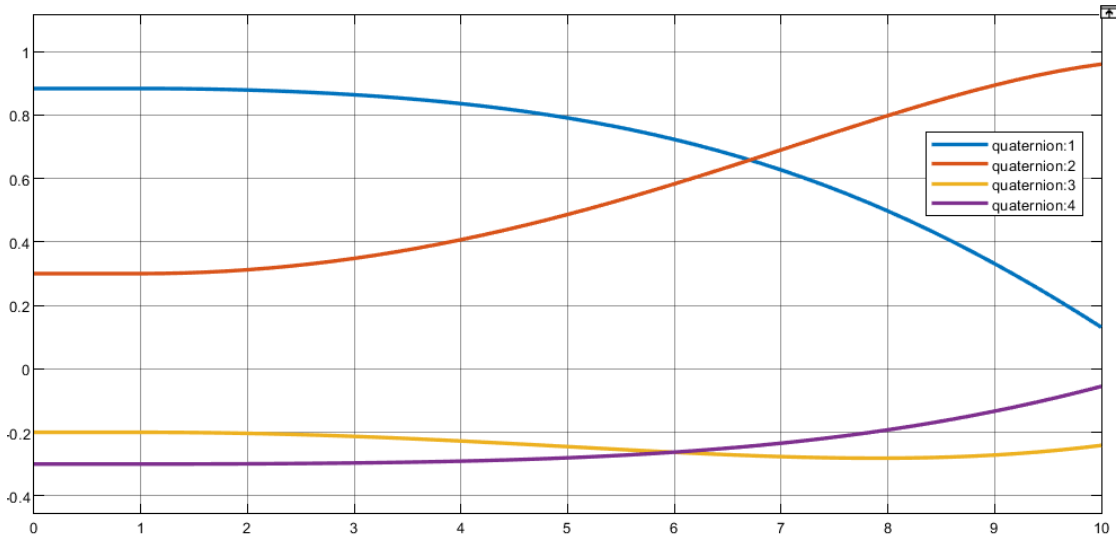

Fig 39: Quaternion of satellite with Non-Diagonal Inertia Matrix for unidirectional step input

Case 2:

Input $\vec{\tau} = u(t-1)\hat{\boldsymbol{\imath}} + u(t-1)\,\hat{\boldsymbol{\jmath}} + u(t-1)\hat{\boldsymbol{k}}$

If step signal is applied along all direction, the response of the systems comes out as below.

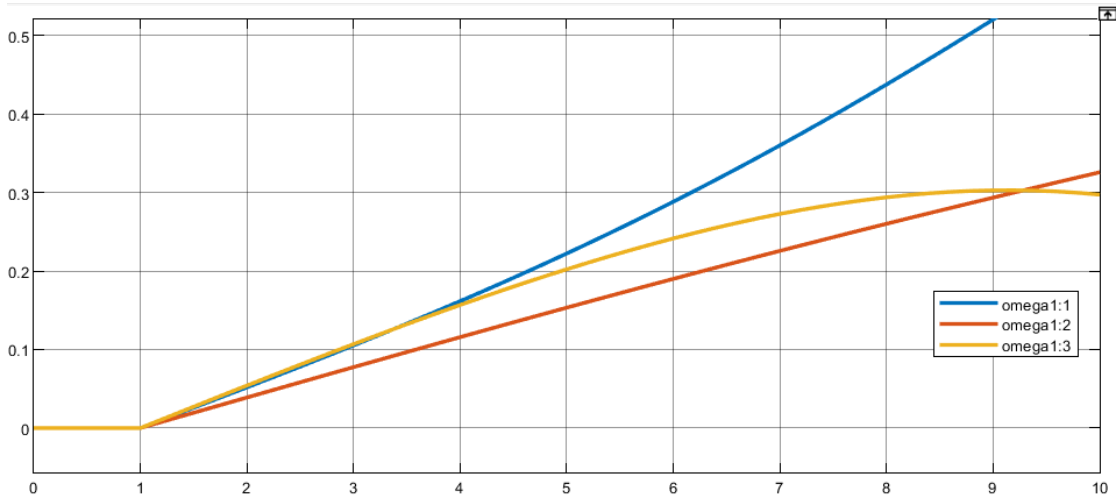

Fig 40: Angular velocity of satellite with Diagonal Inertia Matrix for step input

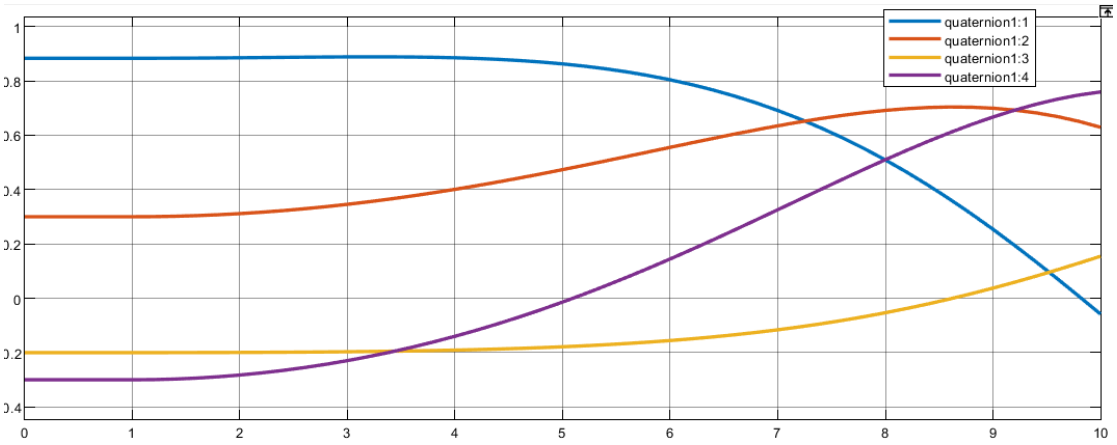

Fig 41: Quaternion of satellite with Diagonal Inertia Matrix for step input

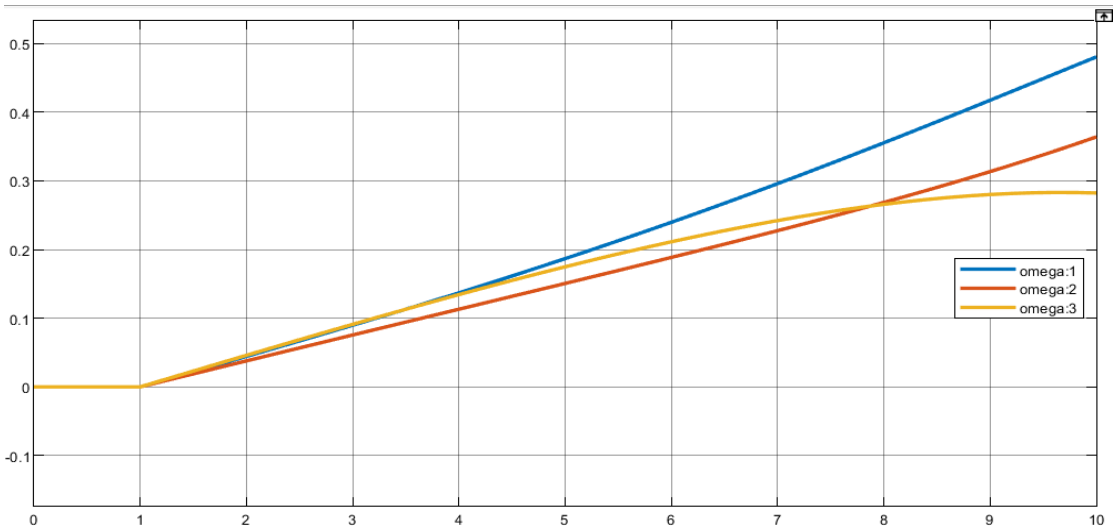

Fig 42: Angular velocity of satellite with Non-Diagonal Inertia Matrix for step input

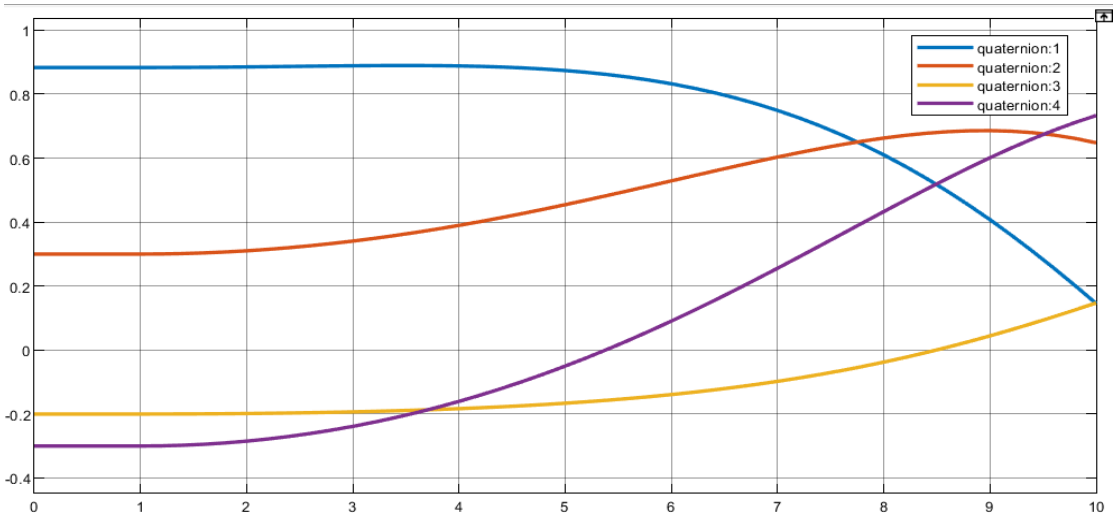

Fig 43: Quaternion of satellite with Non-Diagonal Inertia Matrix for step input

Case 3:

Pulse input $\vec{\tau} = P(t)(\hat{\boldsymbol{\imath}} + \hat{\boldsymbol{\jmath}} + \hat{\boldsymbol{k}})$, where $P(t) = [u(t) - u(t-1)]$

The response of the system is shown below,

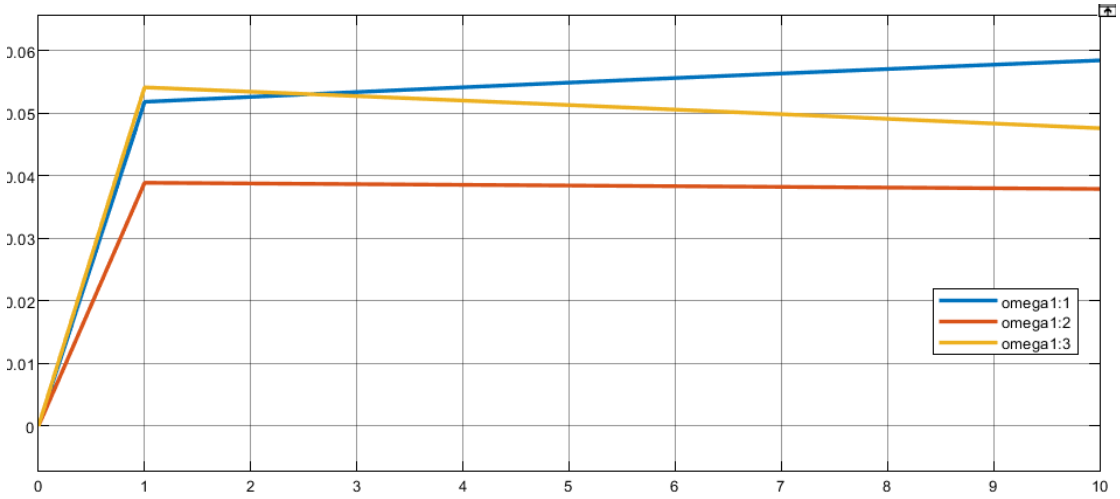

Fig 44: Angular velocity of satellite with Diagonal Inertia Matrix for Pulse input

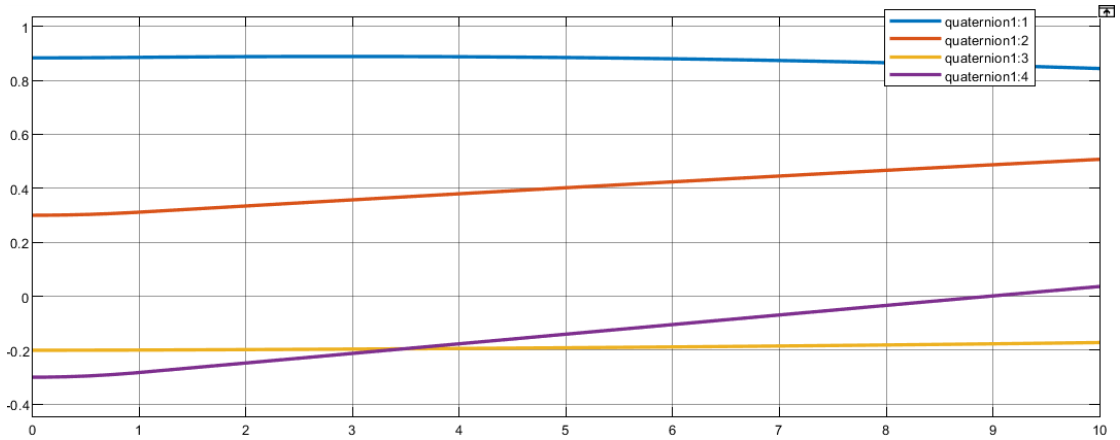

Fig 45: Quaternion of satellite with Diagonal Inertia Matrix for Pulse input

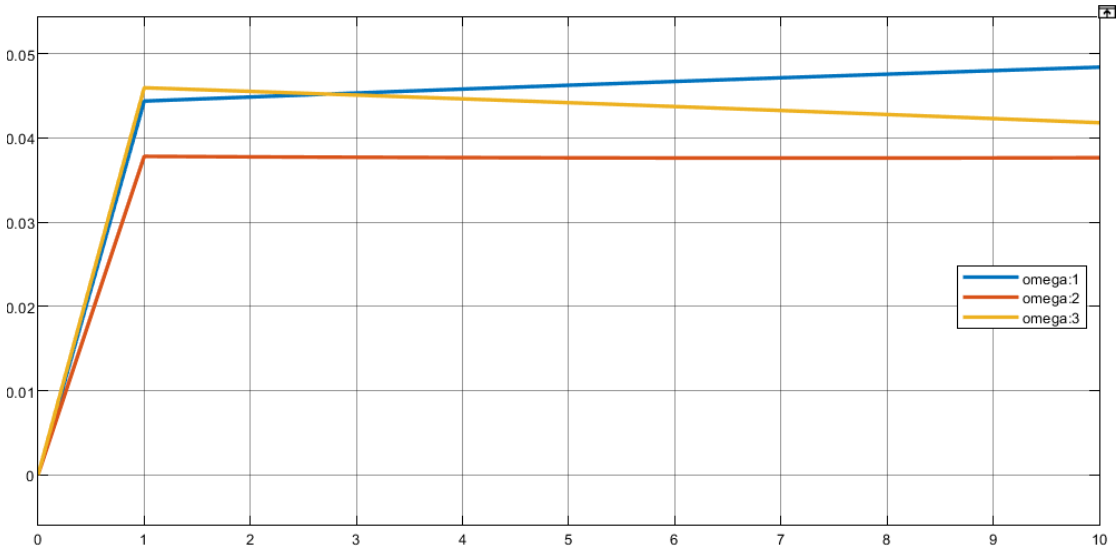

Fig 46: Angular velocity of satellite with Non-Diagonal Inertia Matrix for Pulse input

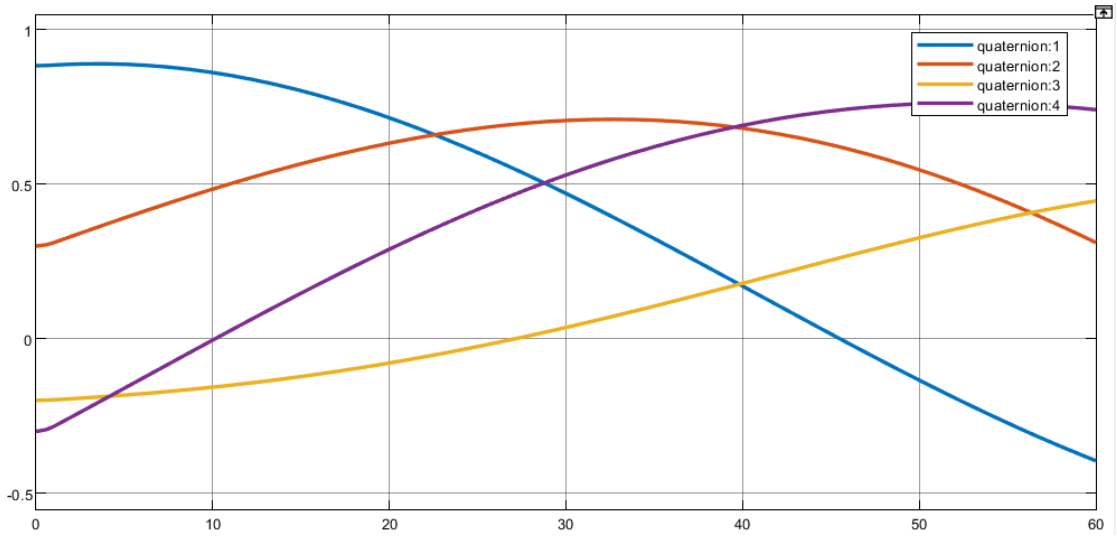

Fig 47: Quaternion of satellite with Non-Diagonal Inertia Matrix for Pulse input

4.3.1 **Effect of Disturbance:**

Now the effect of introducing disturbance to the system will be shown and discussed for the above cases.

$$\text{Disturbance signal} = 0.01\begin{bmatrix}\sin(0.1t)\\ \sin(0.2t)\\ \sin(0.3t)\end{bmatrix} \text{ N-m}$$

Case 1:

System response without any input.

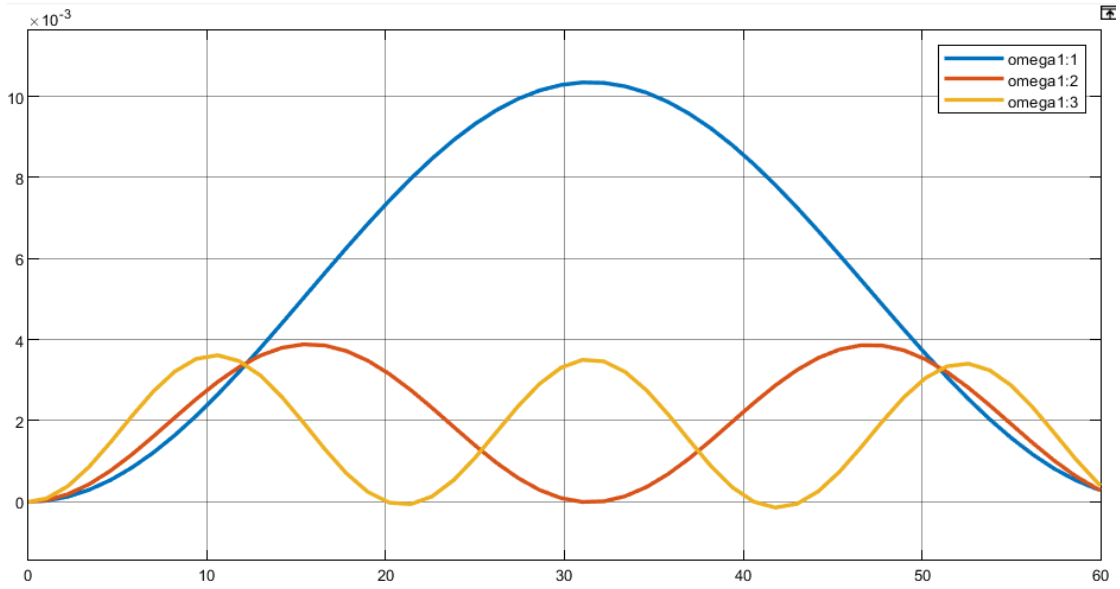

Fig 48: Angular Velocity of Satellite with Diagonal Inertia Matrix for With Disturbance and Without Input

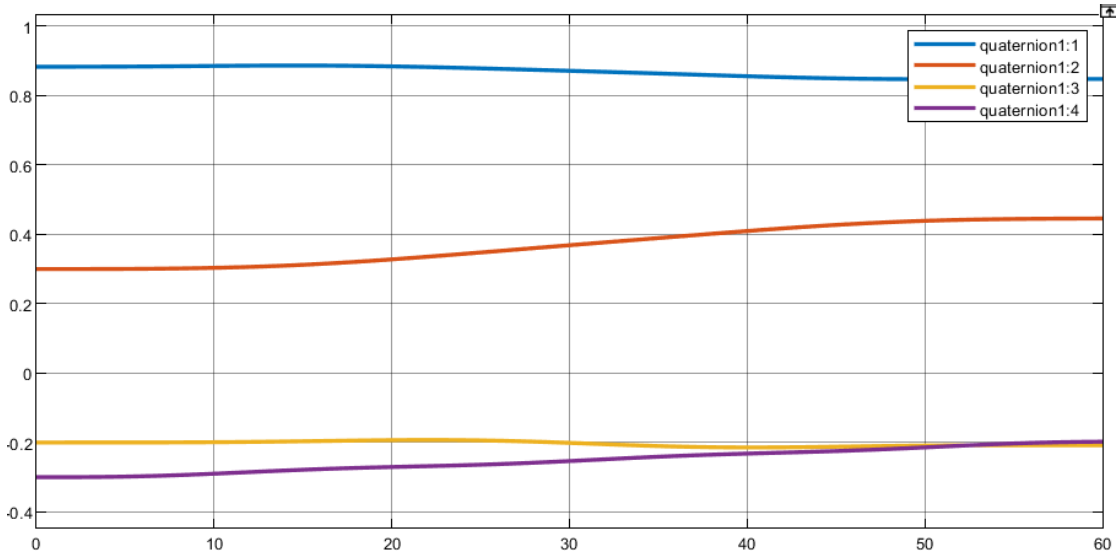

Fig 49: Quaternion of Satellite with Diagonal Inertia Matrix for With Disturbance and Without Input

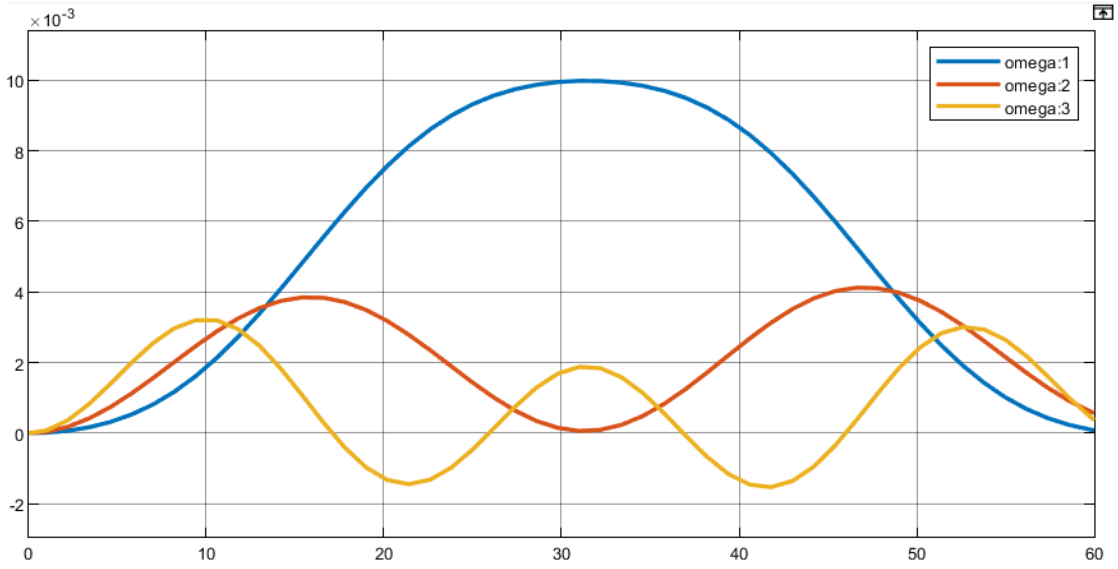

Fig 50: Angular Velocity of Satellite with Non-Diagonal Inertia Matrix for With Disturbance and Without Input

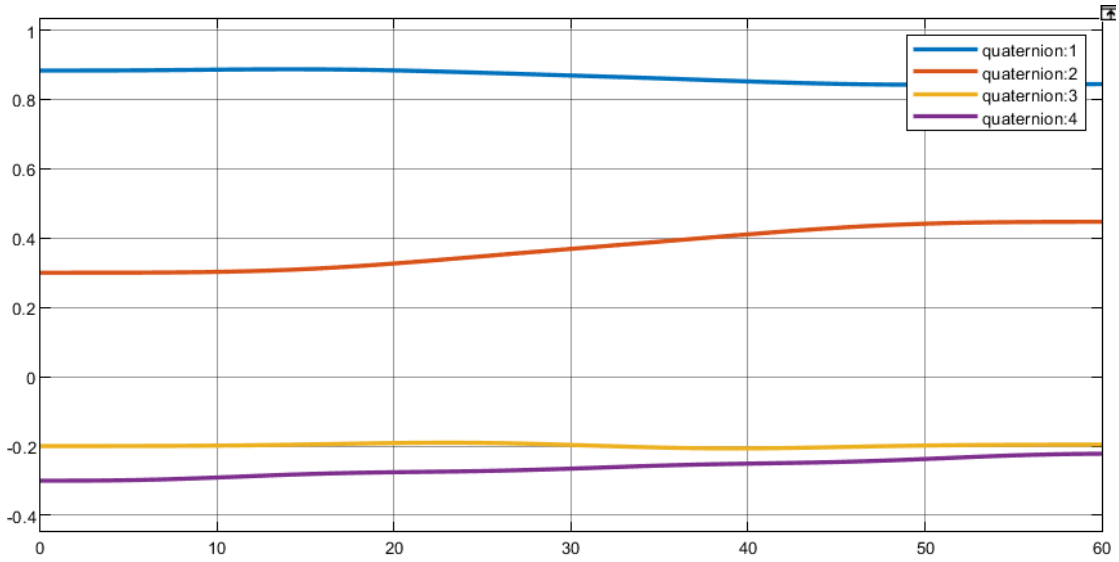

Fig 51: Quaternion of Satellite with Non-Diagonal Inertia Matrix for With Disturbance and Without Input

Case 2:

System response for step input in presence of disturbance.

$$\vec{\tau} = u(t-1)\hat{\boldsymbol{\imath}} + u(t-1)\,\hat{\boldsymbol{\jmath}} + u(t-1)\hat{\boldsymbol{k}}$$

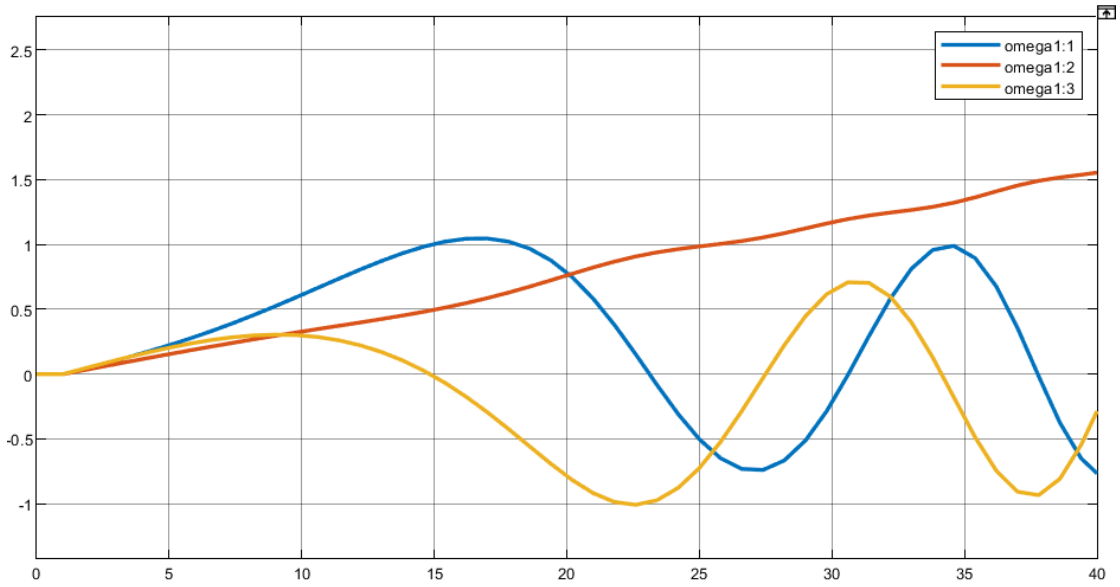

Fig 52: Angular Velocity of Satellite with Diagonal Inertia Matrix for With Disturbance and Step Input

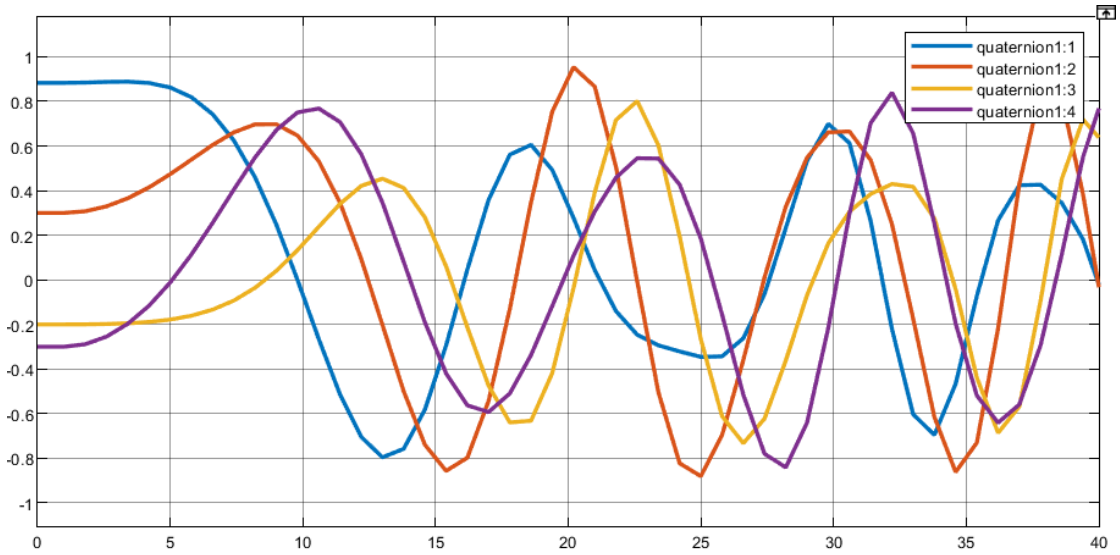

Fig 53: Quaternion of Satellite with Diagonal Inertia Matrix for With Disturbance and Step Input

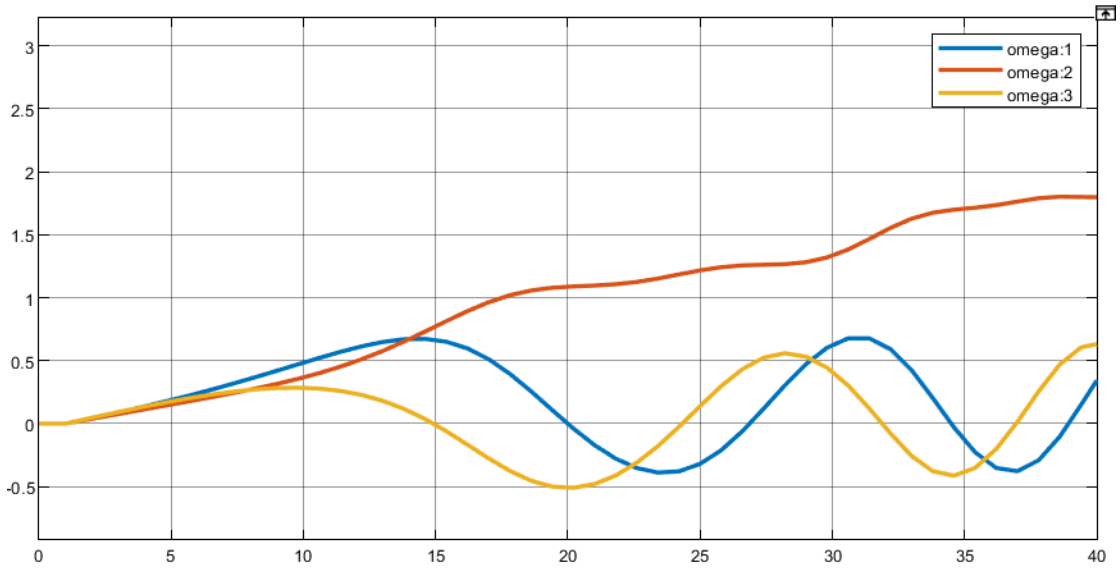

Fig 54: Angular Velocity of Satellite with Non-Diagonal Inertia Matrix for With Disturbance and Step Input

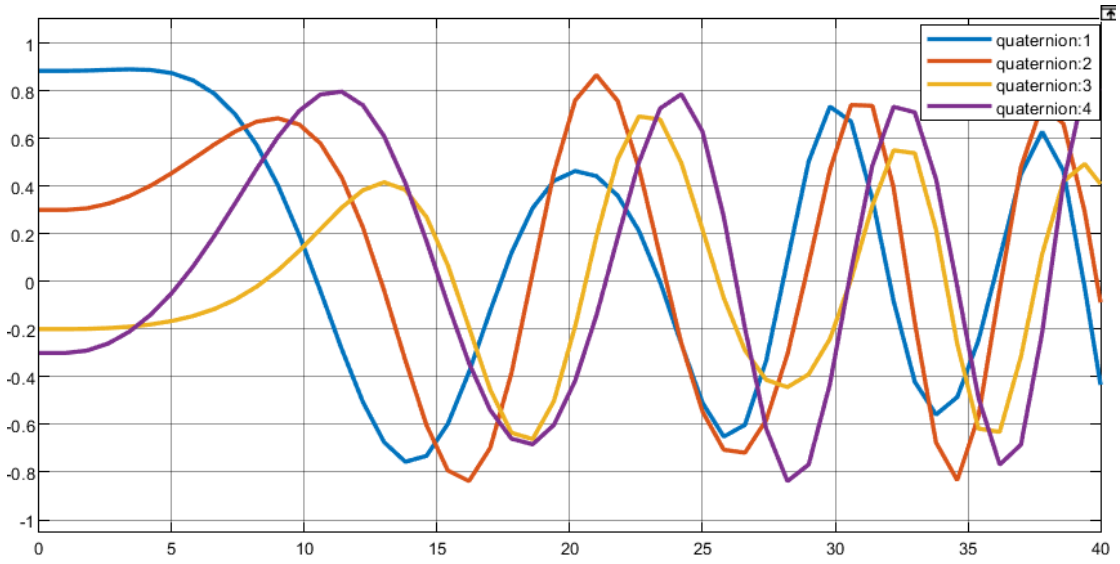

Fig 55: Quaternion of Satellite with Non-Diagonal Inertia Matrix for With Disturbance and Step Input

Case 3:

Pulse input $\vec{\tau} = P(t)(\hat{\boldsymbol{\imath}} + \hat{\boldsymbol{\jmath}} + \hat{\boldsymbol{k}})$, where $P(t) = [u(t) - u(t-1)]$

The response of the system in presence of disturbance is shown below,

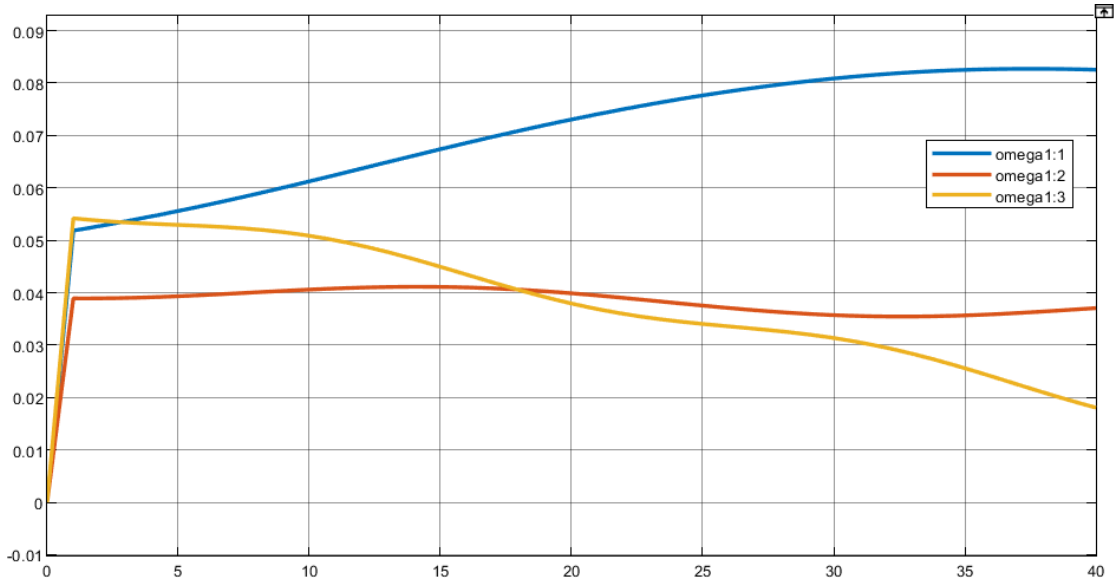

Fig 56: Angular Velocity of Satellite with Diagonal Inertia Matrix for With Disturbance and Pulse Input

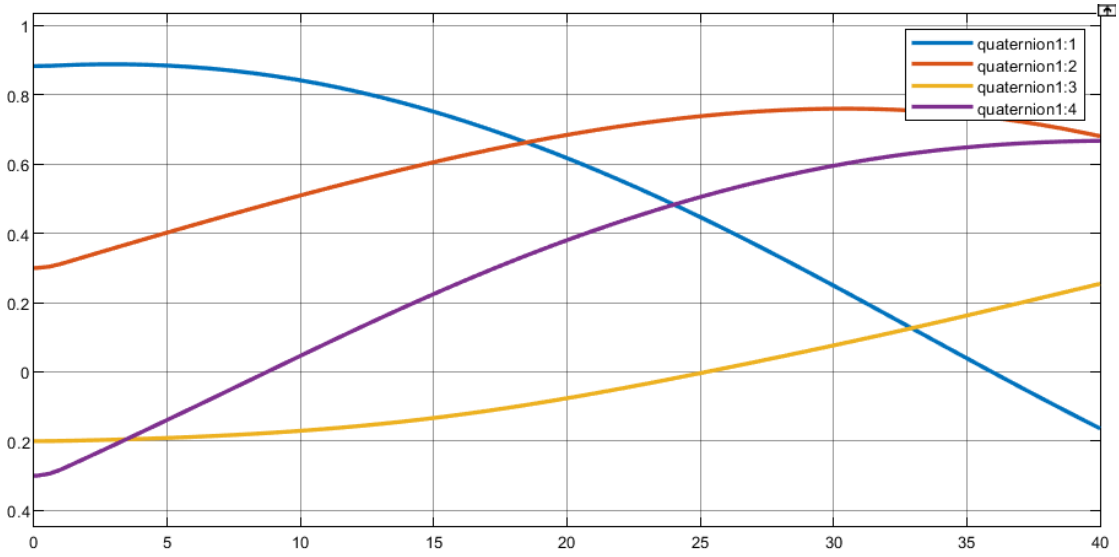

Fig 57: Quaternion of Satellite with Diagonal Inertia Matrix for With Disturbance and Pulse Input

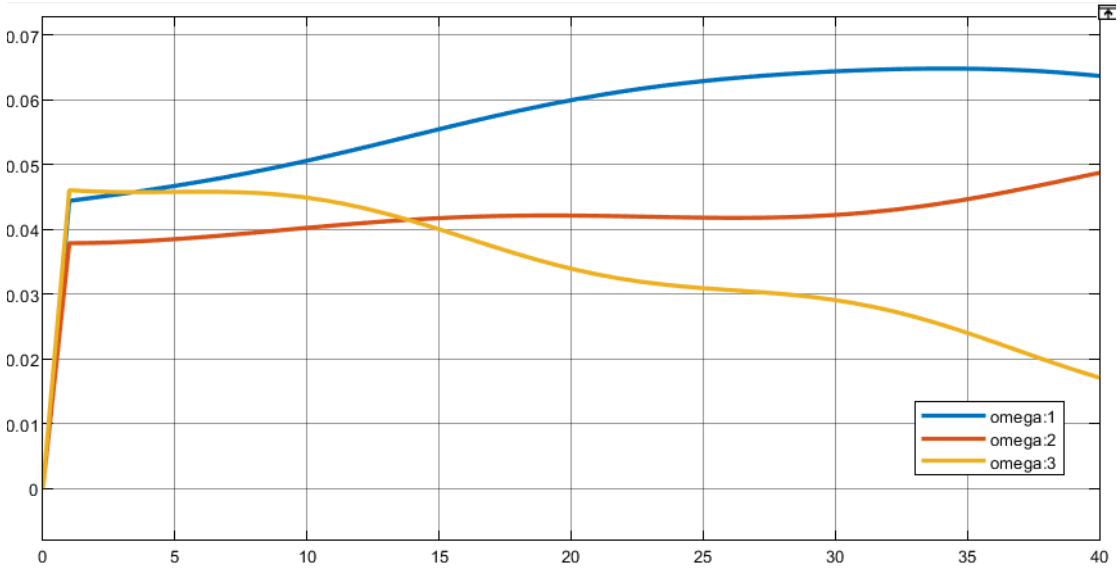

Fig 58: Angular Velocity of Satellite with Non-Diagonal Inertia Matrix for With Disturbance and Pulse Input

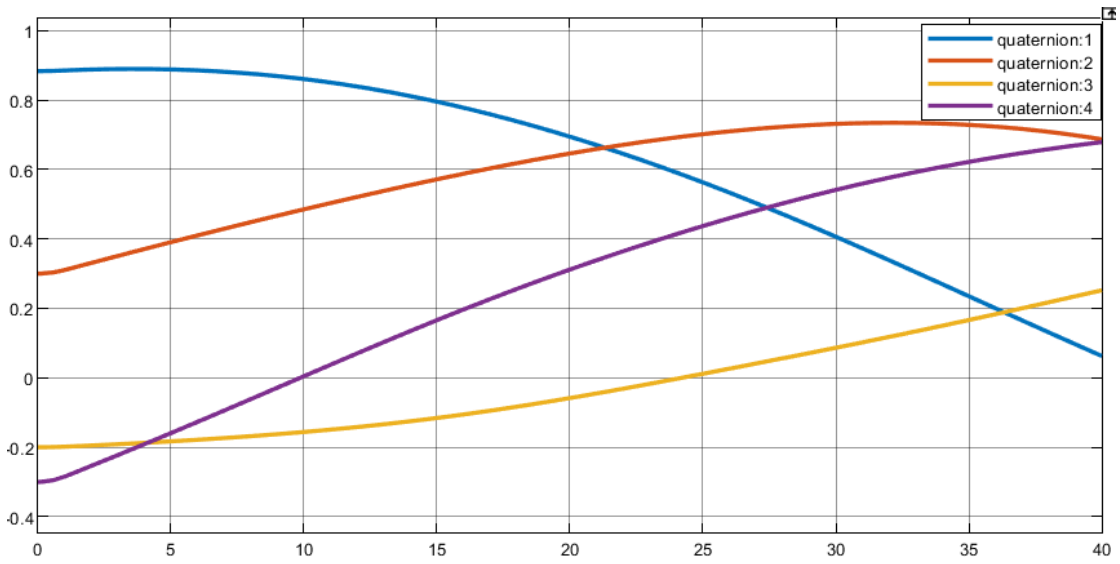

Fig 59: Quaternion of Satellite with Non-Diagonal Inertia Matrix for With Disturbance and Pulse Input

4.4. Open Loop Response of the System (Error Quaternion based model):

Error quaternion-based model is derived based on the minimizing the error quaternion between the actual and reference quaternion of the system. A simulation model has been prepared in Simulink environment to investigate its open loop response for different inputs.

Case 1:

input $\vec{\tau} = u(t)(\hat{\imath} + \hat{\jmath} + \hat{k})$

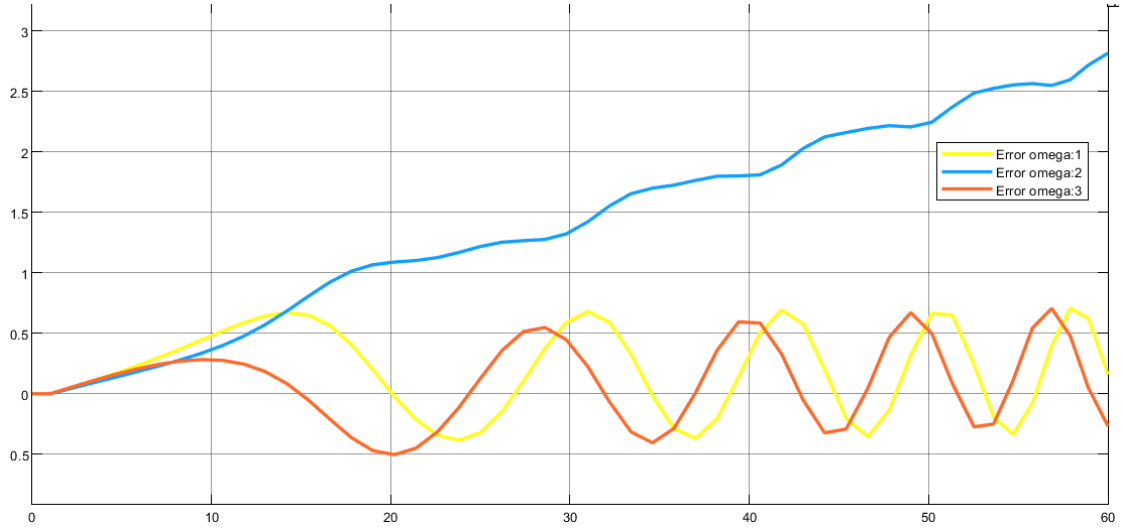

Fig 60: Error Angular Velocity of Satellite for Step Input

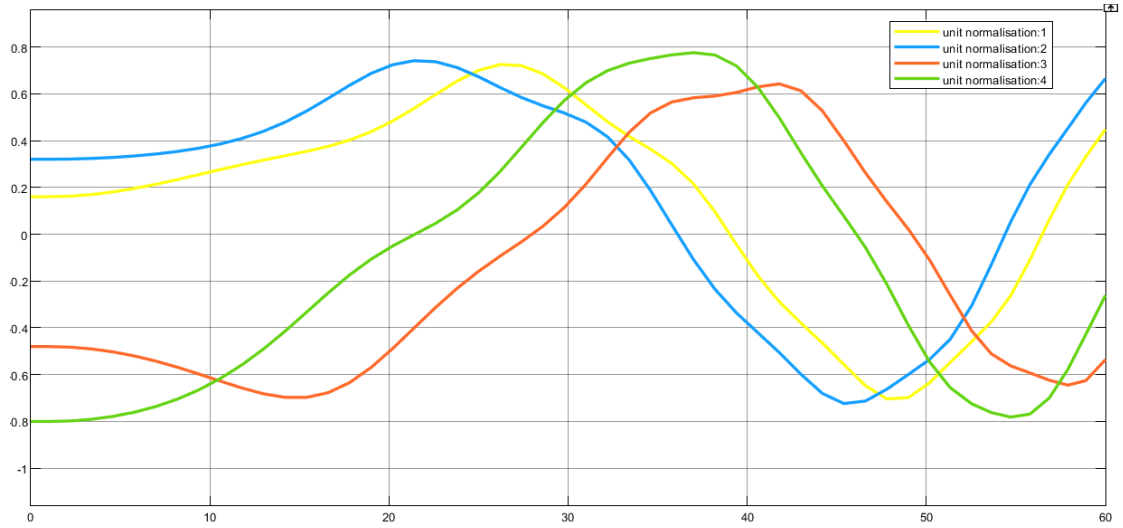

Fig 61: Error Quaternion of Satellite for Step Input

Case 2:

input $\vec{\tau} = P(t)(\hat{\boldsymbol{\imath}} + \hat{\boldsymbol{\jmath}} + \hat{\boldsymbol{k}})$, where $P(t) = [u(t) - u(t-10)]$

Pulse width is taken as 10 sec unlike the previous cases, because of the slow dynamics of the error quaternion model, hence observing the dynamic characteristics required wider pulse.

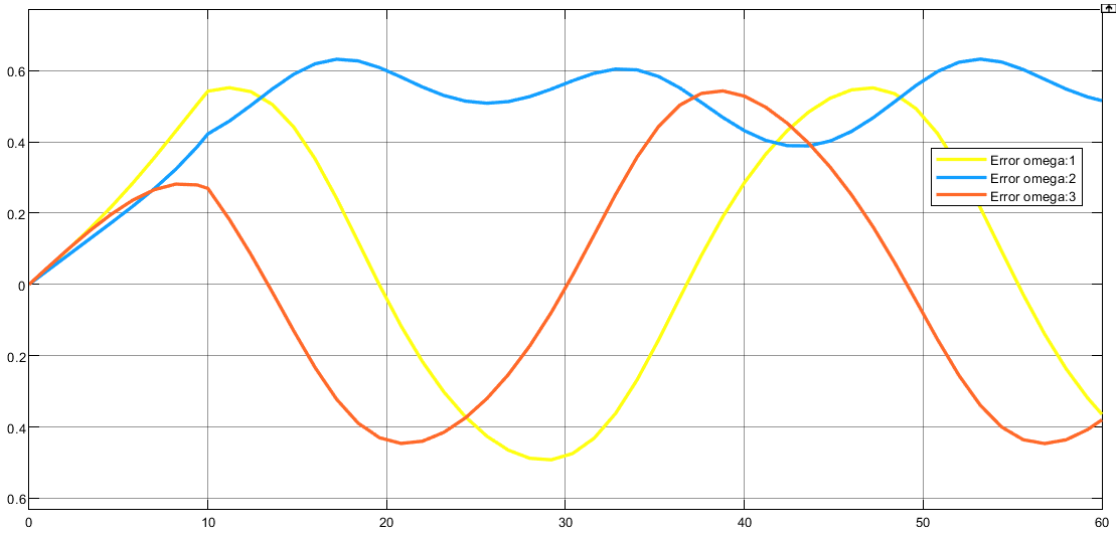

Fig 62: Error Angular Velocity of Satellite for Pulse Input

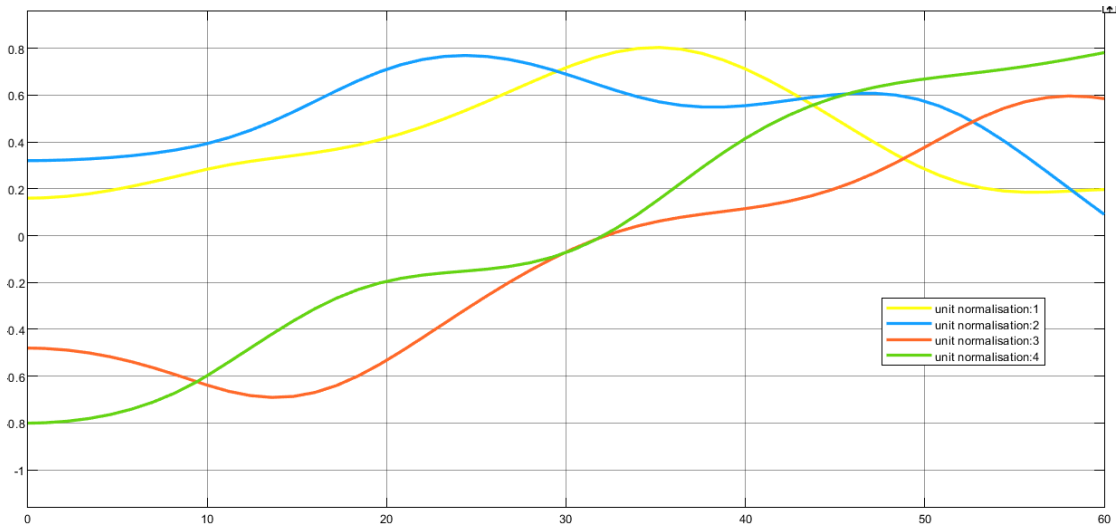

Fig 63: Error Quaternion of Satellite for Pulse Input

4.4.1. Effect of Disturbance:

In this section the effect of disturbance in the error quaternion model will be investigated. The disturbance function assumed is same as the above cases.

Case 1:

Effect of disturbance on error angular velocity and error quaternion is shown without the presence of any input control torque.

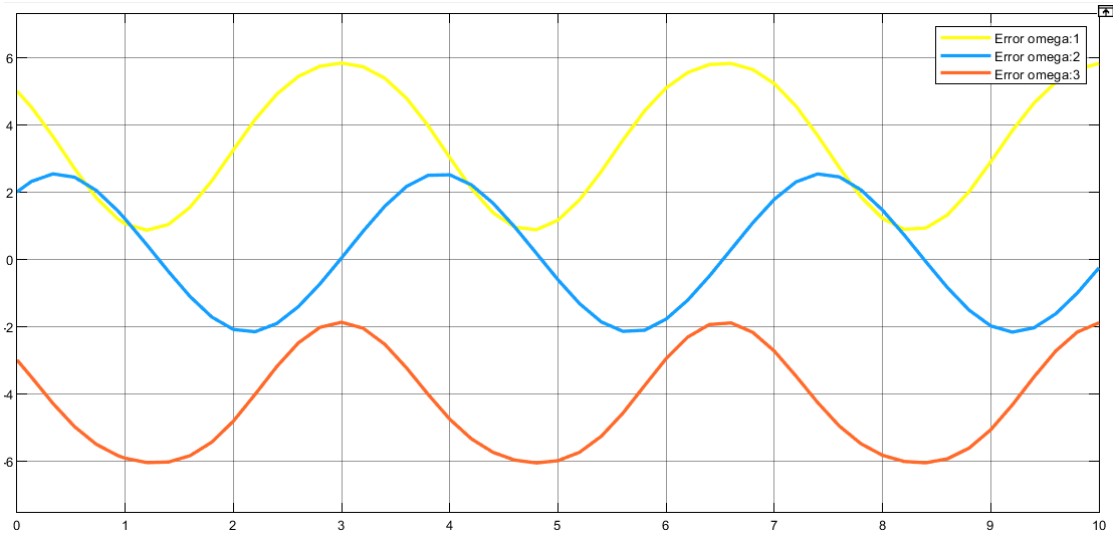

Fig 64: Error Angular Velocity of Satellite in Presence of Disturbance without Any Input

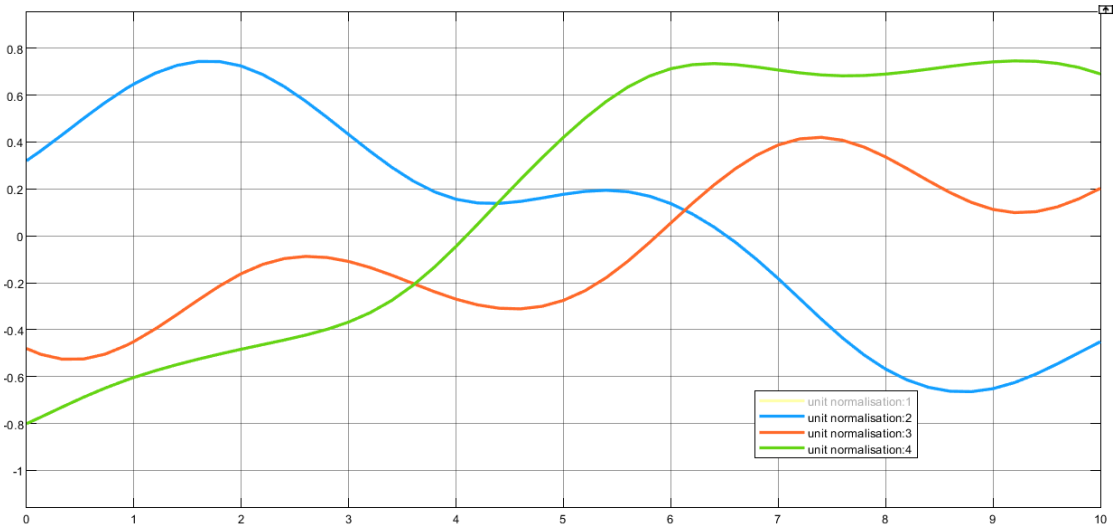

Fig 65: Error Quaternion of Satellite in Presence of Disturbance without Any Input

Case 2:

Effect of disturbance in presence of step input.

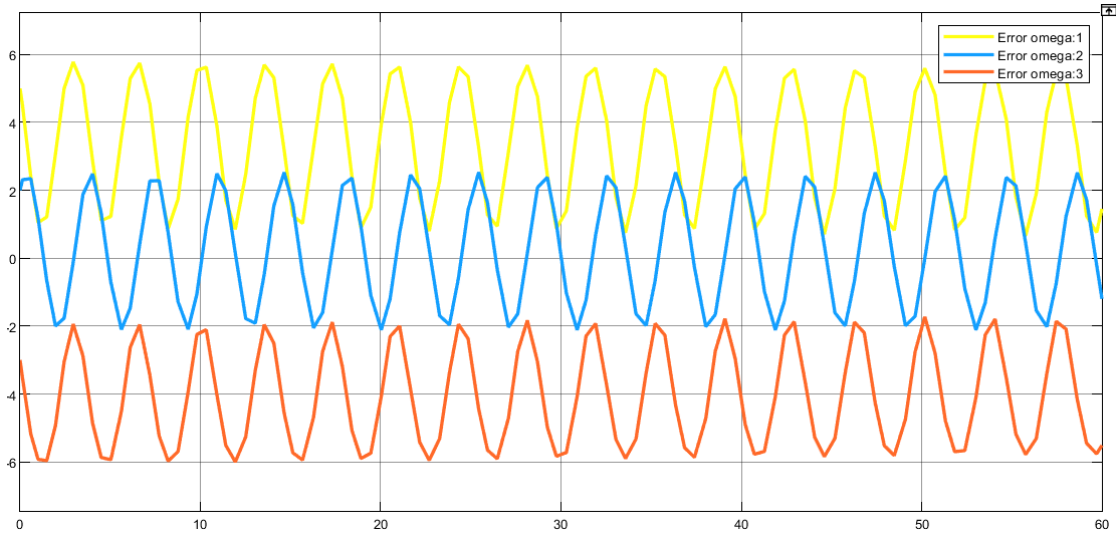

Fig 66: Error Angular Velocity of Satellite in Presence of Disturbance with Step Input

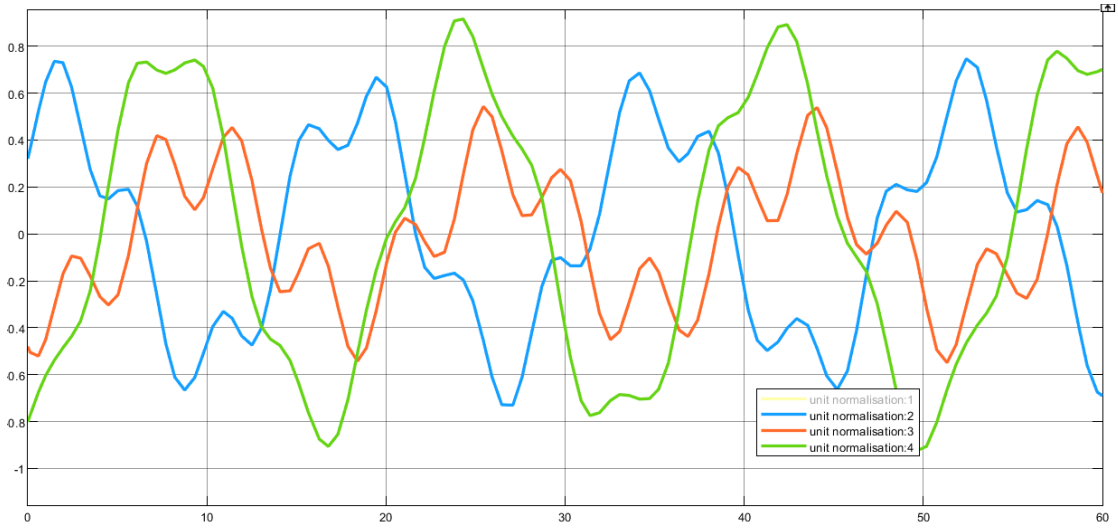

Fig 67: Error Quaternion of Satellite in Presence of Disturbance with Step Input

4.5. Stabilization problem with PID controller:

4.5.1. Quaternion Model:

It is well established from the above results and observations, that the system is inherently unstable. That is why a problem has been constructed where the microsatellite is having a payload (like camera or antenna) which needs to pointed at a particular direction to fulfil mission objectives. That is why the objective of the controller is to stabilize the system at a particular orientation expressed by the quaternion $q =$

$[1\ 0\ 0\ 0]^T$ in presence of disturbance function provided above. Initial orientation of the satellite was assumed to be $q = [0.8832\ \ 0.3\ \ -0.2\ \ 0.3]^T$. The result is shown below.

Firstly the output results with the model with diagonal inertia matrix is shown.

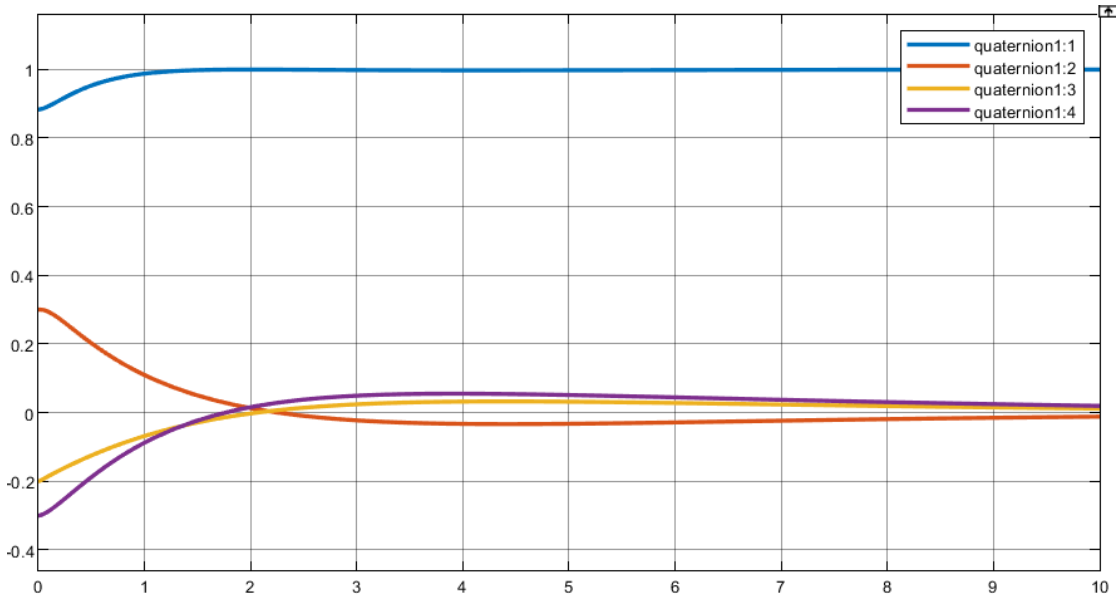

Fig 68: Quaternion of the PID stabilized satellite with Diagonal Inertia Matrix

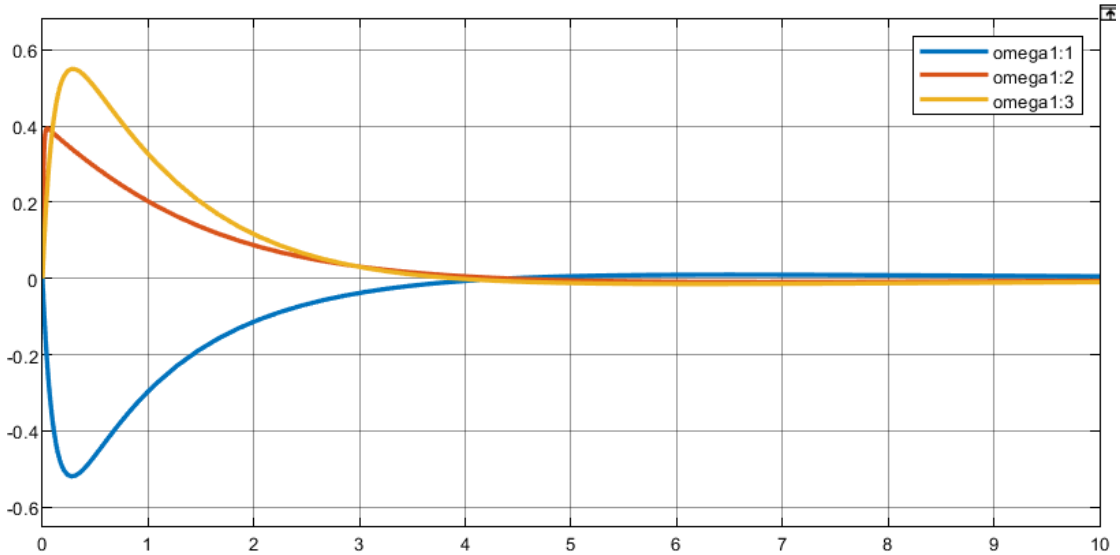

Fig 69: Angular Velocity of the PID stabilized satellite with Diagonal Inertia Matrix

Observation:

The system gets sufficiently stable after 6 seconds and the angular velocities approach sufficiently close to zero at 4 seconds.

As PID controller can only take a scalar quantity as its input, 3 separate PID controllers were used to stabilize the system. The tuned parameters of the controllers are shown below.

Controller Formula $= P + \frac{I}{s} + D\frac{N}{1+\frac{N}{s}}$

Controller Parameter	PID Controller 1	PID Controller 2	PID Controller 3
Proportional (P)	9.588	10.910	6.659
Integral (I)	0.480	0.570	0.289
Derivative (D)	37.346	51.712	37.642
Filter Coefficient (N)	10.490	114.282	10.490

Now, results of PID controller stabilisation for the satellite with non-diagonal inertia matrix is shown below.

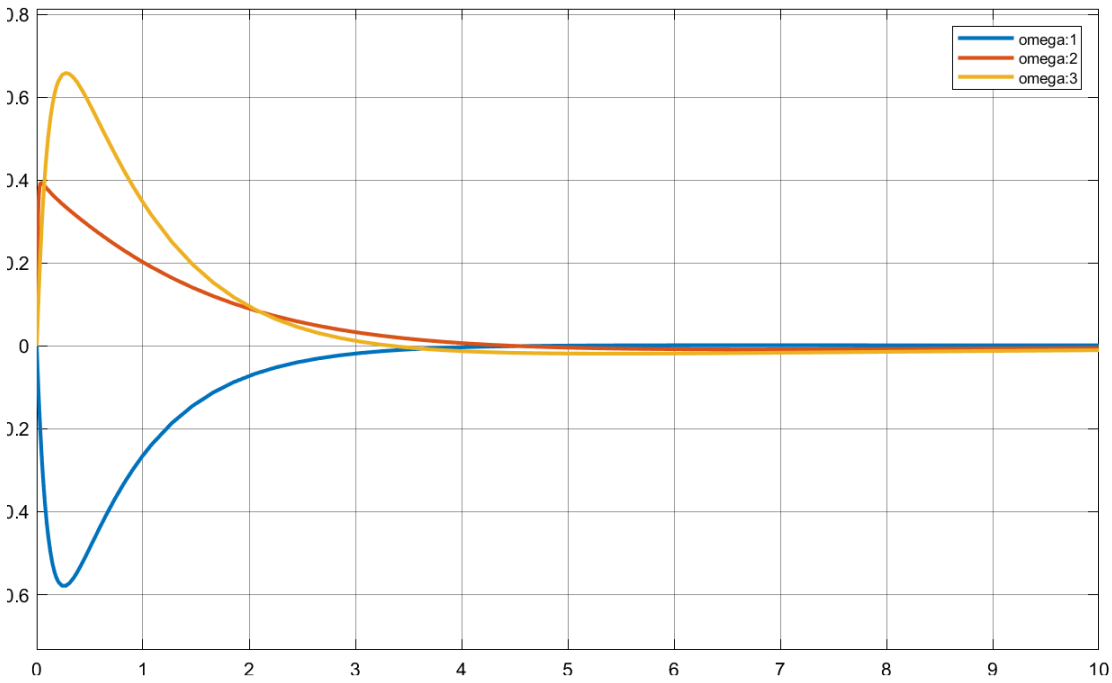

Fig 70: Angular Velocity of the PID stabilized satellite with Non-Diagonal Inertia Matrix

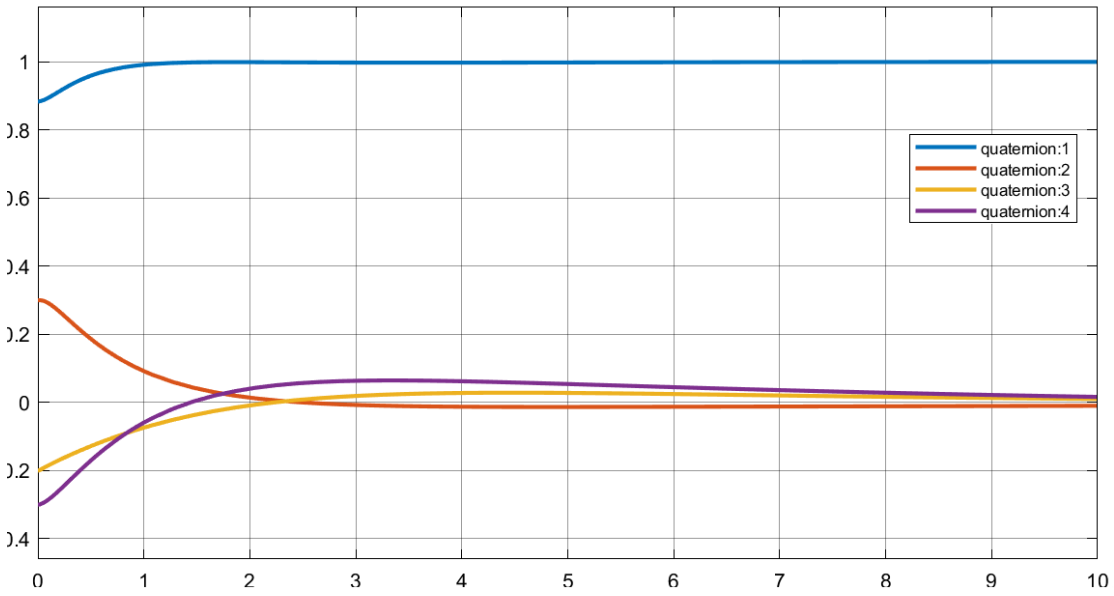

Fig 71: Quaternion of the PID stabilized satellite with Non-Diagonal Inertia Matrix

Three details of PID controllers used in this model are tabulated below.

Controller Parameter	PID Controller 1	PID Controller 2	PID Controller 3
Proportional (P)	9.037	11.391	7.257
Integral (I)	0.434	0.331	0.332
Derivative (D)	35.740	52.183	39.170
Filter Coefficient (N)	10.490	114.282	10.490

4.5.2. Euler Angle Model:

A similar simulation effort was done to stabilise the Euler angle model as well. The non-zero initial Euler angles were $[2\ 1\ -1]$ and they were stabilized to $[0\ 0\ 0]$. The simulation results are shown below for the diagonal inertia matrix model and non-diagonal inertia matrix model.

Details of the PID controller for the diagonal inertia matrix:

Controller Parameter	PID Controller 1	PID Controller 2	PID Controller 3
Proportional (P)	3.602	6.188	4.408
Integral (I)	0.169	0.287	0.205
Derivative (D)	18.894	24.755	17.635
Filter Coefficient (N)	5.454	10.490	10.490

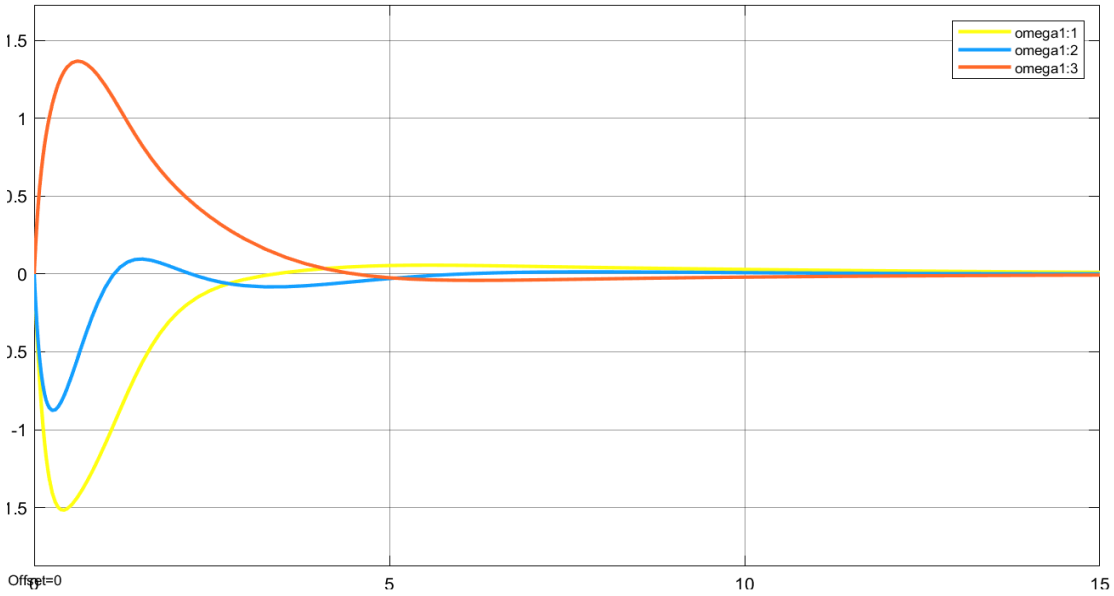

Fig 72: Angular Velocity of the PID stabilized satellite with Diagonal Inertia Matrix

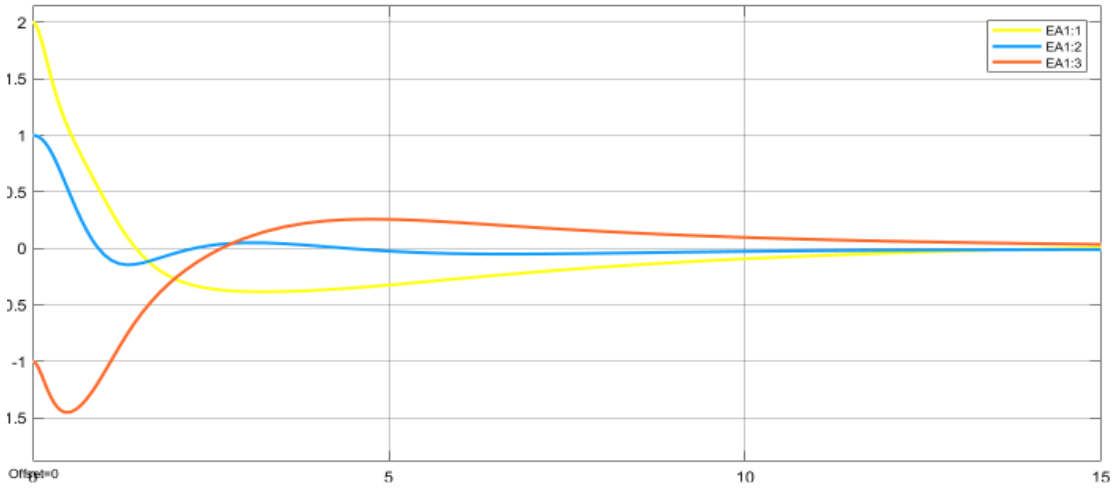

Fig 73: Euler Angle of the PID stabilized satellite with Diagonal Inertia Matrix

Details of the PID controller for the diagonal inertia matrix:

Controller Parameter	PID Controller 1	PID Controller 2	PID Controller 3
Proportional (P)	3.577	4.851	4.457
Integral (I)	0.168	0.228	0.224
Derivative (D)	18.721	25.390	17.320
Filter Coefficient (N)	5.454	5.454	10.490

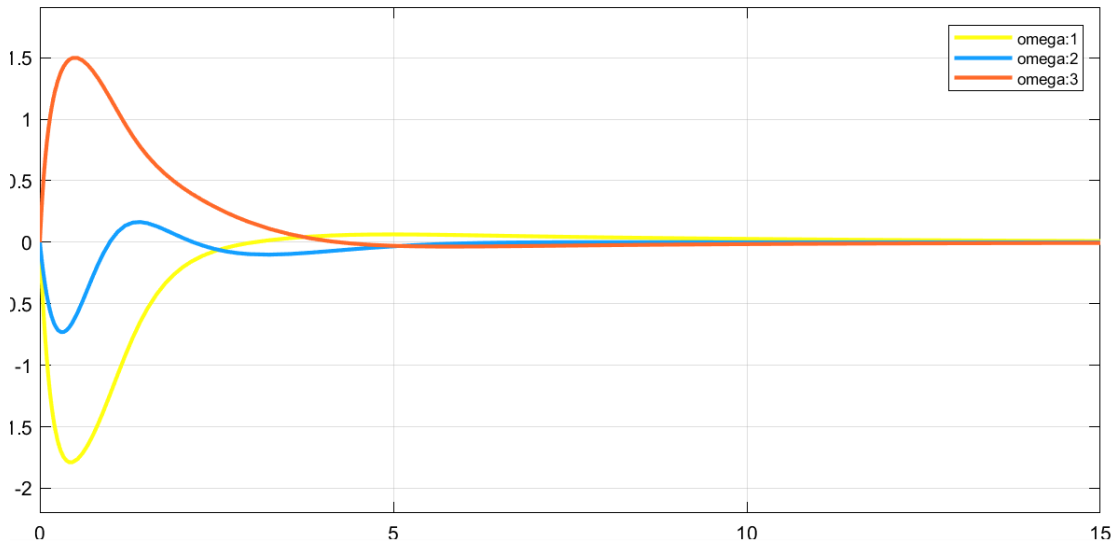

Fig 74: Angular Velocity of the PID stabilized satellite with Non-Diagonal Inertia Matrix

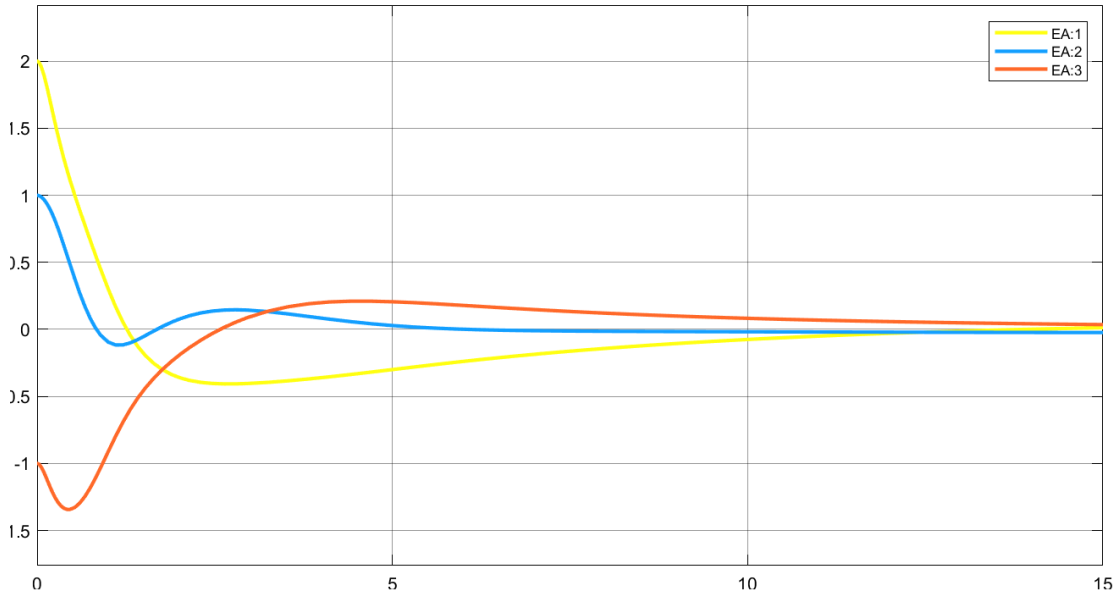

Fig 75: Euler Angle of the PID stabilized satellite with Non-Diagonal Inertia Matrix

Refererence:

[1] V. Jungnell, "Guidance Methods for Earth Observation Satellites," Centre national detudes spatiales Centre spatial de Toulouse, Toulouse, France, Sep. 2012.

[2] S. Janson, "The concept and history of small satellites," *Elsevier eBooks*, pp. 9–55, Jan. 2023, doi: https://doi.org/10.1016/b978-0-12-824541-5.00017-0.

[3] Ovchinnikov, Michael, Vladimir Pen'ko, Olle Norberg, and Stas Barabash. "Attitude control system for the first swedish nanosatellite "MUNIN"." *Acta Astronautica* 46, no. 2-6 (2000): 319-326.

[4] İnce, Fuat. "Nano and micro satellites as the pillar of the 'new space' paradigm." In *Space Environment and International Politics*, pp. 377-396. Transnational Press London, 2020.

[5] de Carvalho, Rogério Atem, Jaime Estela, and Martin Langer, eds. *Nanosatellites: space and ground technologies, operations and economics*. John Wiley & Sons, 2020.

[6] Ovchinnikov, M. Yu, and D. S. Roldugin. "A survey on active magnetic attitude control algorithms for small satellites." *Progress in Aerospace Sciences* 109 (2019): 100546.

[7] Hajiyev, Chingiz, and DEMET Cilden Guler. "Review on gyroless attitude determination methods for small satellites." *Progress in Aerospace Sciences* 90 (2017): 54-66.

[8] He, Liang, Wenjie Ma, Pengyu Guo, and Tao Sheng. "Developments of attitude determination and control system of microsats: A survey." *Proceedings of the Institution of Mechanical Engineers, Part I: Journal of Systems and Control Engineering* 235, no. 10 (2021): 1733-1750.

[9] Stickler, A. Craig, and K. T. Alfriend. "Elementary magnetic attitude control system." *Journal of spacecraft and rockets* 13, no. 5 (1976): 282-287.

[10] Bhat, Sanjit P., and Ajit S. Dham. "Controllability of spacecraft attitude under magnetic actuation." In *42nd IEEE International Conference on Decision and Control (IEEE Cat. No. 03CH37475)*, vol. 3, pp. 2383-2388. IEEE, 2003.

[11] Wen, John Ting-Yung, and Kenneth Kreutz-Delgado. "The attitude control problem." *IEEE Transactions on Automatic control* 36, no. 10 (1991): 1148-1162.

[12] Pittelkau, Mark E. "Optimal periodic control for spacecraft pointing and attitude determination." *Journal of Guidance, Control, and Dynamics* 16, no. 6 (1993): 1078-1084.

[13] Lovera, Marco. "Modelling and simulation of spacecraft attitude dynamics." (2003): 1-9.

[14] De Marchi, Eliana, Luca De Rocco, Giuseppe D. Morea, and Marco Lovera. "Optimal Magnetic Momentum Control for Inertially Pointing Spacecraft." In *Spacecraft Guidance, Navigation and Control Systems*, vol. 425, p. 195. 2000.

[15] Arcara, Paolo, Sergio Bittanti, and Marco Lovera. "Active control of vibrations in helicopters by periodic optimal control." In *Proceedings of the 1997 IEEE international conference on control applications*, pp. 730-735. IEEE, 1997.

[16] Wisniewski, Rafal. "Satellite attitude control using only electromagnetic actuation." (1997).

[17] Wiśniewski, Rafał, and Mogens Blanke. "Fully magnetic attitude control for spacecraft subject to gravity gradient." *Automatica* 35, no. 7 (1999): 1201-1214.

[18] Wisniewski, Rafal, and F. Landis Markley. "Optimal magnetic attitude control." *IFAC Proceedings Volumes* 32, no. 2 (1999): 7991-7996.

[19] Wiśniewski, Rafal, and Jakob Stoustrup. "Periodic H2 synthesis for spacecraft attitude determination and control with a vector magnetometer and magnetorquers." *IFAC Proceedings Volumes* 34, no. 12 (2001): 119-124.

[20] Lovera, Marco. "Periodic H∞ attitude control for satellites with magnetic actuators." *IFAC Proceedings Volumes* 33, no. 14 (2000): 631-636.

[21] Lovera, Marco. "Optimal magnetic momentum control for inertially pointing spacecraft." *European Journal of Control* 7, no. 1 (2001): 30-39.

[22] Silani, Enrico, and Marco Lovera. "Magnetic spacecraft attitude control: a survey and some new results." *Control engineering practice* 13, no. 3 (2005): 357-371.

[23] Zhihong, Man, and Xing Huo Yu. "Terminal sliding mode control of MIMO linear systems." *IEEE Transactions on Circuits and Systems I: Fundamental Theory and Applications* 44, no. 11 (1997): 1065-1070.

[24] Feng, Yong, Xinghuo Yu, and Zhihong Man. "Non-singular terminal sliding mode control of rigid manipulators." *Automatica* 38, no. 12 (2002): 2159-2167.

[25] Singh, Sahjendra N., and Ashok Iyer. "Nonlinear decoupling sliding mode control and attitude control of spacecraft." *IEEE Transactions on Aerospace and Electronic Systems* 25, no. 5 (1989): 621-633.

[26] Vadali, Srinivas Rao. "Variable-structure control of spacecraft large-angle maneuvers." *Journal of Guidance, Control, and Dynamics* 9, no. 2 (1986): 235-239.

[27] Liu, X. J., P. Guan, and J. Z. Liu. "Fuzzy sliding mode attitude control of satellite." In *Proceedings of the 44th IEEE Conference on Decision and Control*, pp. 1970-1975. IEEE, 2005.

[28] Cao, Lu, Xiaolong Li, Xiaoqian Chen, and Yong Zhao. "Minimum sliding mode error feedback control for fault tolerant small satellite attitude control." *Advances in Space Research* 53, no. 2 (2014): 309-324.

[29] Curtis, Howard D. *Orbital mechanics for engineering students: Revised Reprint*. Butterworth-Heinemann, 2020.

[30] Markley, F. Landis, John L. Crassidis, F. Landis Markley, and John L. Crassidis. *Correction to: Fundamentals of Spacecraft Attitude Determination and Control*. Springer New York, 2014.

[31] Stevens, Brian L., Frank L. Lewis, and Eric N. Johnson. *Aircraft control and simulation: dynamics, controls design, and autonomous systems*. John Wiley & Sons, 2015.

[32] Thomson, William Tyrrell. *Introduction to space dynamics*. Courier Corporation, 2012.

[33] Das, Manasi, Smita Sadhu, and Tapan Kumar Ghoshal. "Spacecraft attitude & rate estimation by an adaptive unscented Kalman filter." In *Proceedings of The 2014 International Conference on Control, Instrumentation, Energy and Communication (CIEC)*, pp. 46-50. IEEE, 2014.

[34] Tiwari, Pyare Mohan, S. Janardhanan, and Mashuq un Nabi. "Attitude control using higher order sliding mode." *Aerospace Science and Technology* 54 (2016): 108-113.

[35] Sidi, Marcel J. *Spacecraft dynamics and control: a practical engineering approach*. Vol. 7. Cambridge university press, 1997.